HUMBOLDT BAY POWER PLANT
CALCULATION COVER SHEET

Calculation No.: GEO.HBIP.03.04

☐ Preliminary

☒ Final

Department/Group: HBPP/Geosciences

Unit(s) 0 Structure, System or Component: ISFSI Geotechnical

Type or Purpose of Calculation: Development of Probabilistically Based Spectra for HBIP ISFSI Site

No. of Sheets: 760 include 6 Appendices   Plant Problem Report No. N/A

	Signature	Discipline/Dept	Date
Prepared by:	*By Geosciences*		09/29/2003
Checked by:	*By Geosciences*		09/29/2003
Approved by (Supv):	[signature]	HBIP	10/02/2003

Registered Engineer Approval: (Complete section A for Civil calcs. Complete A or B for others)

A. Insert Engineer Stamp or Seal Below	B.
By Geosciences	Engineer's full name: ______
	Registration Number: ______
	Expiration Date: ______
Expiration Date:	

RECORDS OF REVISIONS

Revision Number	Date	Reasons for Revision & Plant Problem Report Number	Prepared By	Checked By	Approval Regis. Engr.	Approval Supvr.
0	09/29/03	Initial Issue	*Geosci.*	*Geosci.*	*Geosci.*	[signature]

Pacific Gas and Electric Company
Geosciences Department
Calculation Document

Calc Number: GEO.HBIP.03.04
Calc Revision: 00
Calc Date: 9/29/03 NAA
Quality Related: Yes NAA 9/29/03
ITR Verification Method: A

Number of pages: 760 NAA

1.0 CALCULATION TITLE: Development of Probabilistically Based Spectra for the HBIP ISFSI Site

2.0 SIGNATORIES

PREPARED BY:	[signature]	Date:	9/29/03
	Nicholas J. Gregor		Consultant
	Printed Name		Organization
VERIFIED BY:	[signature]	Date:	9/29/03
	Norman A. Abrahamson		PG&E Geosciences
	Printed Name		Organization
APPROVED BY:	Kent S. Ferre	Date:	9/29/03
	Kent S. Ferre		PG&E Geosciences
	Printed Name		Organization

REGISTERED PROFESSIONAL ENGINEER
KENT S. FERRE
C 034629
EXP. 9-30-05
CIVIL
STATE OF CALIFORNIA

Kent S. Ferre

3.0 RECORD OF REVISIONS

Rev. No.	Reason for Revision	Revision Date
00	Initial Calculation Document	09/29/03

4.0 PURPOSE

The purpose of this calculation is to perform a probabilistic seismic hazard analysis (PSHA) for the Humboldt Bay Power Plant site location as requested in AR A0583100 (PG&E, 2003a), that meets the requirements described in Draft RegGuide 3021 (March 2002) and NRC Reg Guide 1.165. Probabilistically determined horizontal ground motion response spectra (5% spectral damping) are developed for a range of return periods for both the fault normal and fault parallel components of motion for hypothetical rock and for the site-specific soil condition at HBIP.

The equal hazard spectra are computed for spectral periods of 0 to 3 seconds. The spectra are not computed for periods greater than 3 seconds because the longest period for which the attenuation relation (for subduction events) is defined is 3 seconds.

5.0 ASSUMPTIONS

5.1 Horizontal Component Attenuation Relationships for Rock Site Conditions for Crustal Earthquakes

The Abrahamson and Silva (1997), Campbell (1997), and Idriss (1991; 1995), and Sadigh et al. (1997) attenuation relationships for horizontal response spectral values (5% spectral damping) are assumed to be representative attenuation relations for rock sites for crustal earthquakes. The basis for this assumption is that these attenuation relations represent the state-of-the practice and are widely used. These four attenuation relations were also used in the deterministic evaluation (PG&E 2002c).

5.2 Horizontal Component Attenuation for Subduction Zone Earthquakes

The Youngs et al. (1997) attenuation relation is assumed to be representative of ground motions from subduction zone earthquakes for both interface and intra-slab events. The basis for this assumption is given below.

There are two types of subduction zone earthquakes: interface earthquakes and intra-slab earthquakes. Although the ground motions for a given magnitude and distance can be very different for these two types of earthquakes, most ground motion attenuation studies for subduction zone earthquakes have not distinguished between these two source types. The exception is Youngs et al. (1997). By separating the two source types for subduction zone earthquakes, Youngs et al. (1997) found a significant difference in ground motions (ground motions from intra-slab earthquakes are about 60% larger than those from interface earthquakes for the same magnitude and distance). This difference is considered to be important, so the Youngs et al. (1997) attenuation relation for rock site conditions, which is considered to be a state-of-practice attenuation relationship for subduction zone earthquakes, is selected for use in this study.

5.3 Attenuation Model Weights

Three crustal horizontal ground motion attenuation relationships and one subduction horizontal ground motion attenuation relationship is used in the PSHA. These attenuation relationships are assumed to be equally weighted when computing the total hazard for the site. The basis for this assumption of equal weighting for the suite of attenuation models is justified because of the lack of a preferred empirical attenuation model.

5.4 Ground Motion Attenuation Model Sigma Truncation

Empirical attenuation models give estimates of median ground motions and an associated uncertainty (i.e., sigma). This uncertainty in the estimated ground motion values is included in the PSHA. However, an upper limit of 3.0 sigma is assumed for the hazard calculations. This assumption of an upper limit on the sigma value for a given attenuation relationship is based on the fact that unrealistically large ground motions can be estimated for large sigma values. If no truncation value on the sigma value is used, these large unrealistic ground motions can control the total hazard at a site, especially for longer return periods.

5.5 Spectral Period Associated with PGA Value for Attenuation Relationships

Each rock attenuation relationship used in the PSHA is defined for PGA as well as a suite of spectral periods. The PGA ground motion values are assumed to be equal to the ground motion value between the spectral period range of 0.01 and 0.03 seconds (i.e., the ground response spectra is constant at the PGA value between these two spectral periods). This assumption is valid based on the observation that for spectral periods less than about 0.03 seconds (i.e., 33 Hz) to 0.01 seconds (i.e., 100 Hz), the computed acceleration response spectra from empirical ground motion recordings in active tectonic regions is approximately constant.

5.6 Magnitude Density Distribution Models

The magnitude density distribution model describes the relative number of large magnitude and moderate magnitude events that occur on a given seismic source. Three alternative magnitude density functions are considered: the truncated exponential model and the maximum magnitude model (pure characteristic) and a composite characteristic model (Youngs and Coppersmith ,1985).

The truncated exponential model is the standard Gutenberg-Richter model that is truncated at the minimum and maximum magnitudes and renormalized so that it integrates to unity. This magnitude density distribution model is assumed to be valid and applicable for all areal source zones (i.e., 100% weighting). The basis for this assumption is that it is standard practice.

The characteristic model assumes that more of the seismic energy is released in large magnitude events than for the truncated exponential model. That is, there are fewer small magnitude events for every large magnitude event for the characteristic model than for the truncated exponential model. There are different models for the characteristic model. Two commonly used models are the characteristic model as defined by Youngs and Coppersmith (1985) and the "maximum magnitude" characteristic model. In this analysis, we will call these two models the characteristic model and maximum magnitude model, respectively. Both of these characteristic magnitude models are used in the PSHA. These two characteristic models are assumed to apply to fault sources. The basis for this assumption is that studies have found that the characteristic model does a better job of matching observed seismicity than the truncated exponential (Geomatrix, 1992) when the total moment rate is constrained by the geologic slip-rate.

5.7 Area-Magnitude scaling Relations for Earthquakes

The Wells and Coppersmith (1994) area-magnitude scaling relationship for all fault types is assumed to be applicable to the seismic sources used in the PSHA. The basis for this assumption is that it is a well-documented and widely used model.

Two empirical relationships developed for subduction zone earthquakes were used to estimate the characteristic magnitude for the Cascadia interface source zone. The Abe (1981, 1984) and Geomatrix (1993) relationships are assumed to be applicable for the Cascadia interface seismic source. The basis for this assumption is that they are well-documented models and were produced based on subduction zone earthquake parameters.

5.8 Width-Magnitude scaling Relations for Earthquakes

The Wells and Coppersmith (1994) width-magnitude scaling relationship for all fault types is assumed to be applicable to the seismic sources used in the PSHA. The basis for this assumption is that the Wells and Coppersmith model is a well-documented and widely used model.

5.9 Directivity Effects on Ground Motion

The empirical attenuation relationships discussed above predict the horizontal ground motions for average directivity conditions. Recent studies (Somerville et al, 1997) have shown that rupture directivity can have a significant effect on horizontal spectra, especially at longer spectra periods (i.e., periods greater than 1.0 second). There are two parts to the directivity effects. First, directivity leads to a systematic difference in the long period ground motion on the two horizontal components: the horizontal component oriented perpendicular (fault normal) to the fault strike is systematically larger than the horizontal component oriented parallel to the fault strike. Second, directivity leads to an increase in the long period motion when the rupture is toward the site (forward directivity effect) and to a decrease in long period motion when the rupture is away from the site (backward directivity effect). Directivity effects are strongest when the slip direction is aligned with the rupture direction (Somerville et al., 1997). For reverse faults, the slip direction and rupture direction are aligned when the rupture direction is up-dip, rather than along strike, which is the case for strike-slip faults.

The basis for using the empirical directivity model in the PSHA is that it is a well-documented empirically based model and widely used model and the relatively short distance from the site location to the fault sources requires the incorporation of directivity effects in the PSHA.

5.10 Regional and seismic source specific b-values

The magnitude recurrence parameters for a given source can be estimated by fitting the Gutenberg-Richter relationship (1956) to a catalog of the observed historical seismicity. Typical b-values based on shallow earthquake catalogs from different regions of the world are between 0.8 and 1.0. The USGS/CDMG hazard maps for California Petersen et al., 1996) assigned a b-value of 0.9 for the PSHA. The revised PSHA maps for California (Cao et al., 2003) assigns a b-value of 0.85. For this PSHA study, a mean b-value of 0.85 was used for shallow crustal fault sources except the San Andreas fault. For the San Andreas fault, the b-value of 0.9 which was used in the 1996 California PSHA map was used.

The basis for assuming a b-value of 0.85 for shallow crustal fault sources (except the San Andreas fault) is that 0.85 represents an average value for California.

5.11 Earthquake Source Mechanism for Background Source Zone

The background source zone comprises a region around the project site location (called Zone D). The style of faulting mechanism assumed for the background source zone is reverse.

The basis for this assumption is that all of the mapped and modeled shallow crustal faults in this immediate region are dipping reverse/thrust faults.

5.12 Source model for Cascadia

It is assumed that the source Characterization of the Cacadia subduction zone given in PG&E (2002a, section 2) is applicable for the southern Cascadia region. The basis for this assumption is that this model is the most up-to-date model that has been focused on the southern Cascadia region.

5.13 Uncertainty in Recurrence Interval for Petrolia Segment

To account for epistemic uncertainty in the mean recurrence interval for the Petrolia Segment, uncertainty of a factor of 1/1.5 and 1.5 are assumed to represent the 5-95% confidence bands, respectively.

The basis for this assumption is that it slightly larger than the uncertainty in the recurrence interval for events on the Eel River Subplate (see Table 6-2). Since there is less information available about the Petrolia subplate, the uncertainty for the Petrolia subplate should be larger than for the Eel River subplate.

5.14 Recurrence Interval for Eel River Subplate

There are no independent evidence of the recurrence rates of earthquakes on the Eel River subplate segment of the Cascadia interface. Therefore, the recurrence interval of the Eel River segment is assumed to be the same as the rate used in characterizing the main Cascadia interface. The basis for this assumption is that the mean recurrence interval from past earthquake on the Eel River subplate (400 yr ± 90 yrs, Table 6-2) is not significantly different from the mean recurrence interval for the main Cascadia interface (440 yrs, Table 6-2).

5.15 Spectrum for Synchronous Rupture

For the case of synchronous rupture of two sources (e.g. Cascadia and Little Salmon fault zone), the response spectrum of the combined ground motion is assumed to be the square root of the sum of the squares (SRSS) of the spectra of the individual sources.

The basis for this assumption is that SRSS is the appropriate method for combining the response spectra from independent events (random vibration theory).

5.16 Characteristic Earthquake for Petrolia Subplate

The 1999 Petrolia earthquake is assumed to represent the characteristic earthquake for the Petrolia subplate. The basis for this assumption is that the 1992 Petrolia earthquake occurred on this segment and its rupture covered the seismogenic part of the Petrolia subplate (PG&E (2002A), page 2-9).

5.17 Rupture Lengths for the Mad River Faults

The characteristic earthquakes for the Mad River faults are assumed to rupture the full length or half of the rupture length. These two alternative models are assumed to be equally likely (e.g. equal weights).

The basis for this assumption is that the individual faults within the Mad River fault zone are discontinuous. Therefore, individual faults may not rupture the entire fault length. The discontinuous nature of the faulting favors the shorter rupture length (e.g. half of the total length of the fault zone), but the faults are closely spaced and the rupture could step over multiple segments, favoring the total rupture length model. Therefore, equal weight is reasonable.

5.18 Megacycle Model

Two alternative recurrence models for the main Cascadia interface (megacycle and independent,) are assumed to be equally applicable (e.g. given equal weight in the logic tree). The basis for this assumption is that the observations suggest that the megathrust earthquakes may have a long term periodic behavior (e.g. megacyle of about 1400 years) as discussed in PG&E (2002a), but the evidence is based only on 8 observations and could result from random chance. Therefore, both the independent and the megacycle model are reasonable models for the recurrence of megathrust earthquakes. The PG&E seismic consulting board also recommended using equal weights for these two alternative models.

5.19 Weights for Normally Distributed Parameters

The parameters that are assumed to be normally distributed, a three branch weighting is assumed:

Parameter Value	Weight
Mean – 1.64 sigma	0.2
Mean	0.6
Mean + 1.64 sigma	0.2

The basis for this assumption is that these values approximately recover the mean and variance of the distribution. The exact values would be 1.64 sigma with weights of 0.185, 0.53, 0.185, but this implies more accuracy than is warranted. These are rounded to weights of 0.2, 0.6, and 0.2. The use of this tree branch logic tree is standard practice.

5.20 Uncertainty in the b-value for the background Zone

The uncertainty in the b-value for the background Zone D is assumed to be the same as for the Gorda plate. The basis for this assumption is that Zone D has a similar mean b-value as Gorda (0.7 vs 0.59) and is cover the same region with the Gorda plate being located below zone D. With the similar mean b-values and similar spatial location, it is reasonable that the uncertainty in the b-value will be similar.

6.0 INPUTS

6.1. Cascadia Interface

The source parameters for the Cascadia interface were developed in calculation GEO.HBIP.02.03. The source parameters are listed in Tables 6-1 and 6-2.

Table 6-1. Cascadia interface seismic source parameters

<table>
<tr><th>Parameter Name</th><th colspan="2">Parameter Value</th><th>Reference</th></tr>
<tr><td>Closest Distance to HBIP</td><td colspan="2">7 km</td><td>PG&E (2002A), page 5-8</td></tr>
<tr><td rowspan="17">Characteristic Magnitude</td><td>Magnitude</td><td>Wt</td><td rowspan="17">GEO.HBIP.02.04, Table 7-5</td></tr>
<tr><td>8.69</td><td>0.045</td></tr>
<tr><td>8.82</td><td>0.045</td></tr>
<tr><td>8.59</td><td>0.105</td></tr>
<tr><td>8.69</td><td>0.105</td></tr>
<tr><td>8.62</td><td>0.030</td></tr>
<tr><td>8.80</td><td>0.030</td></tr>
<tr><td>8.50</td><td>0.070</td></tr>
<tr><td>8.69</td><td>0.070</td></tr>
<tr><td>8.91</td><td>0.045</td></tr>
<tr><td>9.07</td><td>0.045</td></tr>
<tr><td>8.79</td><td>0.105</td></tr>
<tr><td>8.91</td><td>0.105</td></tr>
<tr><td>8.84</td><td>0.030</td></tr>
<tr><td>9.05</td><td>0.030</td></tr>
<tr><td>8.68</td><td>0.070</td></tr>
<tr><td>8.91</td><td>0.070</td></tr>
<tr><td>Fault Mechanism</td><td colspan="2">Subduction Interface</td><td>GEO.HBIP.02.03
Table 8-1</td></tr>
<tr><td>Hypocentral Depth</td><td colspan="2">20</td><td>GEO.HBIP.02.04
Page 4</td></tr>
</table>

Table 6-2. Timing of past earthquakes on the Main Cascadia interface, and the Eel River Subplate. (from PG&E (2002a), Table 2-1)

Main Cascadia Interface (years before present)	Eel River Subplate (years before present)
	~170
Event Y, 300	
	~830
Event W, 1100	
Event U, 1300	~1290
Event S, 1600	~1530
	~1930
Event N, 2500	
Event L, 2900	
Event P, 3100	
Event O, 3900	

6.2 Cascadia – Petrolia Subplate

The Petrolia subplate source is defined by the rupture zone of the 1992 Petrolia earthquake. Therefore the rupture dimensions, and dip angle of the Petrolia earthquake are used to represent the Petrolia subplate.

Tanioka et al. (1995) estimate that it would require 48 years to accumulate the strain that was released during the 1992 Petrolia earthquake at their preferred strain rate of 5.6 cm per year. The mean recurrence interval was taken to be equal to this estimated 48 years.

The input source parameters for the Petrolia subplate are listed in Table 6-3.

Table 6-3. Cascadia – Petrolia Subplate fault seismic source parameters.

Parameter Name	Parameter Value	Reference
Longitude Latitude	-124.470 40.498 -124.470 40.325	Scaled from PG&E (2002a), figure 2-6
Center of rupture of 1992 Petrolia eqk (km)	14	Tanioka et al. (1995), Table 2 (based on depth of mainshock hypocenter)
Dip Angle	11.0	Tanioka et al. (1995), Table 2
Magnitude of 1992 Petrolia Eqk	7.1	Tanioka et al. (1995), page 1095
Seismogenic Fault Length	18	PG&E (2002a), pg 2-9
Horizontal Rupture Width	14	Scaled from PG&E (2002a), figure 2-6
Mean Recurrence Interval	48 yrs	Tanioka et al. (1995), page 1102
Fault Mechanism	Subduction Interface	PG&E (2002a), pg 2-18

6.3 Cascadia – Eel River Subplate

The input parameters for the Eel River source characterization are given in Table 6-4.

Table 6-4. Cascadia – Eel River Subplate fault seismic source input parameters used in the PSHA.

Parameter Name	Parameter Value	Reference
Longitude Latitude	-124.790 40.678 -124.395 40.505 -124.144 40.505	Scaled from PG&E (2002a), Figure 2-6
Fault Length	60 km	Scaled from PG&E (2002a), Figure 2-6
Width of vertical projection of rupture plane (e.g. Horizontal width)	15 km	Scaled from PG&E (2002a), Figure 2-6
Top of Fault (km)	0.0	PG&E (2002a), Figure 2-6 (fault mapped to surface)
Seismogenic Thickness (km)	15.0	GEO.HBIP.02.03, Section 4.3.3
Fault Mechanism	Subduction Interface	PG&E (2002a), page 2-18

6.4 Little Salmon Fault

The Little Salmon fault is considered to be part of the upper plate thrust system that is associated with the Cascadia subduction zone (PG&E (2002A), section 2.4). This thrust system is called the Little Salmon fault system. Offshore, the fault system bends northward, trending parallel to the deformation front of the Cascadia subduction zone (Jennings, 1994). The fault system continues north to the Thompson Ridge fault, which demarks a change from crustal shortening to rotational blocks.

The seismic source parameters for the Little Salmon fault system are given in Table 6-5

Table 6-5. Little Salmon fault system seismic source parameters.

Parameter Name	Parameter Value	Reference
Longitude Latitude	-123.766 40.459 -123.943 40.520 -124.007 40.540 -124.086 40.580 -124.169 40.637 -124.221 40.721 -124.360 40.821 -124.488 40.948 -124.639 41.011	Jennings (1994); PG&E (2002A), figure 2-6
Top of Fault (km)	0.0	Fault reaches the surface PG&E (2002a), figure 2-6
Dip Angle	40.0 (0.20) 45.0 (0.60) 50.0 (0.20)	GEO.HBIP.02.03, Section 4.3.2,
Sseismogenic Thickness (km)	15.0	GEO.HBIP.02.03, section 4.3.3,
Characteristic Magnitude	7.85 (0.1) 7.81 (0.3) 7.78 (0.10) 7.62 (0.25) 7.72 (0.25)	GEO.HBIP.02.03, Table 7-6
Fault Mechanism	Reverse	GEO.HBIP.02.03, Section 4.3.5

6.5 Gorda Plate

The seismic source parameters for the Gorda Plate seismic source are listed in Tables 6-6.

Table 6-6 Gorda Plate seismic source input parameters.

Parameter Name	Parameter Value	Reference
Longitude Latitude	-127.00 40.69 -127.00 42.00 -126.00 42.00 -123.00 41.00 -123.00 40.31 -127.00 40.69	Geomatrix (1995), Figure 2-27;
Top of Slab Longitude, depth	125.0 7.8 124.5 12.2 124.0 20.0 123.5 31.1	Geomatrix (1994), Scaled from Figure 2-8
Seismogenic Thickness (km)	10.0	Geomatrix (1995), page 2-39
Maximum Magnitude	7.00 (0.33) 7.25 (0.34) 7.50 (0.33)	Geomatrix (1995), page 2-40
b-value	0.59 ± 0.06	Geomatrix (1995), Table 2-4
Activity Rate N(M>4)	1.792 ± 0.23	Geomatrix (1995), Table 2-4
Fault Mechanism	Subduction Intraslab	Geomatrix (1995), page 3-15

6.6 Background Seismicity Zone D

Geomatrix (1994) developed a characterization for the background earthquakes in the North American plate in the HBIP region. The Geomatrix (1994) study separated the observed seismicity in the region into events which fell within the upper North American Plate and events that fell within the deeper subducting Gorda plate. The background zone for the North American plate is called Zone D.

Figure 2-11 in the Geomatrix (1994) report shows that the seismicity rate in western part of Zone D is much lower than the seismicity rate for the rest of the zone. To reflect this lower rate of activity, the western edge of Zone D was modified to remove the part of the zone west of longitude −123.58.

Source parameters for Zone D are listed in Table 6-7. The recurrence rates are listed in Table 6-8.

Table 6-7. Background Zone D seismic source input parameters.

Parameter Name	Parameter Value	Reference
Longitude Latitude	-124.500 40.320 -124.596 41.000 -124.374 41.106 -123.586 40.409 -123.505 40.152 -124.500 40.320	Geomatrix (1994) Values scaled from Figure 2-11.
Top of Fault (km)	0	Assumption 5-16
Seismigenic Thickness (km)	15.0	GEO.HBIP.02.03, section 4.3.3,
Maximum Magnitude	Same as for Mad River Fault System	Geomatrix (1994), page 2-34
Fault Mechanism	Reverse	Assumption 5.11

Table 6-8. Magnitude recurrence rates for Zone D. Values are scaled from Geomatrix (1994), Figure 2-12.

Magnitude	Cumulative Annual Frequency (Number of Eqk/yr)
3.0	3.2
3.5	1.2
4.0	0.50
4.5	0.38
5.0	0.16
5.7	0.07
6.3	0.022

6.7 Mad River Fault Zone

The Mad River fault zone is a zone up to 10 km wide consisting of at least five major, northwest-trending, northeast-dipping imbricate thrust faults (Jennings, 1994). Recent studies have identified a fault, called the Greenwood Heights fault, that intersects the northernmost tip of Humboldt Bay. Geomatrix (1994) interprets this fault to mark the southern boundary of the Mad River fault zone. They defined the northwestern extent of the zone based on seismic reflection data (Clarke, 1992), and the southeastern limit of the zone by the approximate location of a cluster of seismicity about latitude 40.5° N that appears to crosscut the Mad River trend. Based on these boundary limits, the Mad River fault zone extends for a total distance of about 80 km.

Because of the greater distance to the site relative to the Little Salmon fault zone and the Cascadia subduction zone sources, the geometry of the Mad River fault zone was simplified and is modeled as two parallel faults that cover the fault zone. The detailed locations of the individual faults that define the Mad River fault zone were not characterized for the PSHA.

Table 6-9. Mad River Fault Zone seismic source input parameters.

Parameter Name	Parameter Value	Reference
Longitude Latitude	-124.404 41.340 -124.295 40.961 -124.009 40.717	Faults mapped to surface PG&E (2002a), figure 2-6 (western edge)
Total Length of Fault Zone	80 km	Scaled from PG&E (2002a), figure 2-6
Top of Fault (km)	0.0	Faults mapped to surface PG&E (2002A), figure 2-6
Dip Angle	40.0 (0.20) 45.0 (0.60) 50.0 (0.20)	Dip angles same as for the Little Salmon Fault (Geomatrix, 1994, page 2-34) Dip angles for Little salmon: GEO.HBIP.02.03, Section 4.3.2
Seismogenic Thickness (km)	15.0	GEO.HBIP.02.03, section 4.3.3,
b-value	0.85	Assumption 5.10
Slip Rate (mm/yr) (across full zone)	5.0 (0.2) 7.0 (0.6) 9.0 (0.2)	Geomatrix (1994), page 2-33
Fault Mechanism	Thrust	Geomatrix (1994), page 2-33

6.8 Mendocino Fault Zone

These parameters for the Mendocino source zone are listed in Table 6-10. Events associated with the Mendocino source zone was assigned to be strike-slip events based on the observed seismicity in the immediate area and the presence of the strike-slip Mendocino fault (Jennings, 1994).

Table 6-10. Mendocino seismic source input parameters.

Parameter Name	Parameter Value	Reference
Longitude Latitude	-123.000 40.140 -123.000 40.310 -127.000 40.690 -127.000 40.250 -123.000 40.140	Scaled from Geomatrix (1995), Figure 2-27;
Top of Fault (km)	0.0	Assumption 5.16
Seismogenic Thickness (km)	15.0	Petersen et al. (1996), Appendix A, page A-11
Maximum Magnitude	7.25 (0.33) 7.50 (0.34) 7.75 (0.33)	Geomatrix (1995), page 2-41
b-value	0.816 ± 0.069	Geomatrix (1995), Table 2-4
Activity Rate N>M=4	2.504 ± 0.280	Geomatrix (1995), Table 2-4
Fault Mechanism	Strike-slip	Petersen et al. (1996), Appendix A, page A-11 (rake=180)

6.9 Northern San Andreas Fault

The San Andreas fault is a major strike-slip fault which runs the entire length of California starting in the north at the Mendocino triple junction and continuing south to the Salton Sea region of southern California. The input source parameters that are given in Table 6-11 below were taken from the CDMG/USGS (Petersen et al., 1996) modeling of the North Coast segment of the Northern San Andreas fault.

Table 6-11. San Andreas fault seismic source input parameters used in the PSHA.

Parameter Name	Parameter Value	Reference
Longitude Latitude	-124.0747 40.0446 -124.0009 39.8063 -123.9790 39.6034 -123.9251 39.4076 -123.8404 39.2072 -123.7009 39.0024 -123.5161 38.8024 -123.3154 38.6006 -123.1354 38.4175 -122.9455 38.2080 -122.7594 38.0005 -122.5884 37.7973 -122.4296 37.6048 -122.2467 37.4044 -122.0238 37.1988 -121.7408 37.0010 -121.4792 36.8068	Jennings (1994)
Top of Fault (km)	0.0	CDMG/USGS (1996), Appendix A, page A-1
Dip Angle	90.0	CDMG/USGS (1996), Appendix A, page A-1
Fault Thickness (km)	12.0	CDMG/USGS (1996), Appendix A, page A-1
b-value	0.85	Assumption 5.10
Slip Rate (mm/yr)	24.0	CDMG/USGS (1996), Appendix A, page A-1
Fault Mechanism	Strike-slip	CDMG/USGS (1996), Appendix A, page A-1
Mean Characteristic magnitude	7.6	CDMG/USGS (1996), Appendix A, page A-1

6.10 Deaggregation Bin Values

The magnitude and distance deaggregation bins from DG3021 Table C-1are listed in Table 6-12.

Table 6-12. Deaggregation bins.

Bin Number	Magnitude Range	Distance Range
1	5.0 – 5.5	0 – 15
2	5.5 – 6.0	15 – 25
3	6.0 – 6.5	25 - 50
4	6.5 – 7.0	50 – 75
5	> 7.0	75 – 100
6		100 – 200
7		200 – 300
8		> 300

6.11 Return Periods for Equal Hazard Spectra

AR A0583100 specifies 8 return periods listed in Table 6-14. Return periods of 25 years and 50 years were added by the project .

Table 6-13. Return periods used to compute the equal hazard spectra.

Return Period	
1 month	AR A0583100
1 yr	AR A0583100
25 yrs	Additional
50 yrs	Additional
100 yrs	AR A0583100
500 yrs	AR A0583100
1,000 yrs	AR A0583100
2,000 yrs	AR A0583100
5,000 yrs	AR A0583100
10,000 yrs	AR A0583100

6.12 Minimum Magnitude for PSHA

The minimum magnitude for the PSHA calculation is 5.0 (DG3021, page 20).

6.13 Northridge High Frequency Spectral Shapes

The acceleration response spectral shape (i.e., SA/PGA) from 5 strong ground motion sites on soil site conditions which recorded large horizontal PGA motions (i.e., average horizontal ground motions of 0.6 g and larger) from the Northridge earthquake are given in GEO.HBIP.03.02 (Table 10-5). These values are listed in Table 6-14 below.

Table 6-14. Average horizontal rock spectral shape based on 12 Northridge strong motion recordings. (from GEO.HBIP.03.02 Table 10-5)

Period (sec)	Average Spectral Shape (Sa/pga)
0.010	1.000
0.020	1.000
0.030	1.016
0.050	1.095
0.075	1.225
0.100	1.384
0.150	1.690
0.200	1.911
0.300	2.368
0.500	1.980
0.750	2.049
1.000	1.682
1.500	1.036
2.000	0.765
3.000	0.451
4.000	0.208

6.15 HBIP Latitude and Longitude Location

The plant site location used in the PSHA was scaled from Jennings et al. (1994)

Latitude	40.742
Longitude	-124.214

6.16 Spectral Periods for Capturing Site Response

Calculation GEO.HBIP.03.02 specified the spectral periods given in Table 6-15 as being adequate to capture the resonances in the site response

Table 6-15. Periods to adequately model site responance

Period (sec) from Calc GEO.HBIP.03.02
0.01
0.03
0.05
0.07
0.10
0.12
0.15
0.17
0.20
0.25
0.30
0.35
0.40
0.50
0.60
0.70
0.80
0.90
1.00
1.20
1.50
1.70
2.00
2.50
3.00
3.50
4.00
5.00
7.00
10.00

7.0 METHOD AND EQUATION SUMMARY

7.1 Regulatory Requirements for PSHA

The two regulatory documents (Draft RG3021 and RG1.165) give requirements for conducting a PSHA, but these requirements are focused on rock sites in the eastern U.S. The main difference in the PSHA requirements between Draft 3021 and RG1.165 is the reference probability. RG1.165 is written for nuclear power plants and uses a median hazard with an annual probability of being exceeded of 10^{-5} (e.g. return period of 100,000 years). Draft Guide 3021 is for an ISFSI and it uses a mean hazard with an annual probability of being exceeded of $5x10^{-4}$ (e.g. return period of 2,000 years). The descriptions of the acceptable methods for computing a PSHA is consistent between these two guides.

7.1.1 Source Characterization

Appendix D of DG 3021 says that acceptable methods for the source characterization (geometry, max mag, recurrence) are given in NUREG/CR-6372. This NUREG is known as the "SSHAC" report. The SSHAC report does not provide clear direction for a hazard analysis. Much of the report is focused on the use of expert opinion. In terms of hazard, the main recommendation in the report is to keep track of epistemic uncertainty and aleatory variability. Aleatory variability is the natural randomness that occurs in the earthquake sizes, locations, and the resulting ground motion. Epistemic uncertainty is the scientific uncertainty that the model of the earthquake source, ground motion attenuation, and site response are correct. Aleatory variability leads to the shape of the hazard curve, whereas, epistemic uncertainty leads to alternative hazard curves (due to limited scientific knowledge, there is uncertainty as to which model of the earthquake behavior is correct).

This calculation follows the SSHAC concepts of aleatory variability and epistemic uncertainty. The epistemic uncertainty is implemented using "logic trees". The epistemic uncertainty can be characterized through fractiles of the hazard curves.

7.1.2 Rock Hazard

The hazard analysis for the rock motion follows the general approach given in DG 3021 and RG1.165. The main difference is that RG1.165 allows the hazard be computed at just two spectral frequencies (1 and 10 Hz), and the equal hazard spectrum is determined using the envelope of two separate spectra based on normalized spectral shapes scaled to the 1 Hz and 10 Hz spectral accelerations.

The use of 1 Hz and 10 Hz are for rock ground motions is applicable to the eastern U.S. because the hazard is typically controlled at high frequencies (e.g. 10 Hz) by a small magnitude local earthquake, whereas, at low frequencies (e.g. 1 Hz) the hazard is typically controlled by a large magnitude distant earthquake (e.g. Charleston or New Madrid). In the eastern US, the rock spectra typically peak at 10 Hz, so this is a good representation of the high frequency content.

This approach of just computing the hazard at just 1 Hz and 10 Hz is not applicable to the horizontal motions at HBIP for several reasons. First, the source characterization at

HBIP includes synchronous rupture of the Little Salmon fault and the Cascadia interface. There are no existing standard spectral shapes available for synchronous rupture. Second, directivity effects may be significant for the HBIP site since it is located along the Little Salmon fault (directly up-dip). Directivity effects are strongly frequency dependent and 1 Hz is not representative of the low frequency directivity effects (0.3 Hz would be much better). Third, 10 Hz is not a good representative frequency for the high frequency ground motion because spectra on typically rock sites in California peak at 5 Hz rather than 10 Hz. This difference can be attributed to the higher rates of attenuation of the crust in California as compared to the eastern U.S.

Therefore, rather than using computing the horizontal rock hazard at just 1 and 10 Hz, spectral the hazard is computed at multiple frequencies that cover the relevant frequency band. The equal hazard spectra are then determined directly from the suite of hazard curves. This is standard practice in modern PSHA.

7.1.3 Soil Hazard

DG-3021 Appendix F gives a vague discussion of incorporation of site-specific site response effects. Appendix F states "It is anticipated that a regulatory guide will be developed that provides guidance on assessing site-specific effects", and then it refers to NUREG/CR-6728. NUREG/CR-6728 presents several alternative methods that can be used for incorporating site response effects into probabilistic analyses (summarized in Table 6-1 of NUREG/CR-6728).

This calculation follows NUREG/CR-6728 approach 3A for incorporating site response effects into PSHA. In this approach, the site amplification factors are modeled as being dependent on the earthquake magnitude and the rock spectral acceleration. The soil amplification factors are then incorporated directly into the hazard integral (equation 6-7 of NUREG/CR-6728).

DG 3021, Appendix C, says to compute the hazard at spectral frequencies of 1 Hz and 10 Hz and then apply spectral shapes (see discussion in section 7.1.1.2). In Approach 3A, the hazard is run for multiple spectral frequencies rather than using just 2 spectral frequencies and spectral shapes.

7.1.4 Vertical Component

The estimation of the vertical spectrum on soil is not discussed in DG3021 or RG1.165. NUREG/CR-6728 gives a method for computing the vertical component for rock sites (section 4-7). In the NUREG/CR-6728 method, the V/H ratio is computed for the controlling earthquake and this ratio is scaled by the horizontal UHS, but no specific recommendations are given for soil sites

For the vertical component, the 1Hz and 10Hz method described in DG3021 is applicable because the vertical rock motion tends to peak at near 10 Hz, directivity effects are much weaker on the vertical component, and the soil site response in the vertical direction is much more linear than for the horizontal component. Rather than computing the rock hazard directly, the vertical ground motion at 1 and 10 Hz is computed by scaling the horizontal hazard curve by the V/H ratio computed for the magnitude and distance determined from the deaggregation.

The detailed steps for the approach and methodology to the development of the probabilistic seismic hazard curves and associated equal hazard response spectra is presented in the following section.

7.2 Method

7.2.1 Compute Required Source Parameters

The source parameters given in Section 6 do not include all of the parameters required for the PSHA input. In this step, the additional required parameters are computed.

7.2.2 Develop Seismic Source Parameter file for PSHA

Develop the seismic source parameters in a file format compatible with the HAZ36h program. This is called the fault file.

7.2.3 Develop Input Parameter file for PSHA

The next step is to develop the necessary run input file for the program. In this file, the site location, requested attenuation models and other various input parameters are assigned.

7.2.4 Execution of HAZ36h PSHA Computer Program

Given the input seismic source parameter file and the input run parameter file, the computer program HAZ36h will compute the probabilistic seismic hazard. The computer program generates five separate output ASCII files (see calculation GEO.HBIP.03.03 for a complete description of the output files).

The hazard is run for four cases: rock fault parallel, rock fault normal, soil fault parallel, and soil fault normal.

7.2.5 Compute Mean Hazard Curves

Total hazard curves are written out in the third output file for each spectral period and attenuation model. In this step, the mean hazard is computed for each spectral period. The weights given to each alternative attenuation relations are used to compute the weighted average.

7.2.6 Compute Equal Hazard Spectra

Using the mean hazard curves from the previous step, the equal hazard spectra are computed by interpolating the hazard curves to the annual relate of events corresponding to the specified return periods. The interpolation is done using linear interpolation of the log values (e.g. log-log interpolation).

7.2.7 Apply Spectral Shape Constraints

The spectral shapes from the equal hazard spectra are computed and compared to the empirical shape from high ground motion values: (Table 6-14). Since the empirical shape was developed using Northridge earthquake recordings, the long period part of the shape is not applicable to smaller magnitude earthquakes.

The main purpose of the spectral shape constraint is to compensate for potential overdamping of the high frequencies at high ground motion values. Therefore, the spectral shape constant is only applied for periods less than or equal to 0.2 sec.

7.2.8 Deaggregate Hazard

Based on the estimated ground motion values for a given probability of exceedance (i.e., return period) and spectral period, the weighted deaggregation values will be computed based on the output deaggregation file from the hazard program. The deaggregation values will be interpolated to the ground motion value that corresponds to the specified return periods.

The deaggregation is computed for peak acceleration, T=0.2 sec, T=1.0 sec, and T=3 sec. These values are consistent with the intent of the deaggregation frequencies specified in DG3021 (e.g. 10 Hz and 1 Hz) in that they capture the long period content and include a period near the peak in the spectrum for California sites.

7.2.9 Compute Vertical Component Equal Hazard Spectra

For each return period (of the UHS), compute the horizontal spectral acceleration for a rock site using the mean magnitude and mean distance from the deaggregation (horizontal comp) for spectral periods of 1 sec and 0.1 sec. Next, compute the vertical soil spectrum for the same events (one for T=1 sec and one for T=0.1 sec). For each case, scale the average horizontal rock UHS by the vertical soil spectrum and divide by horizontal rock spectral acceleration computed for the specific spectral period. Finally, take the maximum of the two spectra to define the UHS for the vertical component for soil.

The rock horizontal is used rather than the soil horizontal because the V/H ratios from the attenuation relations are not applicable to the highly non-linear conditions for HBIP.

This approach is equivalent to multiplying the horizontal UHS by the V(soil)/H(rock) ratio for the specific period (e.g. T=0.1 sec) and then scaling the corresponding spectral shape to match to vertical at the specified period.

For example, for the T=0.1 case, the vertical component is computed using:

$$Sa_{Vsoil}(T) = UHS_{Hrock}(T)\frac{Sa_{Vsoil}(T=0.1, M_{0.1}, D_{0.1})}{Sa_{Hrock}(T=0.1, M_{0.1}, D_{0.1})}\frac{Sa_{Vsoil}(T, M_{0.1}, D_{0.1})}{Sa_{Vsoil}(T=0.1, M_{0.1}, D_{0.1})}$$

which can be simplified to be:

$$Sa_{Vsoil}(T) = UHS_{Hrock}(T)\frac{Sa_{Vsoil}(T, M_{0.1}, D_{0.1})}{Sa_{Hrock}(T=0.1, M_{0.1}, D_{0.1})}$$

7.3 Equations

7.3.1 Equation for log-log interpolation of hazard curves

The interpolation of the hazard curve values is done using linear interpolation on the log annual probability (AP) of exceedance – log ground motion values. Given the annual probability of exceedance values AP_1 and AP_2 at ground motion values SA_1 and SA_2, respectively, then using linear interpolation on the log-log values, the ground motion SA at annual probability AP is given by

$$\ln(SA) = \ln(SA_1) + \left(\ln(AP) - \ln(AP_1)\right) \frac{[\ln(SA_2) - \ln(SA_1)]}{[\ln(AP_2) - \ln(AP_1)]} \qquad (7\text{-}1)$$

7.3.2 Area-Magnitude Scaling Relationships

The Wells and Coppersmith (1994; Table 2A, p. 990) scaling relationship for rupture area as a function of magnitude (using all fault types) is given by

$$Log(A) = -3.49 + 0.91*M \qquad (7\text{-}2)$$

where A is the rupture area in km^2 and M is moment magnitude. The associated uncertainty with this equation is 0.24 as given Wells and Coppersmith (1994; Table 2A, p. 990).

7.3.3 Width-Magnitude Scaling Relationships

The Wells and Coppersmith (1994; Table 2A, p. 990) scaling relationship for rupture width as a function of magnitude (using all fault types) is given by

$$Log(RW) = -1.01 + 0.32*M \qquad (7\text{-}3)$$

where RW is the rupture width in km and M is moment magnitude. The associated uncertainty with this equation is 0.24 as given Wells and Coppersmith (1994; Table 2A, p. 990).

7.3.4 Magnitude-Area Scaling Relationships

The Wells and Coppersmith (1994; Table 2A, p. 990) scaling relationship for magnitude as a function of rupture area (using all fault types) is given by

$$M = 0.98\ Log(RA) + 4.07 \qquad (7\text{-}4)$$

where RA is the rupture area in km^2 and M is moment magnitude. This is the same model used in calculation GEO.HIP.02.03 (see equation 5-1).

The Abe (1981;1984) relation for magnitude as a function of rupture area for subduction zones is given by (Geomatrix, 1995, pg. 2-29)

$$M = Log(RA) + 3.99 \tag{7-5}$$

The Geomatrix (1993) relation for magnitude as a function of rupture area for subduction zones is given by (Geomatrix, 1995, pg 2-29)

$$M = 0.81\ Log(RA) + 4.7 \tag{7-6}$$

7.3.5 Abrahamson and Silva (1997) Attenuation Equation

The Abrahamson and Silva (1997) median spectral acceleration attenuation relation is given by (Abrahamson and Silva, 1997, eq. 3, page 105):

$$\ln(Sa(g)) = f_1(M,R_{rup}) + Ff_3(M,R_{rup}) + HWf_4(M,R_{rup}) + Sf_5(PGA_{rock}) \tag{7-7}$$

where M is the moment magnitude, R_{rup} is the rupture distance, F is the style of faulting factor (F=1 for reverse, F=0.5 for reverse/oblique, and F=0 otherwise), S is a site factor (S=0 for rock, S=1 for soil), and HW is a hangingwall factor (HW=1 for sites on the hanging wall and HW=0 otherwise).

For $M > c_1$ the $f_1(M,R)$ equation is given by (Abrahamson and Silva, 1997, eq. 4, page 105):

$$f_1(M,R) = a_1 + a_4(M - c_1) + a_{12}(8.5 - M)^n + [a_3 + a_{13}(M - c_1)]\ln R \tag{7-8}$$

and

$$f_1(M,R) = a_1 + a_2(M - c_1) + a_{12}(8.5 - M)^n + [a_3 + a_{13}(M - c_1)]\ln R \tag{7-9}$$

for $M <= c_1$, where $c_1 = 6.4$ (Abrahamson and Silva, 1997, table 3, page 108). The distance R is given by (Abrahamson and Silva, 1997, eq. 5, page 105):

$$R = \sqrt{R_{rup}^2 + c_4^2} \tag{7-10}$$

The non-linear soil response (Abrahamson and Silva, 1997, eq. 10, page 106) is modeled by:

$$f_5(PGA_{rock}) = a_{10} + a_{11}\ln(PGA_{rock} + c_5) \tag{7-11}$$

Substituting eq. 7-8, and 7-10 into eq. 7-7, the median spectral acceleration for M>6.4 on rock (S=0) for strike-slip earthquakes is

$$\ln(Sa(g)) = a_1 + a_4(M - c_1) + a_{12}(8.5 - M)^n + [a_3 + a_{13}(M - c_1)]\ln(\sqrt{R_{rup}^2 + c_4^2}) \quad (7\text{-}12)$$

and for M<= 6.4:

$$\ln(Sa(g)) = a_1 + a_2(M - c_1) + a_{12}(8.5 - M)^n + [a_3 + a_{13}(M - c_1)]\ln(\sqrt{R_{rup}^2 + c_4^2}) \quad (7\text{-}13)$$

Substituting eq. 7-8, 7-10, and 7-11 into eq. 7-7, the median spectral acceleration for M>6.4 on soil (S=1) for strike-slip earthquakes for M>6.4 is

$$\ln(Sa(g)) = a_1 + a_4(M - c_1) + a_{12}(8.5 - M)^n + [a_3 + a_{13}(M - c_1)]\ln(\sqrt{R_{rup}^2 + c_4^2}) + a_{10} + a_{11}\ln(PGA_{rock} + c_5) \quad (7\text{-}14)$$

and for M≤6.4 is:

$$\ln(Sa(g)) = a_1 + a_2(M - c_1) + a_{12}(8.5 - M)^n + [a_3 + a_{13}(M - c_1)]\ln(\sqrt{R_{rup}^2 + c_4^2}) + a_{10} + a_{11}\ln(PGA_{rock} + c_5) \quad (7\text{-}15)$$

The coefficients for eq. 7-12 to 7-15 are listed in Tables 7-1 and 7-2 for the horizontal and vertical components, respectively.

The standard deviations, for M ≥7.0 are given by (Abrahamson and Silva, 1997, eq. 13, page 106).

$$\sigma = b_5 - 2b_6 \quad (7\text{-}16)$$

The coefficients for the standard deviation for the horizontal and vertical components are also listed in Tables 7-1 and 7-2.

Table 7-1. Coefficients for the Abrahamson and Silva (1997) attenuation relation for horizontal spectral acceleration (from Abrahamson and Silva, Table 3 and 4, pages 108 and 109)

Period (s)	C_4	a_1	a_2	a_3	a_4	a_{10}	a_{11}	a_{12}	a_{13}	n	c_5	b_5	b_6
0.0	5.60	1.640	0.512	-1.1450	-0.144	-0.417	-0.230	0.000	0.17	2	0.03	0.70	0.135
0.03	5.60	1.690	0.512	-1.1450	-0.144	-0.470	-0.230	0.014	0.17	2	0.03	0.70	0.135
0.05	5.60	1.870	0.512	-1.1450	-0.144	-0.620	-0.267	0.0280	0.17	2	0.03	0.71	0.135
0.075	5.58	2.037	0.512	-1.1450	-0.144	-0.628	-0.280	0.0300	0.17	2	0.03	0.73	0.135
0.10	5.50	2.160	0.512	-1.1450	-0.144	-0.598	-0.280	0.0280	0.17	2	0.03	0.74	0.135
0.15	5.27	2.407	0.512	-1.1450	-0.144	-0.577	-0.280	0.0050	0.17	2	0.03	0.75	0.135
0.20	5.10	2.406	0.512	-1.1150	-0.144	-0.445	-0.245	-0.0138	0.17	2	0.03	0.77	0.135
0.30	4.80	2.114	0.512	-1.0350	-0.144	-0.219	-0.195	-0.0360	0.17	2	0.03	0.78	0.135
0.40	4.52	1.860	0.512	-0.9880	-0.144	-0.065	-0.160	-0.0518	0.17	2	0.03	0.79	0.135
0.50	4.30	1.615	0.512	-0.9515	-0.144	0.085	-0.121	-0.0635	0.17	2	0.03	0.80	0.130
0.75	3.90	1.160	0.512	-0.8852	-0.144	0.320	-0.059	-0.0862	0.17	2	0.03	0.81	0.123
1.00	3.70	0.828	0.512	-0.8383	-0.144	0.423	0.000	-0.1020	0.17	2	0.03	0.83	0.118
1.50	3.55	0.260	0.512	-0.7721	-0.144	0.600	0.040	-0.1200	0.17	2	0.03	0.84	0.110
2.00	3.50	-0.150	0.512	-0.7250	-0.144	0.610	0.040	-0.1400	0.17	2	0.03	0.85	0.105
3.00	3.50	-0.690	0.512	-0.7250	-0.144	0.630	0.040	-0.1726	0.17	2	0.03	0.87	0.097
4.00	3.50	-1.130	0.512	-0.7250	-0.144	0.640	0.040	-0.1956	0.17	2	0.03	0.88	0.092
5.00	3.50	-1.460	0.512	-0.7250	-0.144	0.664	0.040	-0.2150	0.17	2	0.03	0.89	0.087

Table 7-2. Coefficients for the Abrahamson and Silva (1997) attenuation relation for vertical spectral acceleration for M > 6.4 (from Abrahamson and Silva, page 116)

Period (sec)	C_4	a_1	a_2	a_3	a_4	a_{10}	a_{11}	a_{12}	a_{13}	n	c_5	b_5	b_6
0.0	6.00	1.642	0.909	-1.2520	0.275	-0.140	-0.22	0.0000	0.06	3	0.3	0.76	0.085
0.03	6.00	2.100	0.909	-1.3168	0.275	-0.140	-0.22	0.0000	0.06	3	0.3	0.76	0.085
0.05	6.00	2.620	0.909	-1.3700	0.275	-0.140	-0.22	-0.0002	0.06	3	0.3	0.76	0.085
0.075	6.00	2.750	0.909	-1.3700	0.275	-0.129	-0.22	-0.0007	0.06	3	0.3	0.76	0.085
0.10	6.00	2.700	0.909	-1.3700	0.275	-0.114	-0.22	-0.0010	0.06	3	0.3	0.76	0.085
0.12	6.00	2.480	0.909	-1.2986	0.275	-0.104	-0.22	-0.0015	0.06	3	0.3	0.74	0.075
0.15	6.00	2.170	0.909	-1.2113	0.275	-0.093	-0.22	-0.0022	0.06	3	0.3	0.72	0.063
0.17	5.72	1.960	0.909	-1.1623	0.275	-0.087	-0.220	-0.0025	0.06	3	0.3	0.70	0.056
0.20	5.35	1.648	0.909	-1.0987	0.275	-0.078	-0.22	-0.0030	0.06	3	0.3	0.69	0.050
0.24	4.93	1.312	0.909	-1.0274	0.275	-0.069	-0.22	-0.0035	0.06	3	0.3	0.69	0.050
0.30	4.42	0.878	0.909	-0.9400	0.275	-0.057	-0.22	-0.0042	0.06	3	0.3	0.69	0.050
0.40	3.77	0.478	0.909	-0.8776	0.275	-0.043	-0.22	-0.0050	0.06	3	0.3	0.69	0.050
0.50	3.26	0.145	0.909	-0.8291	0.275	-0.031	-0.22	-0.0060	0.06	3	0.3	0.69	0.050
0.75	2.50	-0.344	0.909	-0.7488	0.275	-0.010	-0.22	-0.0083	0.06	3	0.3	0.69	0.050
1.00	2.50	-0.602	0.909	-0.7404	0.275	0.004	-0.22	-0.0115	0.06	3	0.3	0.69	0.050
1.50	2.50	-0.966	0.909	-0.7285	0.275	0.025	-0.22	-0.0180	0.06	3	0.3	0.69	0.050
2.00	2.50	-1.224	0.909	-0.7200	0.275	0.040	-0.22	-0.0240	0.06	3	0.3	0.69	0.050
3.00	2.50	-1.581	0.909	-0.7200	0.275	0.040	-0.22	-0.0431	0.06	3	0.3	0.72	0.050
4.00	2.50	-1.857	0.909	-0.7200	0.275	0.040	-0.22	-0.0565	0.06	3	0.3	0.75	0.050
5.00	2.50	-2.053	0.909	-0.7200	0.275	0.040	-0.22	-0.0670	0.06	3	0.3	0.78	0.050

7.3.6 Estimation of b-values

The maximum likelihood estimate for a b-value is given by Utsu (1970), page 387, equation 158:

$$b = \frac{s \ \log e}{\sum M_i - sM_s} \qquad (7\text{-}17)$$

where Ms is the minimum magnitude, s is the number of earthquakes. Dividing by the numerator and denominator by "s", this can be rewritten as

$$b = \frac{1}{\ln(10)} \frac{1}{M_{mean} - M_{\min}} \qquad (7\text{-}18)$$

8.0 SOFTWARE

The validated computer program HAZ36h was used to perform the probabilistic seismic hazard analysis calculations. This use of this program has been validated in calculation GEO.HBIP.03.03, rev 0.

In the validation calculation, GEO.HBIP.03.03, the program is referred to generically as "HAZ36". Following preliminary calculations of the hazard, the program was modified to allow for a larger problem to be run. The final version, HAZv36H, which was used in this calculation was the version that was verified in GEO.HBIP.03.03. This can be confirmed by comparing the executable files in the "PROGRAM" directory of the CD ROM attached to GEO.HBIP.03.02 (rev 0) and GEO.HBIP.03.04 (rev 0).

9.0 BODY OF CALCULATION

9.1 Develop Seismic Source Parameter file for PSHA

9.1.1 Cascadia Main Interface

9.1.1.1 Recurrence Interval

Table 6-2 lists the years BP of previous earthquakes on the Cascadia interface. The inter-event intervals computed using these earthquake dates are listed in Table 9.1-1. Using these values, the mean recurrence interval is 514 years (± 116 years); however, the events appear to occur in triplets, with each triplet defining one mega-cycle (see Table 9.1-1). The time interval for one megacycle is 1400 years, and within a cycle, the recurrence interval ranges from 200 to 400 years, with a mean of 280 years (± 42 years). For application, the mean recurrence interval for the independent model is rounded to 500 ± 100 years and the mean recurrence interval for the megacycle model is rounded to 300 years ± 40 years.

Two earthquake models are considered to characterize the recurrence intervals: one based on the timing of the individual events and one based on the megacycle model. In the megacycle model, we are currently within the cycle, so the shorter interval is appropriate for the application of this model to the current hazard. The two models are given equal weight (assumption 5-18)

Within each model, the uncertainty in the mean recurrence interval is considered. The alternative values were set at 1.64 standard deviations above and below the mean. When used with weights of 0.2, 0.6, and 0.2, these values will approximate the mean and variance of a normal distribution (assumption 5-19).

For the megacycle model, 1.64 standard deviation = 40 yrs * 1.64 = 66 years, which is rounded to 70 years. The three mean recurrence intervals are then 230 years, 300 years, and 370 years.

For the independent model, 1.6 standard deviation = 100 yrs * 1.64 = 164 years, which is rounded to 160 years. The three mean recurrence intervals are then 340 years, 500 years, and 660 years.

The resulting alternative estimates of the mean recurrence interval for the main Cascadia interface are given in Table 9.1-2.

9.1.1.2 Characteristic Magnitude

The alternative estimates of the mean characteristic magnitude of the Cascadia interface source are given below in Table 9.1-3 (from Table 6-1). These estimates are grouped together into 0.1 magnitude steps in the right hand column of Table 9.1-3. The sum of the weights for each magnitude range are then listed in Table 9.1-4.

9.1.1.3 Source Parameters of input in PSHA calculation

The source parameters for the Cascadia interface required for the PSHA calculation are listed in Table 9.1-5. The right hand column of this table gives the source of the input.

Table 9-1.1. Recurrence intervals for Cascadia events.

Main Cascadia Interface (years before present)	Inter-Event Time (years)	
	300+	Open interval, but use 300 in computing the mean
Event Y, 300		
	800	
Event W, 1100		Start MegaCycle
	200	
Event U, 1300		
	300	1400 yrs
Event S, 1600		
	900	
Event N, 2500		Start MegaCycle
	400	
Event L, 2900		
	200	1400 yrs
Event P, 3100		
	800	
Event O, 3900		Start MegaCycle

Table 9.1-2 Logic Tree for Recurrence Intervals for Main Cascadia

Recurrence Interval	Model	Model wt	Uncertainty Wt	Total Wt
230	Megacycle	0.5	0.2	0.1
300	Megacycle	0.5	0.6	0.3
370	Megacycle	0.5	0.2	0.1
340	Independent	0.5	0.2	0.1
500	Independent	0.5	0.6	0.3
660	Independent	0.5	0.2	0.1

Table 9.1-3. Weights for the mean characteristic magnitude for Cascadia (from section 6, Table 6-1)

Magnitude	Wt	Rounded Mag
8.69	0.045	8.7
8.82	0.045	8.8
8.59	0.105	8.6
8.69	0.105	8.7
8.62	0.030	8.6
8.80	0.030	8.8
8.50	0.070	8.5
8.69	0.070	8.7
8.91	0.045	8.9
9.07	0.045	9.1
8.79	0.105	8.8
8.91	0.105	8.9
8.84	0.030	8.8
9.05	0.030	9.1
8.68	0.070	8.7
8.91	0.070	8.9

Table 9.1-4. Logic tree for the mean characteristic magnitude for Cascadia

Magnitude	Weight
8.5	0.070
8.6	0.135
8.7	0.290
8.8	0.210
8.9	0.220
9.0	0.000
9.1	0.075

Table 9.1-5 Table of input parameters used for Cascadia main interface

<table>
<tr><th>Parameter Name</th><th colspan="2">Parameter Value</th><th>Source</th></tr>
<tr><td>Closest Distance to HBIP</td><td colspan="2">7 km</td><td>Table 6-1</td></tr>
<tr><td rowspan="8">Characteristic Magnitude</td><td>Mag</td><td>Wt</td><td rowspan="8">Table 9.1-4</td></tr>
<tr><td>8.5</td><td>0.070</td></tr>
<tr><td>8.6</td><td>0.135</td></tr>
<tr><td>8.7</td><td>0.290</td></tr>
<tr><td>8.8</td><td>0.210</td></tr>
<tr><td>8.9</td><td>0.220</td></tr>
<tr><td>9.0</td><td>0.000</td></tr>
<tr><td>9.1</td><td>0.075</td></tr>
<tr><td>Fault Mechanism</td><td colspan="2">Subduction Interface</td><td>Table 6-1</td></tr>
<tr><td>Hypocentral Depth</td><td colspan="2">20</td><td>Table 6-1</td></tr>
<tr><td>Rupture timing</td><td colspan="2">Synchronous with little salmon Fault</td><td>PG&E (2002a), page 2-11</td></tr>
</table>

9.1.2 Petrolia Subplate

9.1.2.1 Mean characteristic magnitude

The 1999 Petrolia earthquake is assumed to represent the characteristic earthquake for this subplate (assumption 5.16). Two approaches are used to estimate the mean characteristic earthquake for the Petrolia subplate: (1) use the magnitude of 1992 Petrolia earthquake directly, and (2) use the rupture length of the Petrolia subplate along with a magnitude-area relation. Both estimates of characteristic magnitudes were used in the PSHA with equal weighting.

In the first approach, the magnitude of the 1992 Petrolia earthquake is 7.1 (Table 6-3).

In the second approach, the rupture dimensions of the 1992 Petrolia subplate are taken from Table 6-3:

Seimogenic fault length = 18 km
Horizontal rupture width = 14 km
Dip = 11

The down dip width is given by

Down-dip Width = horizontal width / cos(dip) = 14km / cos (11) = 14.3 km

The difference between 14 km and 14.3 km is less than the accuracy of the estimate of the km 14 width, so it is rounded to 14 km.

The mean characteristic earthquake magnitude is estimated from the two empirical magnitude rupture area relationships (equations 7-5 and 7-6).

$$M = \log(RA) + 3.99 = \log(18*14) + 3.99 = 6.39$$

$$M = 0.81 \log(RA) + 4.7 = 0.81 \text{ Log}(18*14) + 4.7 = 6.65$$

The average of the magnitudes from these two models is 6.5.

9.1.2.2 Mean Recurrence Interval

The best estimate of the mean recurrence interval is 48 years (Table 6-3). The 5-95% uncertainty range is assumed to be covered by a factor of 1.5 (assumption 5.13). Using this ratio, the alternative estimates of the mean recurrence interval are:

48 yr * 1.5 = 72 yr
48 yr * 1.0 = 48 yr
48 yr / 1.5 = 32 yr

9.1.2.3 Top of Rupture

The top of the rupture is computed by subtracting one-half of the vertical rupture width from the center of the rupture.

From table 6-3, the center of the rupture is at a depth of 14 km.

The vertical rupture width is given by

Vertical Rupture Width = rupture Width * sin(dip) = 14 * sin(11) = 2.7 km

The top of the rupture is then:

Top of Rup = Center of Rup – 0.5 Vertical Rup Width = 14 – 0.5*2.7 = 12.65 km

9.1.2.4 Source Parameters of input in PSHA calculation

The source parameters for the Petrolia subplate required for the PSHA calculation are listed in Table 9.1-5. The right hand column of this table gives the source of the input.

Table 9.1-6. Source parameters for Petrolia subplate

Parameter Name	Parameter Value	Source
Longitude Latitude	-124.470 40.498 -124.470 40.325	Table 6-3
Top of rupture of 1992 Petrolia eqk (km)	12.65	Section 9.1.2.3
Dip Angle	11.0 E	Table 6-3
Fault Thickness (km)	2.7	Section 9.1.2.3
Mean Characteristic Magnitude	7.1 (0.5) 6.5 (0.5)	Section 9.1.2.1
Magnitude pdf	Max Mag	Assumption 5.6
Mean Recurrence Interval	32 yrs (0.2) 48 yrs (0.6) 72 yrs (0.2)	Section 9.1.2.2
Rupture Area (M) Model	Eq. 7-2	Assumption 5.7
Rupture Width (M) Model	Eq. 7-3	Assumption 5.8
b-value	Not used	
Fault Mechanism	Subduction Interface	Table 6-3

9.1.3 Eel River Subplate

9.1.3.1 Mean Characteristic Earthquake

From Table 6-3, the Eel River Subplate has the following parameters:

Length = 60 km
Crustal thickness= 15 km
Surface width of 15 km

For a crustal thickness of 15km and a surface width of the rupture zone of 15 km, then the fault must be dipping 45 degrees and the down-dip width is sqrt(2) x 15 km= 21 km.

The mean characteristic earthquake magnitude is estimated from the two empirical magnitude rupture area relationships (equations 7-5 and 7-6).

$$M = \log(RA) + 3.99 = \log(60*21) + 3.99 = 7.09$$

$$M = 0.81 \log(RA) + 4.7 = 0.81 \operatorname{Log}(60*21) + 4.7 = 7.21$$

The average of the magnitudes from these two models is 7.15.

Since the 1992 Petrolia earthquake had a larger than average stress-drop, a second method for estimating the mean characteristic earthquake was used that considered the same static stress-drop as implied by the 1992 Petrolia rupture. The characteristic magnitude is estimated by adding the 0.6 magnitude units to the magnitude computed using the mag-area relation. The value of 0.6 is the difference between the magnitude of the Petrolia earthquake (M7.1) and the magnitude expected for that size rupture (M6.7). Using this approach, the mean characteristic magnitude is M_w=7.75. These two estimates, 7.15 and 7.75 were given equal weighting in the PSHA.

9.1.3.2 Source Parameters of input in PSHA calculation

The source parameters for the Eel River subplate required for the PSHA calculation are listed in Table 9.1-6. The right hand column of this table gives the source of the input.

Table 9.1-7. Source parameters for Eel River subplate

Parameter Name	Parameter Value	Source
Longitude Latitude	-124.790 40.678 -124.395 40.505 -124.144 40.505	Table 6-4
Top of fault	0	Table 6-4
Dip Angle	45.0 NE	Table 6-4
Seismogenic Thickness (km)	15.0	Table 6-4
Mean Characteristic Magnitude	7.15 (0.5) 7.75 (0.5)	Section 9.1.2.1
Magnitude pdf	Max Mag	Assumption 5.6
Mean Recurrence Interval	230 (0.1) 300 (0.3) 370 (0.1) 340 (0.1) 500 (0.3) 660 (0.1)	Table 9.1-2
Rupture Area (M) Model	eq. 7-2	Assumption 5.7
Rupture Width (M) Model	eq. 7-3	Assumption 5.8
b-value	Not used	
Fault Mechanism	Subduction Interface	Table 6-4

9.1.4 Little Salmon Fault System

9.1.4.1 Coordinates of the LSF fault system

The LSF fault system extends for over 300 km, but for this calculation, we are only concerned that the rupture distance is correct. Since the magnitude pdf is the maximum magnitude model. Then each earthquake should rupture past the site. Therefore, the distance should be 0.5 km (GEO.HBIP.02.03). This distance of 0.5 km is based on detailed locations of the Bay Entrance strand of the LSF system. The coordinate of the LSF was modified so that the closest distance would be consistent with the 0.5 km distance to the Bay Entrance strand. The modified coordinates are:

-124.169	40.637	
-124.21	40.73	(Changed from –124.221, 40.721)
-124.360	40.821	

Only the closest fault segments were included for simplicity, since the other parts of the fault are not important for this calculation (once the magnitude is set)

9.1.4.2 Mean Recurrence Interval

The mean recurrence interval is set based on the mena recurrence interval for the Main Cascadia interface (Section 9.1.1). The values are from table 9.1-2.

9.1.4.3 Source Parameters of input in PSHA calculation

The source parameters for the Little Salmon Fault System required for the PSHA calculation are listed in Table 9.1-8. The right hand column of this table gives the source of the input.

Table 9.1-8. Source parameters for Little Salmon fault system

Parameter Name	Parameter Value	Source
Longitude Latitude	-124.169 40.637 -124.221 40.721 -124.360 40.821	Section 9.1.4.1 The
Top of fault	0	Table 6-5
Dip Angle	40.0 (0.20) 45.0 (0.60) 50.0 (0.20)	Table 6-5
Seismogenic Thickness (km)	15.0	Table 6-5
Mean Characteristic Magnitude	7.85 (0.1) 7.81 (0.3) 7.78 (0.10) 7.62 (0.25) 7.72 (0.25)	Table 6-5
Magnitude pdf	Max Mag	Assumption 5.6
Mean Recurrence Interval	230 (0.1) 300 (0.3) 370 (0.1) 340 (0.1) 500 (0.3) 660 (0.1)	Table 9.1-2
Rupture Area (M) Model	eq. 7-2	Assumption 5.7
Rupture Width (M) Model	eq. 7-3	Assumption 5.8
b-value	Not used	
Fault Mechanism	Reverse	Table 6-5

9.1.5 Mad River Fault System

9.1.5.1 Slip-Rate

The slip-rate over the Mad River fault system (Table 6-9) is distributed equally over two parallel faults, representative of the Mad River system. Half of the slip-rates listed in Table 6-9 are applied to each sub-fault, resulting in slip-rates of 2.5, 3.5, and 4.5 mm/yr with weights of 0.2, 0.6, and 0.2.

9.1.5.2 Mean Characteristic Magnitude

The total length of the mad River fault zone is 80 km (Table 6-9). The rupture length is assumed to be either the full length or one-half the length (assumption 5.17). This gives two rupture lengths: 40 km and 80 km with equal weight.

The down-dip length can be computed from the dip and the seismogenic thickness:

Down-Dip Width = thickness / sin(dip)

The alternative dips for the mad River fault are given in Table 6-9: 40, 45, and 50 degrees. Using the three dips and the two rupture lengths leads to 6 mean characteristic magnitudes listed in Table 9.1-8. Grouping the weights for the magnitudes that are equal leads to the mean magnitudes and weights given in Table 9.1-10.

Table 9.1-9. Computation of mean characteristic earthquakes for the Mad River Fault System

Dip	Thickness (km)	dip wt	Downdip Width (km)	Length (km)	Length wt	Area (km^2)	mag	Total Wt
40	15	0.2	23.3	80	0.5	1867	7.3	0.1
45	15	0.6	21.2	80	0.5	1697	7.2	0.3
50	15	0.2	19.6	80	0.5	1567	7.2	0.1
40	15	0.2	23.3	40	0.5	933	7.0	0.1
45	15	0.6	21.2	40	0.5	849	6.9	0.3
50	15	0.2	19.6	40	0.5	783	6.9	0.1

Table 9.1-10. Mean characteristic earthquakes for the Mad River Fault System

Magnitude	Weight
6.9	0.4
7.0	0.1
7.2	0.4
7.3	0.1

9.1.5.3 Location of the Mad River Subfaults

The mad River fault system is simplified into two subfaults. Subfault A follows the western edge of the fault zone closest to the site. The coordinates of this edge are listed in Table 6-9. The width of the Mad River zone is about 10 km (Figure 2-6 from PG&E (2002A)). The location of subfault B is computed by shifting the location of subfault A

10 km to the east. For this latitude (e.g. 40 degrees), a 10 km shift corresponds to 0.117 degrees in latitude (10/(111.12*cos(40)).

9.1.5.4 Source Parameters of input in PSHA calculation

The source parameters for the Mad River Fault Zone required for the PSHA calculation are listed in Tables 9.1-11 and 9.1.12 for subfaults A and B. The right hand column of this table gives the source of the input.

Table 9.1-11. Source parameters for Mad River fault system (subfault A)

Parameter Name	Parameter Value	Source
Longitude Latitude	-124.404 41.340 -124.295 40.961 -124.009 40.717	Table 6-9, Section 9.1.5.3
Top of fault	0	Table 6-9
Dip Angle	40.0 (0.20) 45.0 (0.60) 50.0 (0.20)	Table 6-9
Seismogenic Thickness (km)	15.0	Table 6-9
Mean Characteristic Magnitude	6.9 (0.4) 7.0 (0.1) 7.2 (0.4) 7.3 (0.1)	Table 9.1-10
Magnitude pdf	Y&C characteristic	Assumption 5.6
Slip rate (mm/yr)	2.5 (02) 3.5 (0.6) 4.5 (0.2)	Section 9.1.5.1
Rupture Area (M) Model	eq. 7-2	Assumption 5.7
Rupture Width (M) Model	eq. 7-3	Assumption 5.8
b-value	0.85	Assumption 5.10
Fault Mechanism	Reverse	Table 6-5

Table 9.1-12. Source parameters for Mad River fault system (subfault B)

Parameter Name	Parameter Value	Source
Longitude Latitude	-124.287 41.340 -124.178 40.961 -123.892 40.717	Table 6-9, Section 9.1.5.3
Top of fault	0	Table 6-9
Dip Angle	40.0 (0.20) 45.0 (0.60) 50.0 (0.20)	Table 6-9
Seismogenic Thickness (km)	15.0	Table 6-9
Mean Characteristic Magnitude	6.9 (0.4) 7.0 (0.1) 7.2 (0.4) 7.3 (0.1)	Table 9.1-10
Magnitude pdf	Y&C characteristic	Assumption 5.6
Slip rate (mm/yr)	2.5 (02) 3.5 (0.6) 4.5 (0.2)	Section 9.1.5.1
Rupture Area (M) Model	eq. 7-2	Assumption 5.7
Rupture Width (M) Model	eq. 7-3	Assumption 5.8
b-value	Not used	
Fault Mechanism	Reverse	Table 6-5

9.1.6 Gorda

9.1.6.1 b-values

Table 6-6 gives the b-value for the Gorda zone: 0.59 ± 0.06.

Using plus and minus 1.64 standard deviations leads to b-values of

$$0.59 + 1.64*0.06 = 0.69$$
$$0.59 - 1.64*0.06 = 0.49$$

The alternative b-values are 0.49, 0.59, and 0.69 with weights of 0.2, 0.6, and 0.2.

9.1.6.2 Activity Rates

From Table 6-6, the rate of earthquakes > M4 is 1.792 ± 0.23. The uncertainty in the activity rate for M>4 (0.23/1.792 13%) is negligible compared to the uncertainty in the b-value for characterizing the rates of larger magnitude earthquakes.

Considering only the uncertainty in the b-value, the activity rate for M>5 is given by

N(M>5) = N(M>4) 10^(-b)

Using the three b-values from section 9.1.6.1, the alternative activity rates are given in Table 9.1-3.

Table 9.1-3. Alternative activity rates for the Gorda zone.

b-value	N(M>4)	N(M>5)
0.49	1.792	0.58
0.59	1.792	0.46
0.69	1.792	0.37

9.1.6.3 Subdivision of the Gorda Plate

The Gorda plate dips under the HBIP site. A cross-section showing the depth dependence of the Gorda plate as a function of the longitude is shown in Figure 2-8 of Geomatrix (1994). This depth dependence is modeled by subdividing the Gorda plate into four zones shown in Figure 9.1-1.

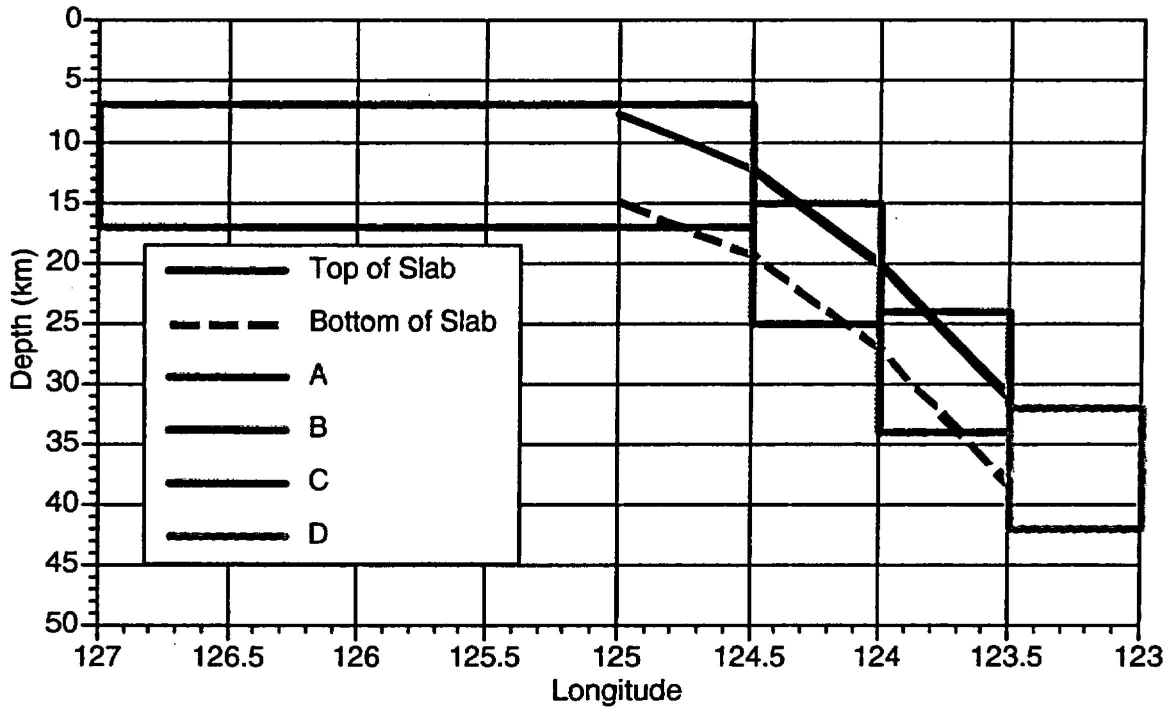

Figure 9.1-1. Model of the depth dependence of the Gorda plate.

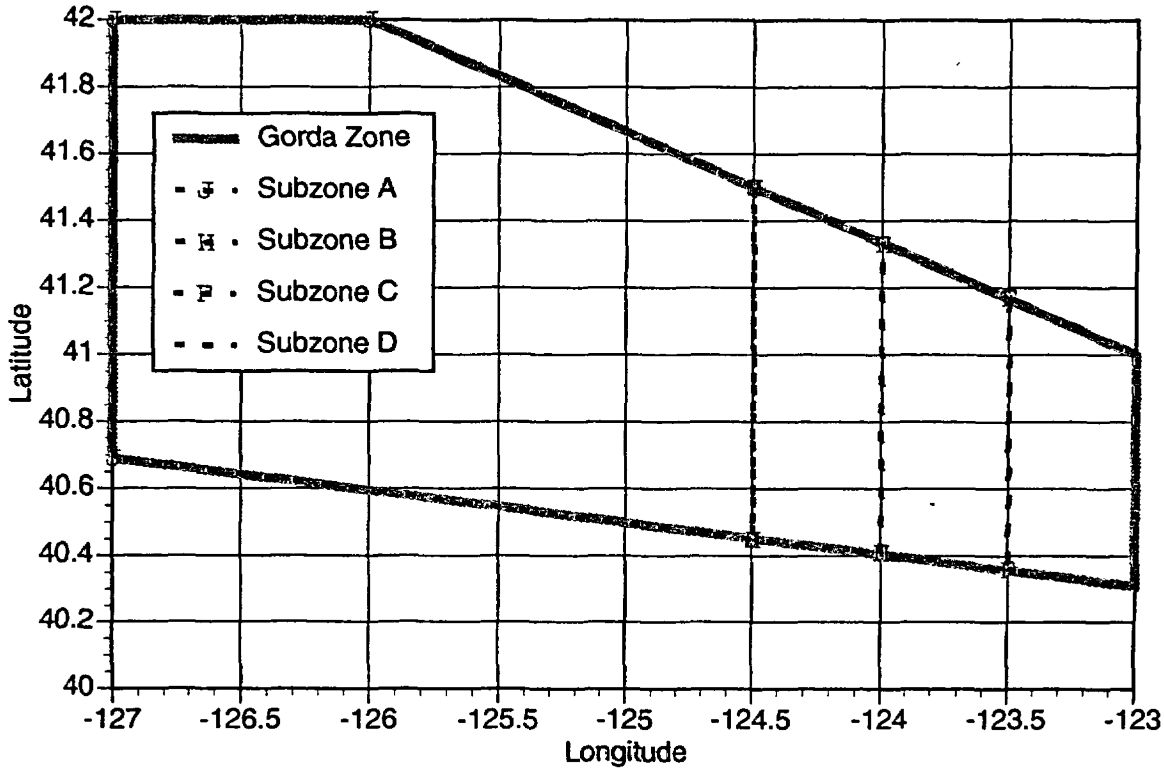

Figure 9.1-2. Map of the subzones used for the Gorda plate.

The activity rates computed in section 9.1.6.2 are partitioned onto these four subzones of the Gorda plate based on the fraction of the total area in each subzone.

Table 9.1-14. Activity rates for Gorda subzones.

Subzone	Area (km^2)	Fractional Area	Scaled Activity Rate 1 (total=0.58)	Scaled Activity Rate 2 (total=0.46)	Scaled Activity Rate 3 (total=0.37)
A	29,700	0.71	0.412	0.327	0.263
B	4,600	0.11	0.064	0.051	0.041
C	4,000	0.096	0.056	0.044	0.036
D	3,500	0.084	0.049	0.039	0.031
Total	41,800				

9.1.6.4 Source Parameters of input in PSHA calculation

The source parameters for the Gorda plate are listed in tables 9.1-15 to 9.1-18.

Table 9.1-15. Parameters for Gorda subzone A.

Parameter Name	Parameter Value	Source
Longitude Latitude	-127.00 40.69 -127.00 42.00 -126.00 42.00 -124.50 41.50 -124.50 40.45 -127.00 40.69	Figure 9.1-2
Top of Slab (km)	7	Figure 9.1-1
Seismogenic Thickness (km)	10.0	Table 6-6
Maximum Magnitude	7.00 (0.33) 7.25 (0.34) 7.50 (0.33)	Table 6-6
b-value	0.49 (0.2) 0.59 (0.6) 0.69 (0.2)	Section 9.1.6.1
Activity Rate N(M>5)	b=0.49, rate = 0.412 b=0.59, rate = 0.327 b=0.69, rate = 0.263	Section 9.1.6.3
Magnitude pdf	Truncated exponential	Assumption 5.6
Fault Mechanism	Subduction Intraslab	Geomatrix (1995), page 3-15

Table 9.1-16. Parameters for Gorda subzone B.

Parameter Name	Parameter Value	Source
Longitude Latitude	-124.50 41.50 -124.50 40.45 -124.00 40.41 -124.00 41.33 -124.5 41.50	Figure 9.1-2
Top of Slab (km)	15	Figure 9.1-1
Seismogenic Thickness (km)	10.0	Table 6-6
Maximum Magnitude	7.00 (0.33) 7.25 (0.34) 7.50 (0.33)	Table 6-6
b-value	0.49 (0.2) 0.59 (0.6) 0.69 (0.2)	Section 9.1.6.1
Activity Rate N(M>5)	b=0.49, rate = 0.064 b=0.59, rate = 0.051 b=0.69, rate = 0.041	Section 9.1.6.3
Magnitude pdf	Truncated exponential	Assumption 5.6
Fault Mechanism	Subduction Intraslab	Geomatrix (1995), page 3-15

Table 9.1-17. Parameters for Gorda subzone C.

Parameter Name	Parameter Value	Source
Longitude Latitude	-124.00 40.41 -124.00 41.33 -123.50 41.17 -123.50 40.36 -124.00 40.41	Figure 9.1-2
Top of Slab (km)	24	Figure 9.1-1
Seismogenic Thickness (km)	10.0	Table 6-6
Maximum Magnitude	7.00 (0.33) 7.25 (0.34) 7.50 (0.33)	Table 6-6
b-value	0.49 (0.2) 0.59 (0.6) 0.69 (0.2)	Section 9.1.6.1
Activity Rate N(M>5)	b=0.49, rate = 0.056 b=0.59, rate = 0.044 b=0.69, rate = 0.036	Section 9.1.6.3
Magnitude pdf	Truncated exponential	Assumption 5.6
Fault Mechanism	Subduction Intraslab	Geomatrix (1995), page 3-15

Table 9.1-18. Parameters for Gorda subzone D.

Parameter Name	Parameter Value	Source
Longitude Latitude	-123.50 41.17 -123.50 40.36 -123.00 40.31 -123.00 41.00 -123.50 41.17	Figure 9.1-2
Top of Slab (km)	32	Figure 9.1-1
Seismogenic Thickness (km)	10.0	Table 6-6
Maximum Magnitude	7.00 (0.33) 7.25 (0.34) 7.50 (0.33)	Table 6-6
b-value	0.49 (0.2) 0.59 (0.6) 0.69 (0.2)	Section 9.1.6.1
Activity Rate N(M>5)	b=0.49, rate = 0.049 b=0.59, rate = 0.039 b=0.69, rate = 0.031	Section 9.1.6.3
Magnitude pdf	Truncated exponential	Assumption 5.6
Fault Mechanism	Subduction Intraslab	Geomatrix (1995), page 3-15

9.1.7 Mendocino

9.1.7.1 b-values

Table 6-10 gives the b-value for the Mendocino zone: 0.816 ± 0.069.

Using plus and minus 1.64 standard deviations leads to b-values of

$$0.816 + 1.64*0.069 = 0.93$$
$$0.816 - 1.64*0.069 = 0.70$$

The alternative b-values are 0.70, 0.816, and 0.93 with weights of 0.2, 0.6, and 0.2.

9.1.7.2 Activity Rates

From Table 6-10, the rate of earthquakes > M4 is 2.504 ± 0.28. The uncertainty in the activity rate for M>4 (0.28/2.504 11%) is negligible compared to the uncertainty in the b-value for characterizing the rates of larger magnitude earthquakes.

Considering only the uncertainty in the b-value, the activity rate for M>5 is given by

$$N(M>5) = N(M>4)\ 10^{(-b)}$$

Using the three b-values from section 9.1.7.1:

Table 9.1-19. Alternative activity rates for the Mendocino zone.

b-value	N(M>4)	N(M>5)
0.816	2.504	0.38
0.93	2.504	0.29
0.70	2.504	0.50

9.1.7.3 Source Parameters of input in PSHA calculation

- The source parameters for the Mendocino zone are given in Table 9.1-20

Table 9.1-20. Source parameters for the Mendocino zone.

Parameter Name	Parameter Value	Reference
Longitude Latitude	-123.000 40.140 -123.000 40.310 -127.000 40.690 -127.000 40.250 -123.000 40.140	Table 6-10
Top of Fault (km)	0.0	Table 6-10
Seismogenic Thickness (km)	15.0	Table 6-10
Maximum Magnitude	7.25 (0.33) 7.50 (0.34) 7.75 (0.33)	Table 6-10
b-value	0.816 (0.6) 0.70 (0.2) 0.93 (0.2)	Section 9.1.7.1
Activity Rate N>M=5	b=0.816 rate = 0.38 b=0.70 rate = 0.50 b=0.93 rate = 0.29	Section 9.1.7.2
Magnitude pdf	Truncated exponential	Assumption 5.6
Fault Mechanism	Strike-slip	Table 6-10

9.1.8 San Andreas

9.1.8.1 Source Parameters of input in PSHA calculation

The parameters for the San Andreas fault required for the PSHA calculation are listed in Table 9.1-21.

Table 9.1-21. Parameters for San Andreas fault

Parameter Name	Parameter Value	Reference
Longitude Latitude	-124.0747 40.0446 -124.0009 39.8063 -123.9790 39.6034 -123.9251 39.4076 -123.8404 39.2072 -123.7009 39.0024 -123.5161 38.8024 -123.3154 38.6006 -123.1354 38.4175 -122.9455 38.2080 -122.7594 38.0005 -122.5884 37.7973 -122.4296 37.6048 -122.2467 37.4044 -122.0238 37.1988 -121.7408 37.0010 -121.4792 36.8068	Table 6-11
Top of Fault (km)	0.0	Table 6-11
Dip Angle	90.0	Table 6-11
Fault Thickness (km)	12.0	Table 6-11
b-value	0.85	Table 6-11
Slip Rate (mm/yr)	24.0	Table 6-11
Magnitude pdf	Youngs and Coppersmith characteristic	Assumption 5.6
Fault Mechanism	Strike-slip	Table 6-11
Mean Char mag	7.6	Table 6-11

9.1.9 Background Zone (Zone D)

9.1.9.1 b-value for zone D

The recurrence rates for zone D are listed in Table 9.1-22 (from Table 6-8).

Table 9.1-22. Recurrence rates for Background Zone D

Mag	Cumulative Annual Frequency (Number of Eqk/yr)	Incremental Rate of Earthquakes	Center Mag
3.0	3.2	2	3.25
3.5	1.2	0.7	3.75
4.0	0.50	0.12	4.25
4.5	0.38	0.22	4.75
5.0	0.16	0.09	5.35
5.7	0.07	0.048	6.00
6.3	0.022	0.022	6.50*

* Mag 6.5 is used for M>6.3.

The mean magnitude is computed by multiplying the center magnitude by the incremental rate and dividing by the rate > M_{min}.

That is

$$M_{mean} = \frac{\sum n(M_i)M_i}{N(M>3)} = 3.62$$

The b value is computed using equation 7-18.

$$b = \frac{1}{\ln(10)}\frac{1}{M_{mean}-M_{\min}} = \frac{1}{2.3}\frac{1}{(3.62-3)} = 0.70$$

The uncertainty in the b-value for zone D is assumed to be equal to the uncertainty for the Gorda plate (assumption 5-20). The uncertainty in the b-value for Gorda is 0.06. Therefore, using ±1.64 sigma, results in ±0.10 in the b-value. The three alternative b-values are 0.60, 0.70, and 0.80 with weights of 0.2, 0.6, 0.2, respectively.

9.1.9.2 Activity Rates

From Table 9.1.-22, the rate of earthquakes > M3 is3.2/yr. Considering the uncertainty in the b-value, the activity rate for M>5 is given by

$$N(M>5) = N(M>3)\ 10^{(-2b)}$$

Using the three b-values from section 9.1.9.1, the activity rates are given in Table 9.1-23

Table 9.1-23. Alternative activity rates for the Mendocino zone.

b-value	N(M>3)	N(M>5)
0.60	3.2	0.20
0.70	3.2	0.13
0.80	3.2	0.08

9.1.9.3 Source Parameters of input in PSHA calculation

The parameters for the San Andreas fault required for the PSHA calculation are listed in Table 9.1-24.

Table 9.1-24. Parameters for background zone D

Parameter Name	Parameter Value	Reference
Longitude Latitude	-124.500 40.320 -124.596 41.000 -124.374 41.106 -123.586 40.409 -123.505 40.152 -124.500 40.320	Table 6-7
Top of Fault (km)	0	Table 6-7
Seismigenic Thickness (km)	15.0	Table 6-7
Maximum Magnitude	6.9 (0.4) 7.0 (0.1) 7.2 (0.4) 7.3 (0.1)	Same as Mad River (Table 6-7) Table 9.1-10
Fault Mechanism	Reverse	Table 6-7
b-value	0.60 (0.2) 0.70 (0.6) 0.80 (0.2)	section 9.1.9.1
N(M>5)	b=0.60, rate =0.20 b=0.70, rate =0.13 b=0.80, rate =0.08	section 9.1.9.2
Magnitude pdf	Truncated exponential	Assumption 5.6

9.2 Develop Input Parameter file for PSHA

9.2.1 Fault Parameter File

The PSHA computer program HAZ36h requires an input file in addition to the fault parameter file discussed in Section 9.1 above. The input parameters discussed in section 9.1 are set in these input files. The fault file is listed in Appendix 1 and is given on the enclosed CD-ROM.

9.2.2 Run Parameter File

The run parameter file includes the selected attenuation relations (for rock or soil) and component, the truncation of the variability of the attenuation relation, the site location, and the ground motion levels for computing the hazard. The ground motion levels were selected so that the equal hazard spectrum could be determined for return period up to 10,000 years. The shortest return period are limited by the minimum magnitude and the spatial extent of the sources.

Calculation GEO.HBIP.03.02 specifies a set of 30 spectral periods to cover the site resonances (Table 6-15). Based on preliminary hazard calculations, not all 30 periods are needed to adequately characterize the spectra. Therefore, a subset of 15 periods was used for the final hazard runs. These 15 periods are shown in Table 9.2-1. Periods greater than 3 sec were not included because the Youngs et al (1997) attenaution relation is only defined for periods up to 3 seconds. Periods less than 0.1 sec were not included (other than PGA) because the Youngs et atl (1997) attenuation relation is only defined for period greater than 0.075 sec (except for PGA). The peak of the spectrum was sampled at all of the specified periods, but away from the peak, only every other period was used. The reason for reducing the number of periods was to reduce the calculation times.

The input files are listed in Appendices 2-5 and are also given on the enclosed CD-ROM.

Table 9.2-1 Periods used for the PHSA calculation.

Period (sec) from Calc GEO.HBIP.03.02	Period (Sec) Used in final PSHA calculation
0.01 (PGA)	X
0.03 (PGA)	
0.05	
0.07	
0.10	X
0.12	
0.15	X
0.17	
0.20	X
0.25	X
0.30	X
0.35	X
0.40	X
0.50	X
0.60	X
0.70	
0.80	X
0.90	
1.00	X
1.20	
1.50	X
1.70	
2.00	X
2.50	
3.00	X
3.50	
4.00	
5.00	
7.00	
10.00	

9.3 Execution of HAZ36 PSHA Computer Program

Given the run parameter files and corresponding fault parameter files, the PHSA computer program HAZ36h was run to generate the hazard curves. The computer program generates a suite of five output files which are described in GEO.HBIP.03.02 – Verification of PHSA software HAZ36, Revision 0 (PG&E, 2003b). The complete set of output files are given on the enclosed CD-ROM. The output files with the mean hazard curves for each attenuation relation are listed in Appendices 1-4.

The results are summarized in a series of plots and tables in sections 9.4, 9.5, 9.6, and 9.7 for the rock FN component, rock FP component, soil FN component, and soil FP component, respectively. In each section, the following plots are tables are included:

- Hazard curves showing the hazard by source for PGA, 0.2 sec, 1.0 sec, and 3.0 sec
- Equal hazard spectra (tables and figures)
- Mag-Dist deaggregation of the hazard for PGA, 0.2 sec, 1.0 sec, and 3.0 sec

9.4 Rock Hazard for the Fault Normal Component

The hazard curves are shown in Figures 9.4-1 to 9.4-4 for spectral periods of 0.0 (PGA), 0.2 sec, 1.0 sec, and 3.0 sec, respectively. The total hazard curve is interpolated using equation 7-1 to compute the equal hazard spectra for return periods of 1, 25, 50, 100, 500, 1000, 2000, 5000, and 10000 years. The equal hazard spectra are listed in Table 9.4-1 and are plotted in Figure 9.4-5.

The deaggregation in magnitude and distance space for a 2000 year return period for spectral periods of 0.0 (PGA), 0.2 sec, 1.0 sec, and 3.0 sec is shown in Figures 9.5-6, 9.6-7, 9.6-8, and 9.6-9, respectively. These plots show that at all period, the hazard dominated by the Cascadia – Little Salmon synchronous rupture.

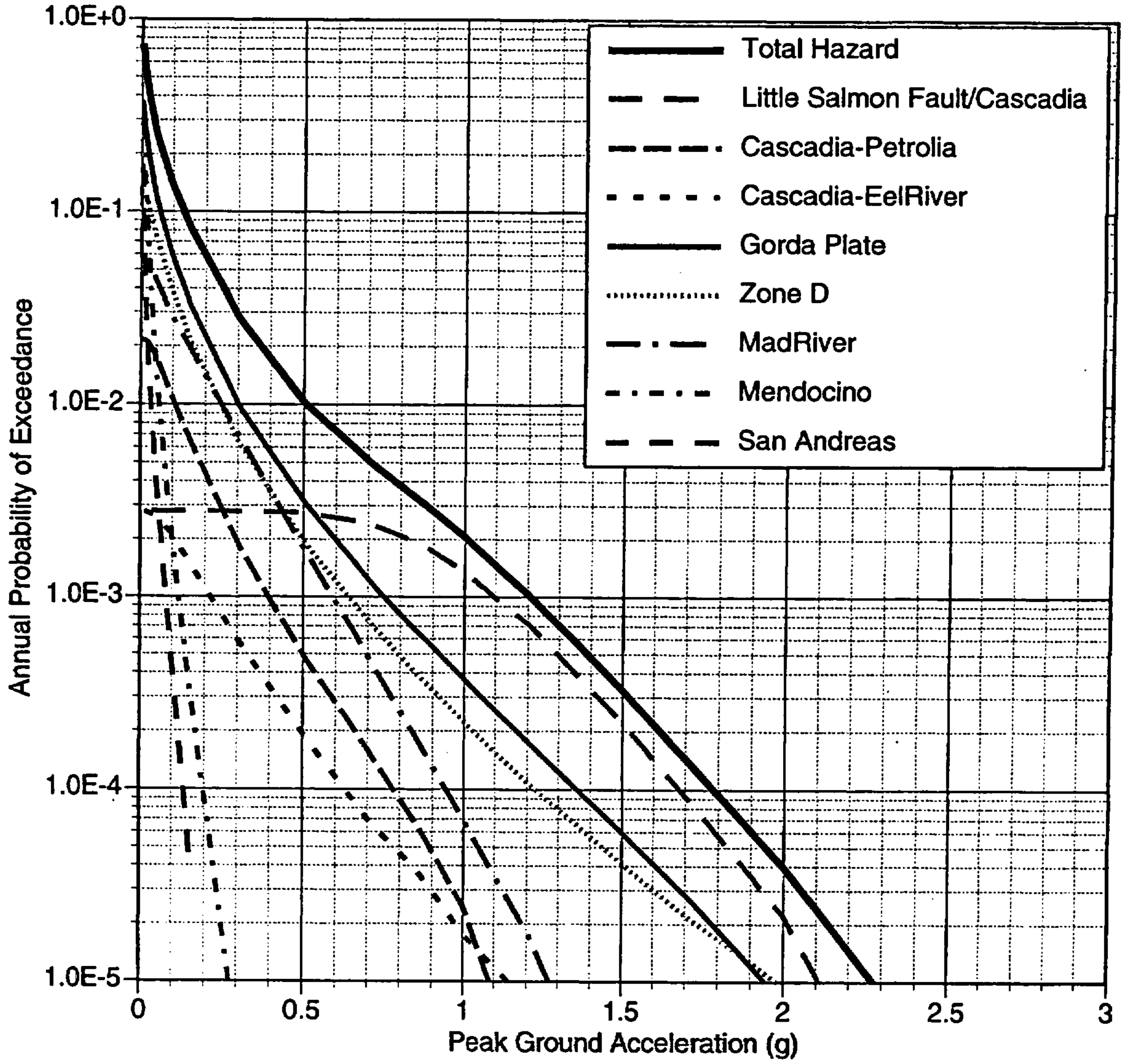

Figure 9.4-1. Mean hazard curve by source, FN component, Rock, PGA

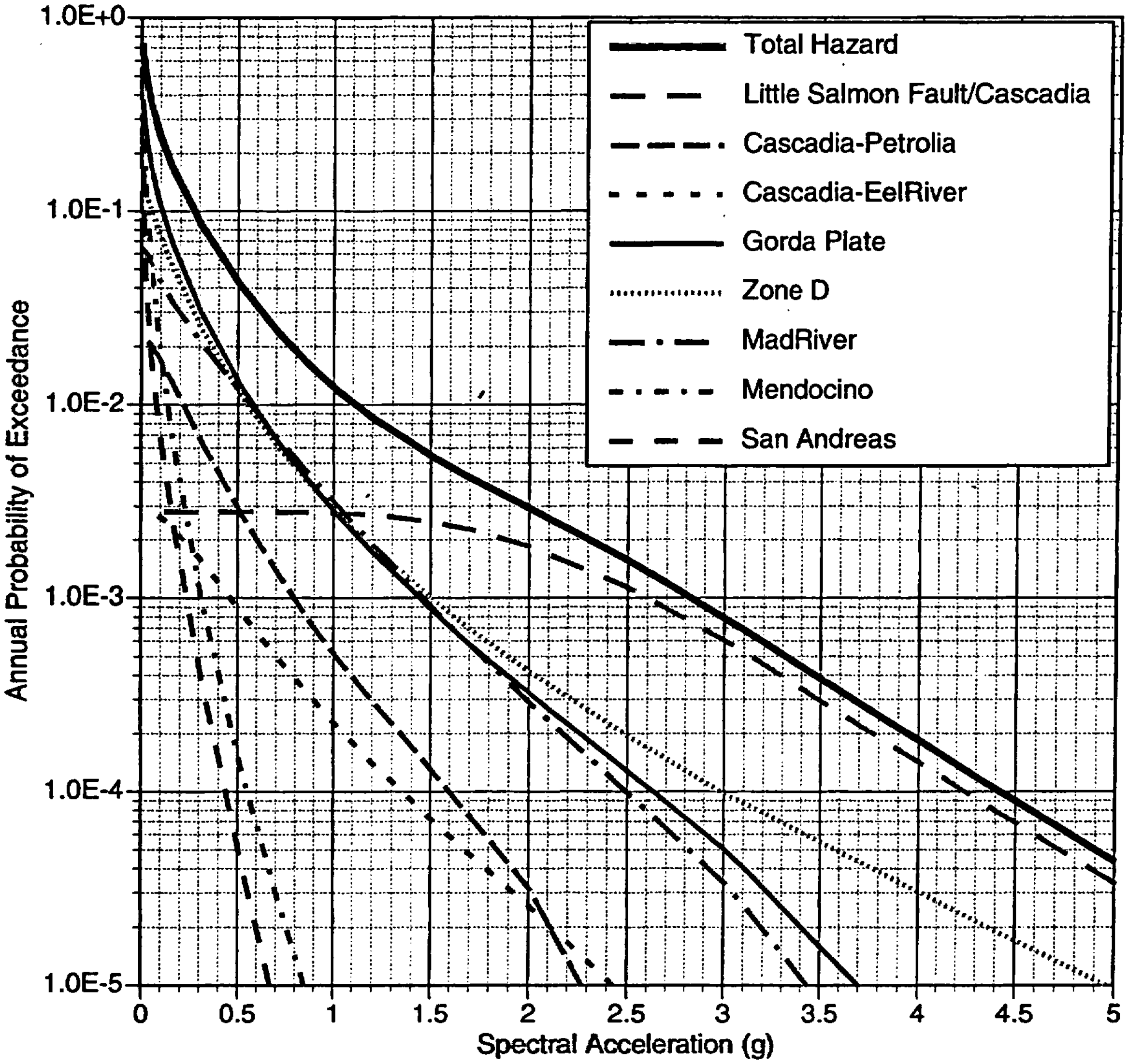

Figure 9.4-2. Mean hazard curve by source, FN component, Rock, T=0.2 sec

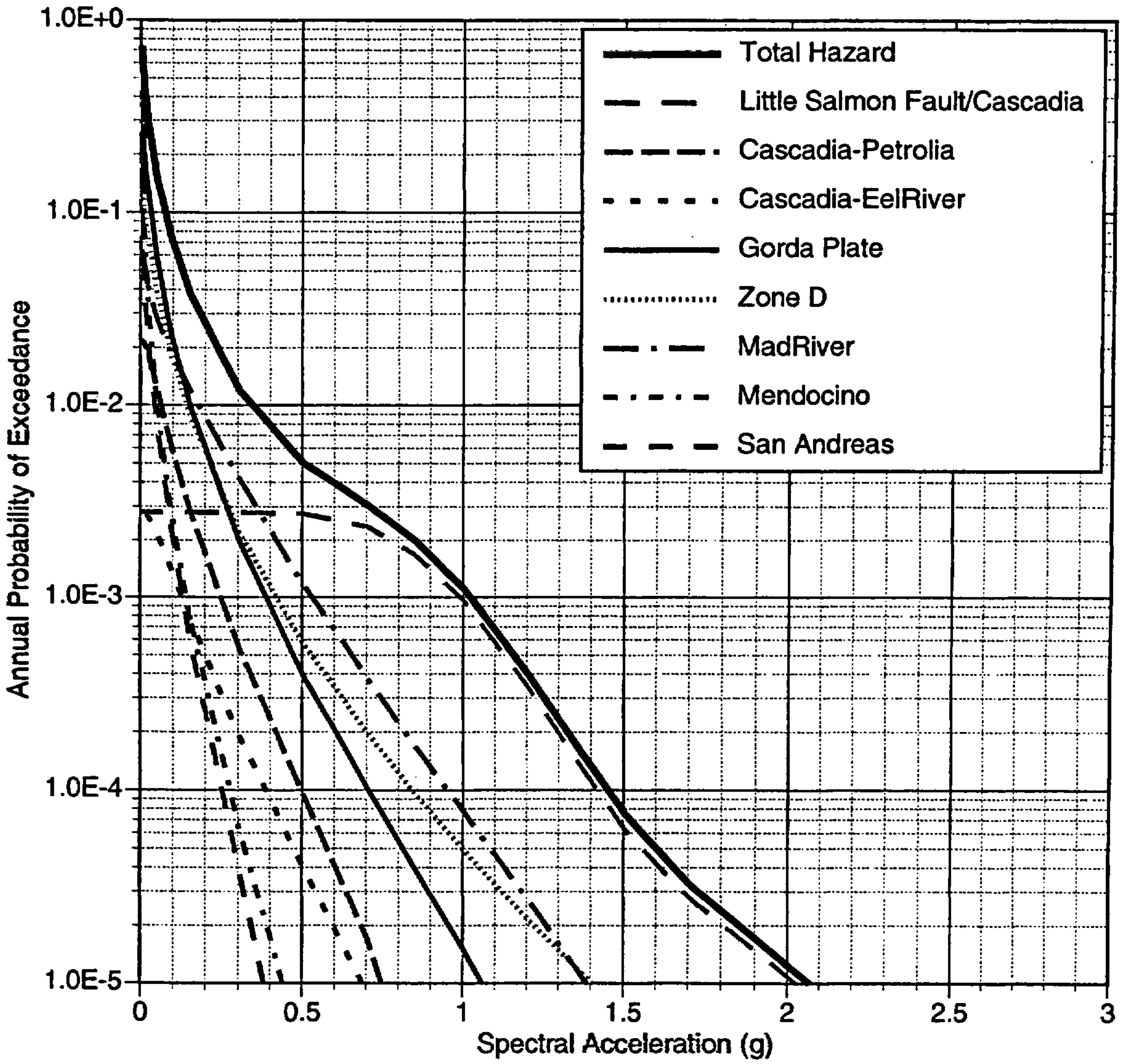

Figure 9.4-3. Mean hazard curve by source, FN component, Rock, T=1.0 sec

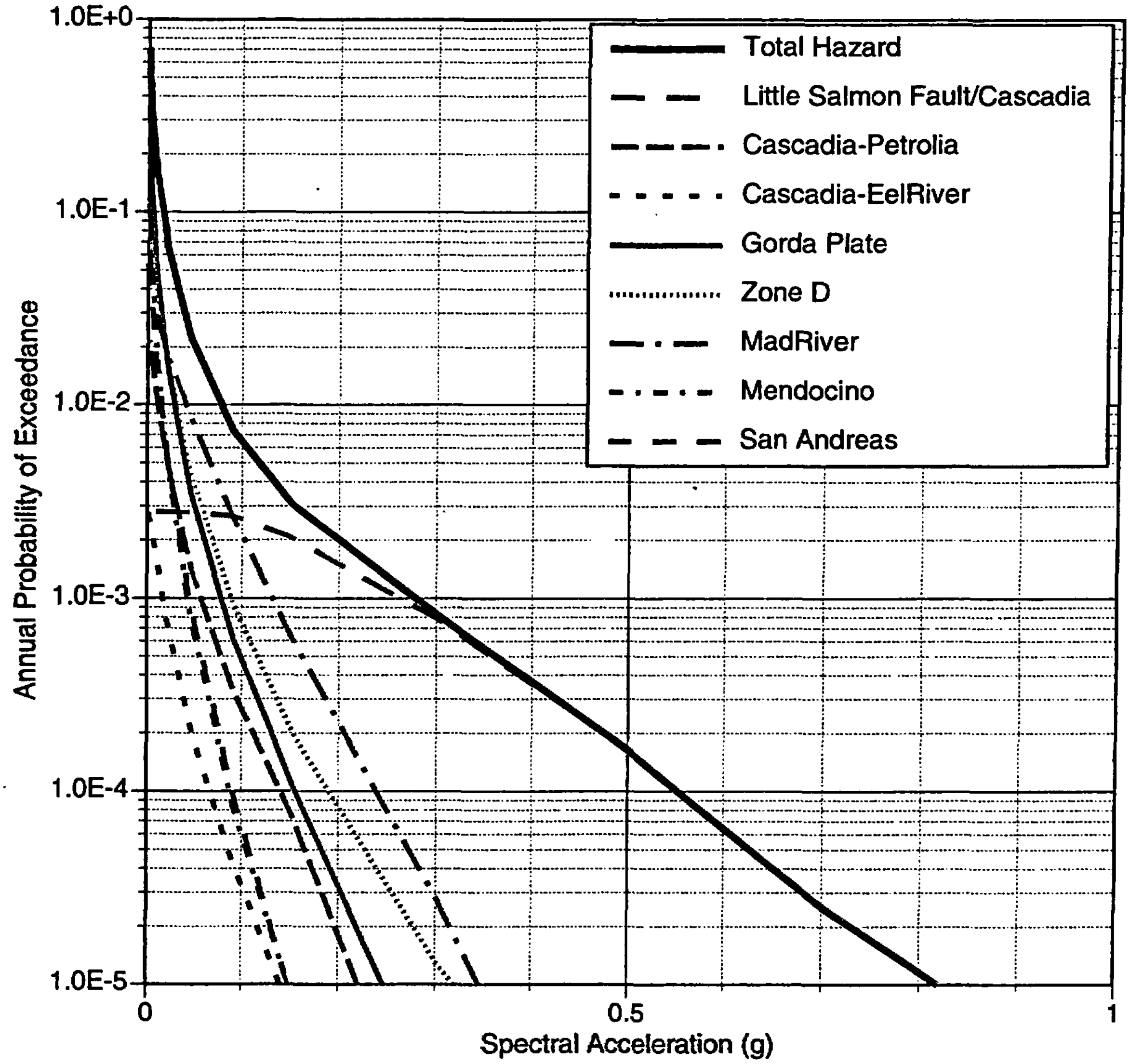

Figure 9.4-4. Mean hazard curve by source, FN component, Rock, T=3.0 sec

Table 9.4-1 Equal hazard spectra (g) for the fault normal component for rock site conditions.

Period (sec)	1 Yr	25 yr	50 yr	100 yr	500 yr	1,000 yr	2,000 yr	5,000 yr	10,000 yr
0.01	0.0031	0.2392	0.3567	0.5050	1.0038	1.2046	1.3770	1.6116	1.7746
0.03	0.0031	0.2392	0.3567	0.5050	1.0038	1.2046	1.3770	1.6116	1.7746
0.10	0.0051	0.4739	0.7003	0.9874	1.9180	2.2938	2.6647	3.1087	3.3901
0.15	0.0056	0.5147	0.7643	1.0870	2.1860	2.6738	3.1111	3.6067	4.0334
0.20	0.0057	0.5180	0.7738	1.1064	2.2869	2.8133	3.2488	3.8176	4.3133
0.25	0.0054	0.4738	0.7142	1.0262	2.1669	2.6883	3.1470	3.6958	4.1736
0.30	0.0050	0.4351	0.6610	0.9558	2.0612	2.5685	3.0401	3.5653	4.0221
0.40	0.0042	0.3615	0.5530	0.8053	1.7978	2.2449	2.6815	3.2065	3.5847
0.50	0.0037	0.3126	0.4766	0.6962	1.6081	2.0283	2.3997	2.8776	3.1860
0.60	0.0032	0.2557	0.3943	0.5830	1.3696	1.7500	2.0821	2.5074	2.8100
0.80	0.0022	0.1839	0.2868	0.4249	1.0528	1.2490	1.3986	1.5944	1.7408
1.00	0.0017	0.1440	0.2202	0.3335	0.8473	1.0184	1.1526	1.3160	1.4438
1.50	0.0011	0.0860	0.1350	0.2050	0.5188	0.6531	0.7788	0.9297	1.0406
2.00	0.0005	0.0575	0.0926	0.1399	0.3471	0.4620	0.5668	0.7089	0.8008
3.00	0.0002	0.0291	0.0483	0.0743	0.1889	0.2717	0.3514	0.4686	0.5457

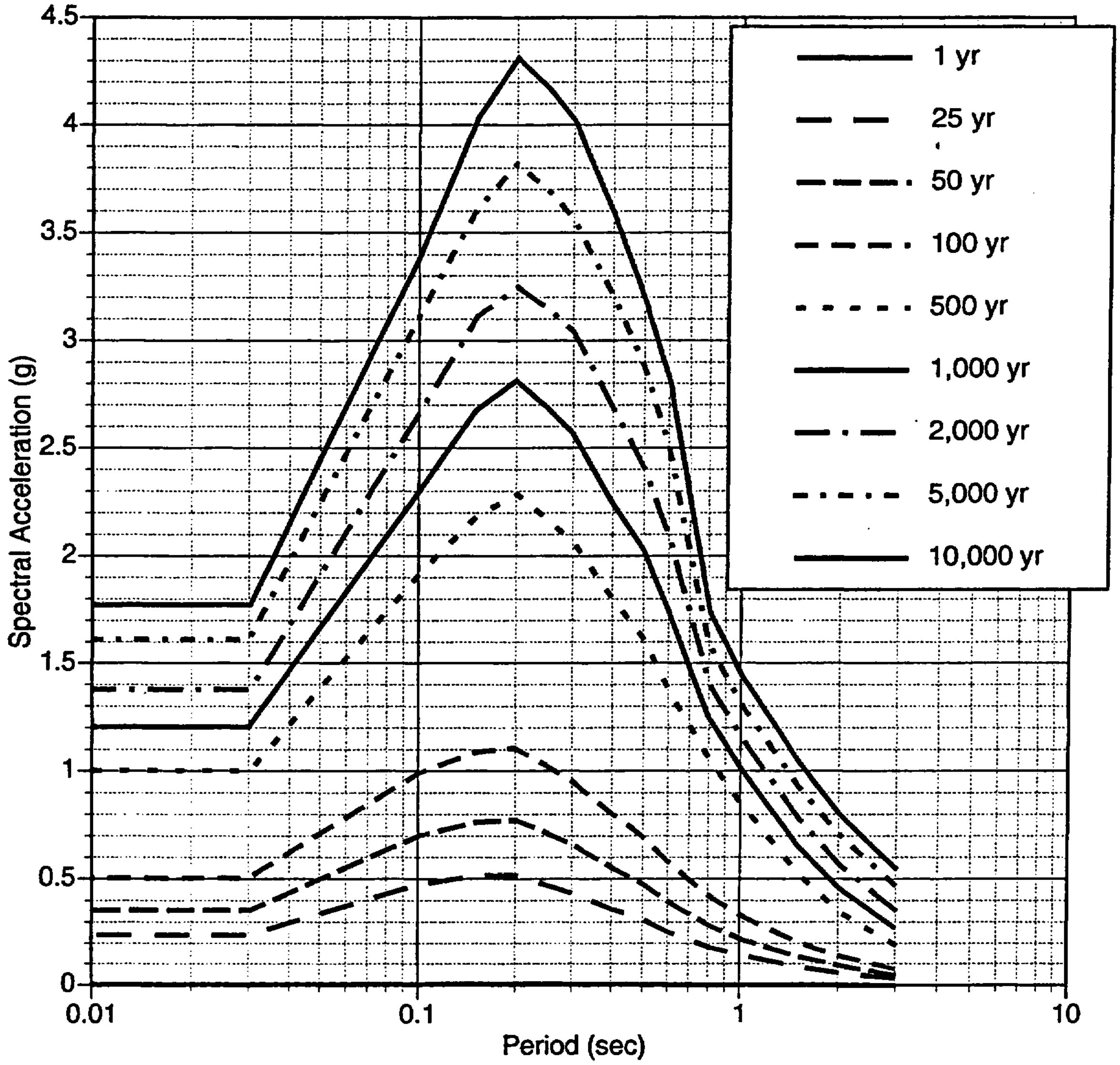

Figure 9.4-5. Equal hazard spectra for the FN component, rock site conditions

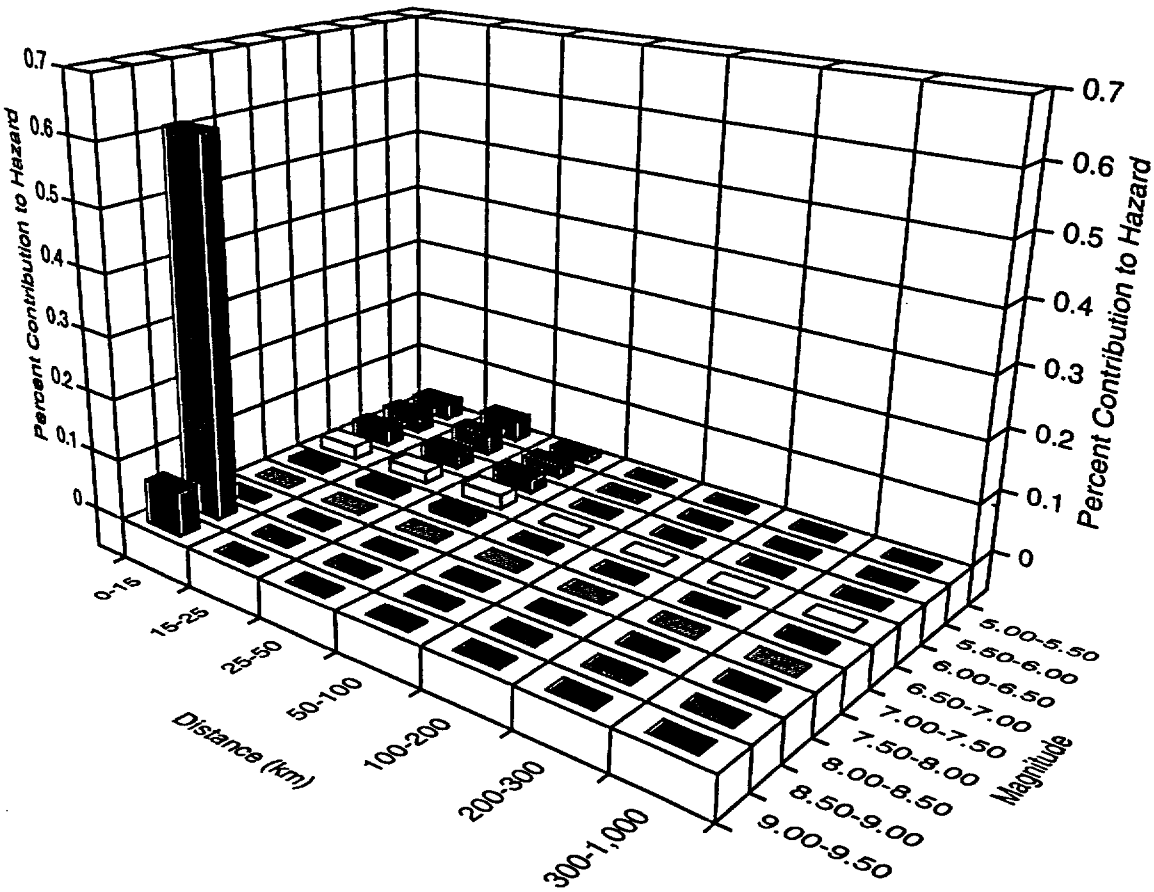

Figure 9.4-6 Deaggregation for the FN component, Rock site conditions, PGA, for a 2,000 yr return period.

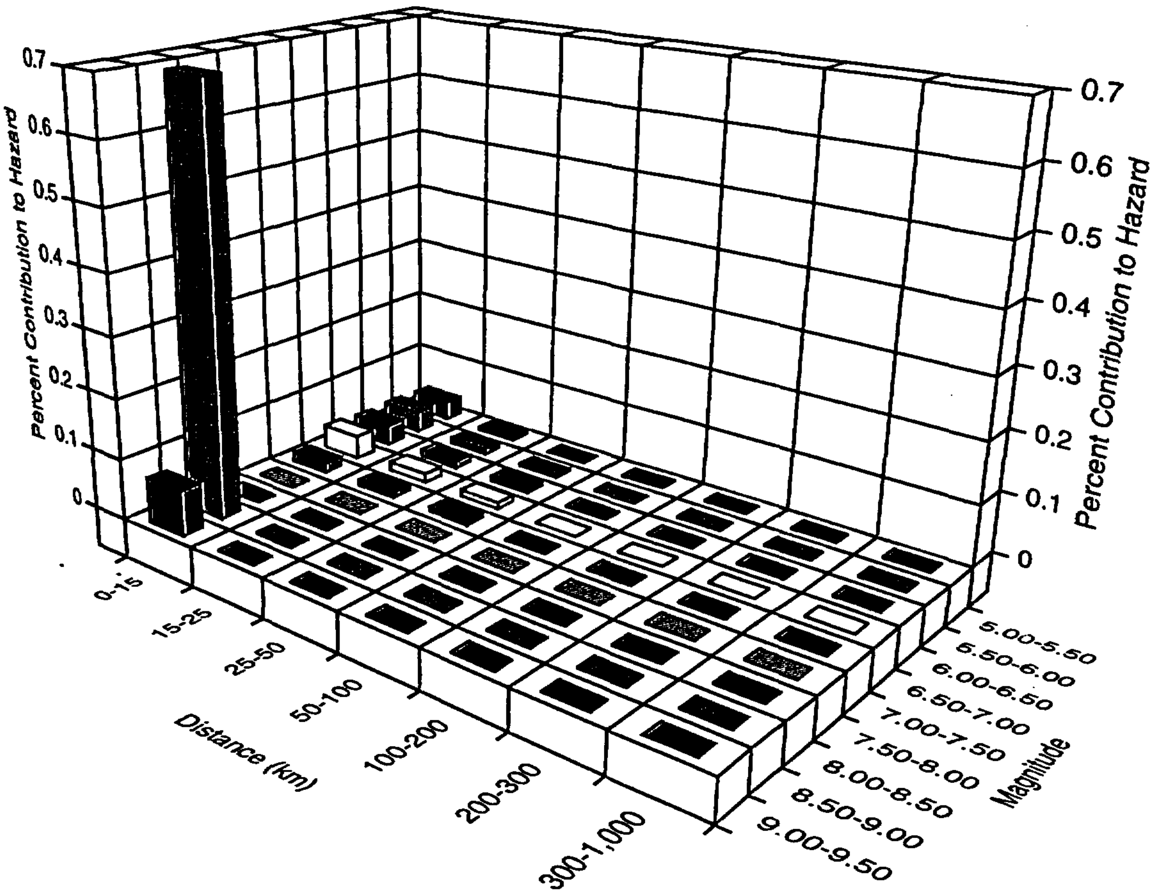

Figure 9.4-7 Deaggregation for the FN component, Rock site conditions, T=0.2 sec, for a 2,000 yr return period.

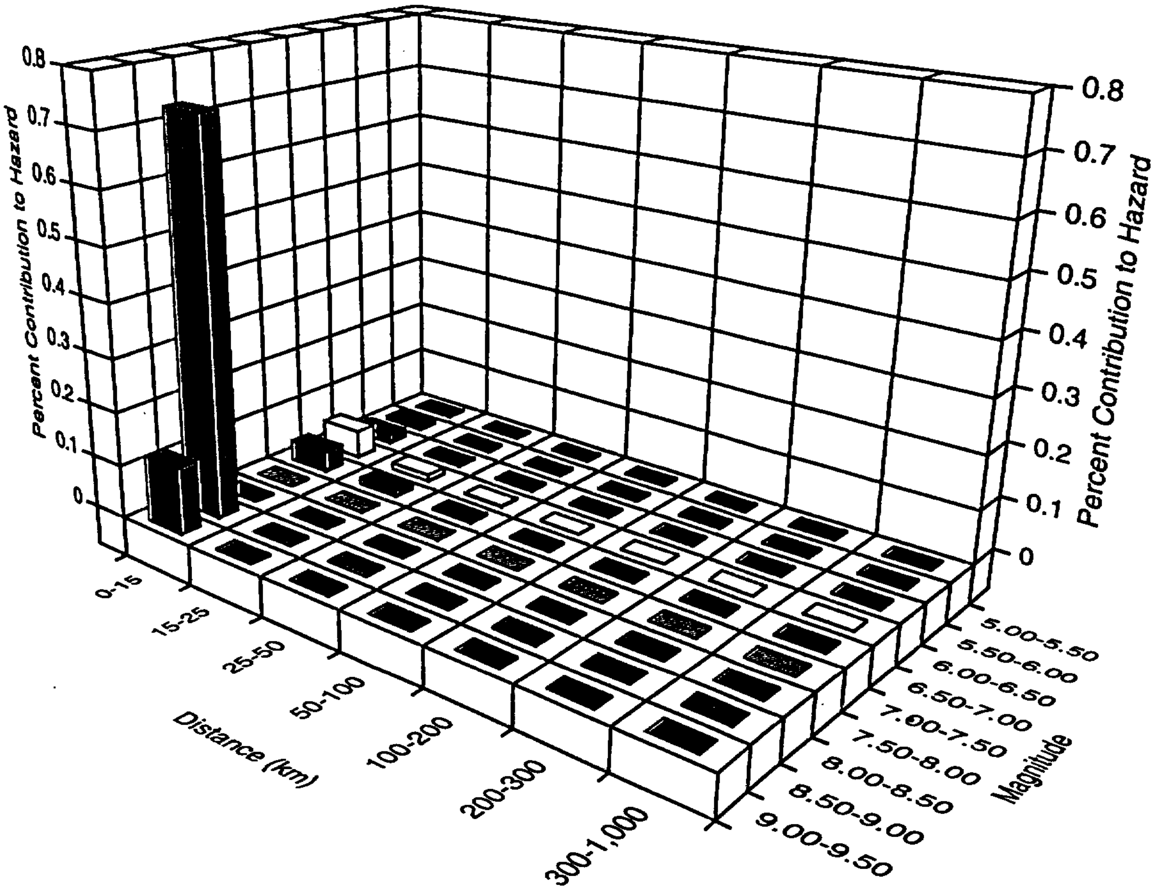

Figure 9.4-8 Deaggregation for the FN component, Rock site conditions, T=1.0 sec, for a 2,000 yr return period.

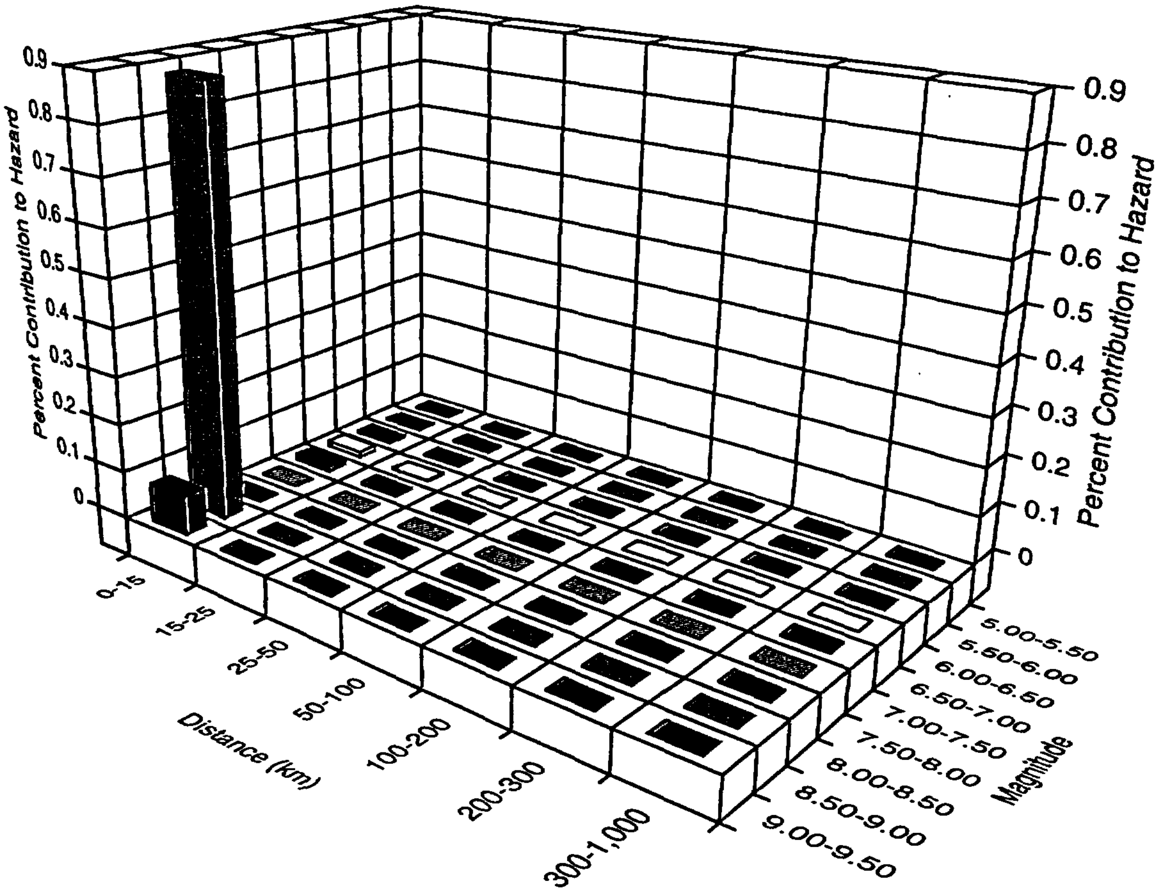

Figure 9.4-9 Deaggregation for the FN component, Rock site conditions, T=3.0 sec, for a 2,000 yr return period.

9.5 Rock Hazard for the Fault Parallel Component

The FP component is identical to the FN component for periods less than 0.6 sec. Therefore, the hazard is only recomputed for spectral period of 0.8 sec, 1.0 sec, 1.5 sec, 2.0 sec, and 3.0 sec.

The hazard curves are shown in Figures 9.5-1 to 9.5-2 for spectral periods1.0 sec, and 3.0 sec, respectively. The total hazard curve is interpolated using equation 7-1 to compute the equal hazard spectra for return periods of 1, 25, 50, 100, 500, 1000, 2000, 5000, and 10000 years. The equal hazard spectra are listed in Table 9.5-1 and are plotted in Figure 9.5-3.

The deaggregation in magnitude and distance space for a 2000 year return period for spectral periods of 1.0 sec, and 3.0 sec is shown in Figures 9.5-4 and 9.5-5, respectively. These plots show that at long periods, the hazard dominated by the Cascadia – Little Salmon synchronous rupture.

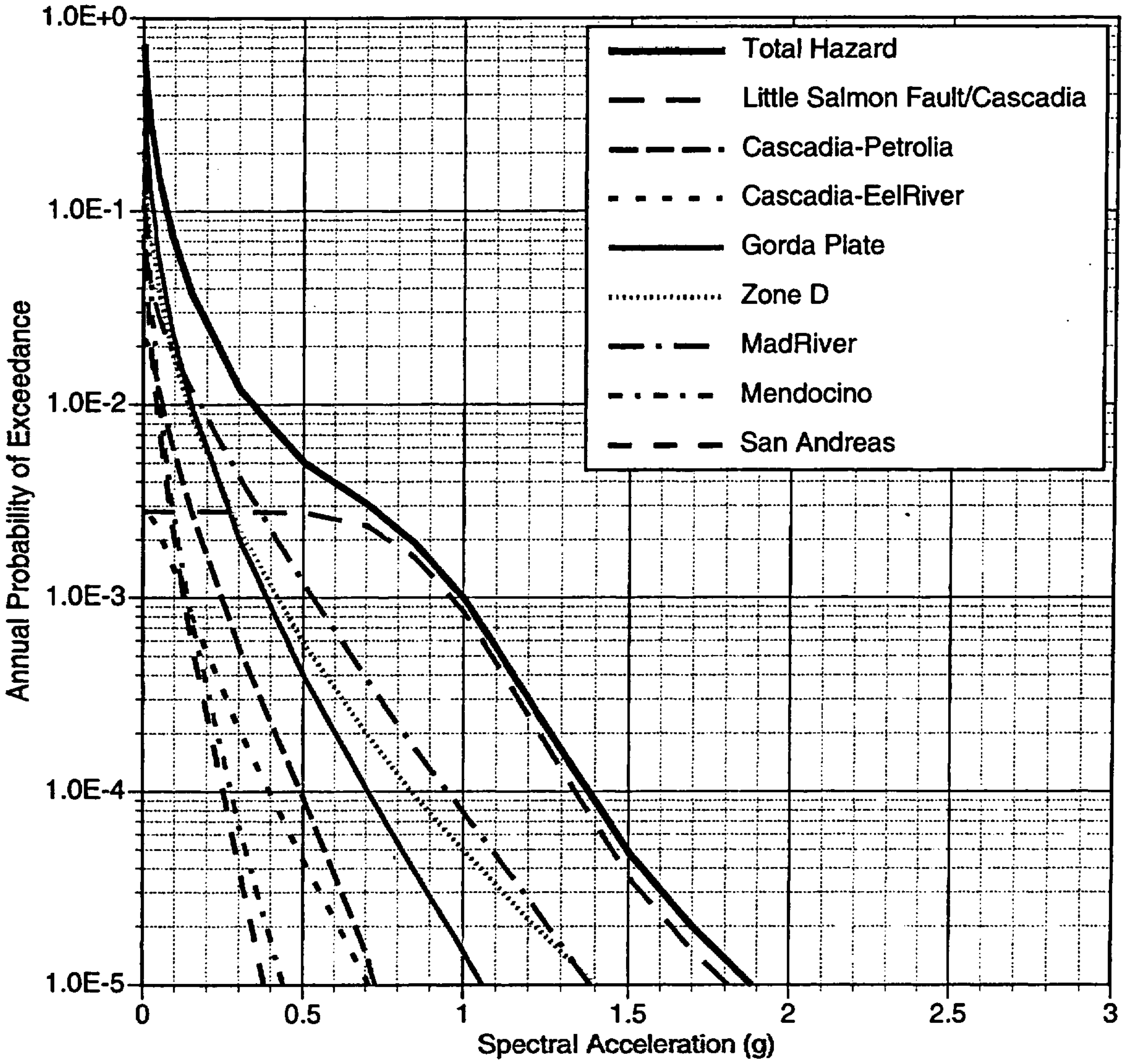

Figure 9.5-1. Mean hazard curve by source, FP component, Rock, T=1.0 sec.

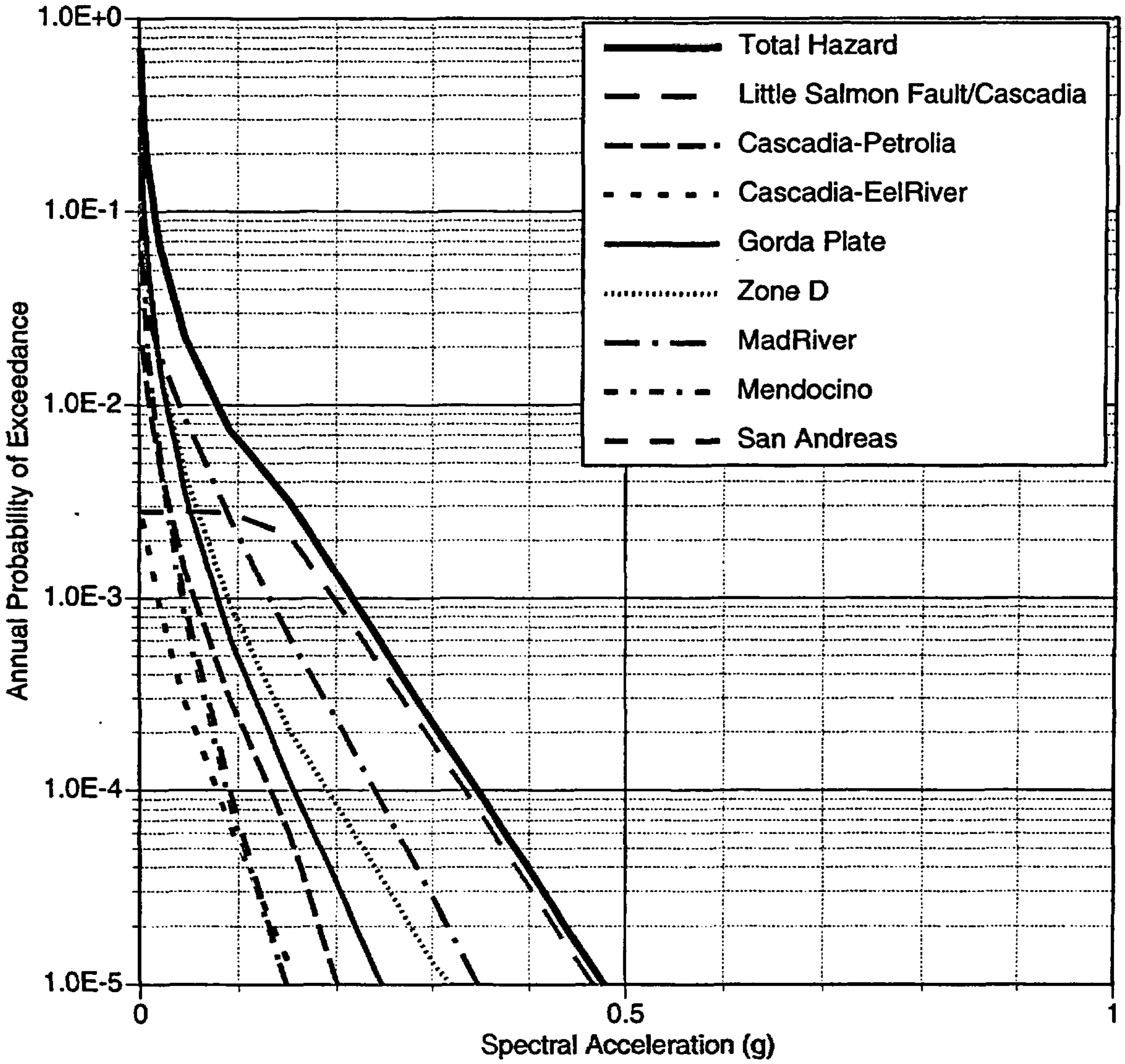

Figure 9.5-2. Mean hazard curve by source, FP component, Rock, T=3.0 sec.

Table 9.5-1 Equal hazard spectra (g) for the fault parallel component for rock site conditions.

Period (sec)	1 Yr	25 yr	50 yr	100 yr	500 yr	1,000 yr	2,000 yr	5,000 yr	10,000 yr
0.01	0.0031	0.2392	0.3567	0.5050	1.0038	1.2046	1.3770	1.6116	1.7746
0.03	0.0031	0.2392	0.3567	0.5050	1.0038	1.2046	1.3770	1.6116	1.7746
0.10	0.0051	0.4739	0.7003	0.9874	1.9180	2.2938	2.6647	3.1087	3.3901
0.15	0.0056	0.5147	0.7643	1.0870	2.1860	2.6738	3.1111	3.6067	4.0334
0.20	0.0057	0.5180	0.7738	1.1064	2.2869	2.8133	3.2488	3.8176	4.3133
0.25	0.0054	0.4738	0.7142	1.0262	2.1669	2.6883	3.1470	3.6958	4.1736
0.30	0.0050	0.4351	0.6610	0.9558	2.0612	2.5685	3.0401	3.5653	4.0221
0.40	0.0042	0.3615	0.5530	0.8053	1.7978	2.2449	2.6815	3.2065	3.5847
0.50	0.0037	0.3126	0.4766	0.6962	1.6081	2.0283	2.3997	2.8776	3.1860
0.60	0.0032	0.2557	0.3943	0.5830	1.3696	1.7500	2.0821	2.5074	2.8100
0.80	0.0022	0.1839	0.2866	0.4246	1.0461	1.2352	1.3724	1.5597	1.6925
1.00	0.0017	0.1439	0.2203	0.3338	0.8371	0.9964	1.1082	1.2591	1.3709
1.50	0.0011	0.0861	0.1351	0.2056	0.5096	0.6045	0.7099	0.8087	0.8877
2.00	0.0005	0.0575	0.0926	0.1401	0.3314	0.4021	0.4880	0.5607	0.6171
3.00	0.0002	0.0291	0.0483	0.0747	0.1690	0.2022	0.2418	0.3036	0.3361

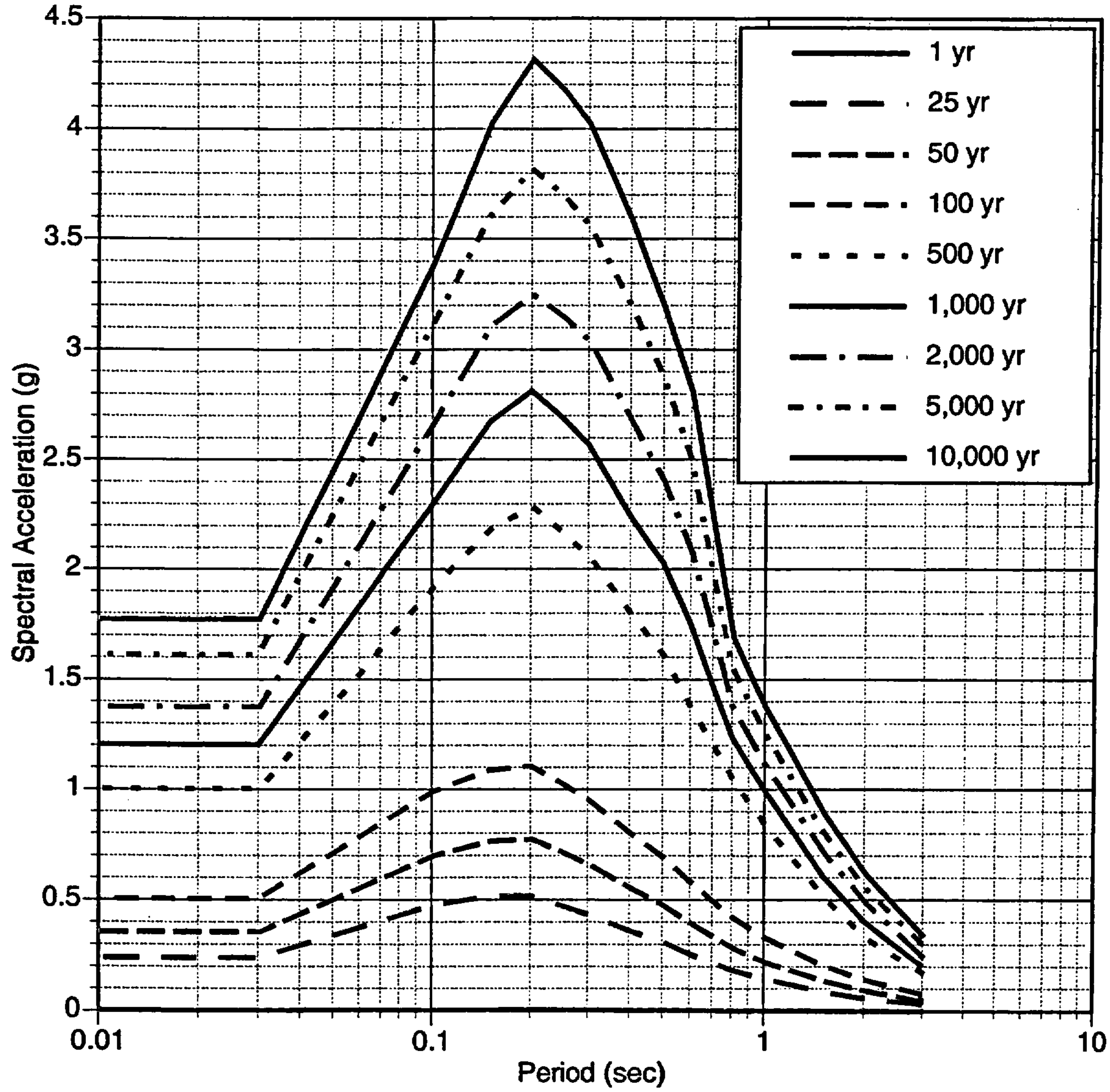

Figure 9.5-3. Equal hazard spectra for the FP component, rock site conditions

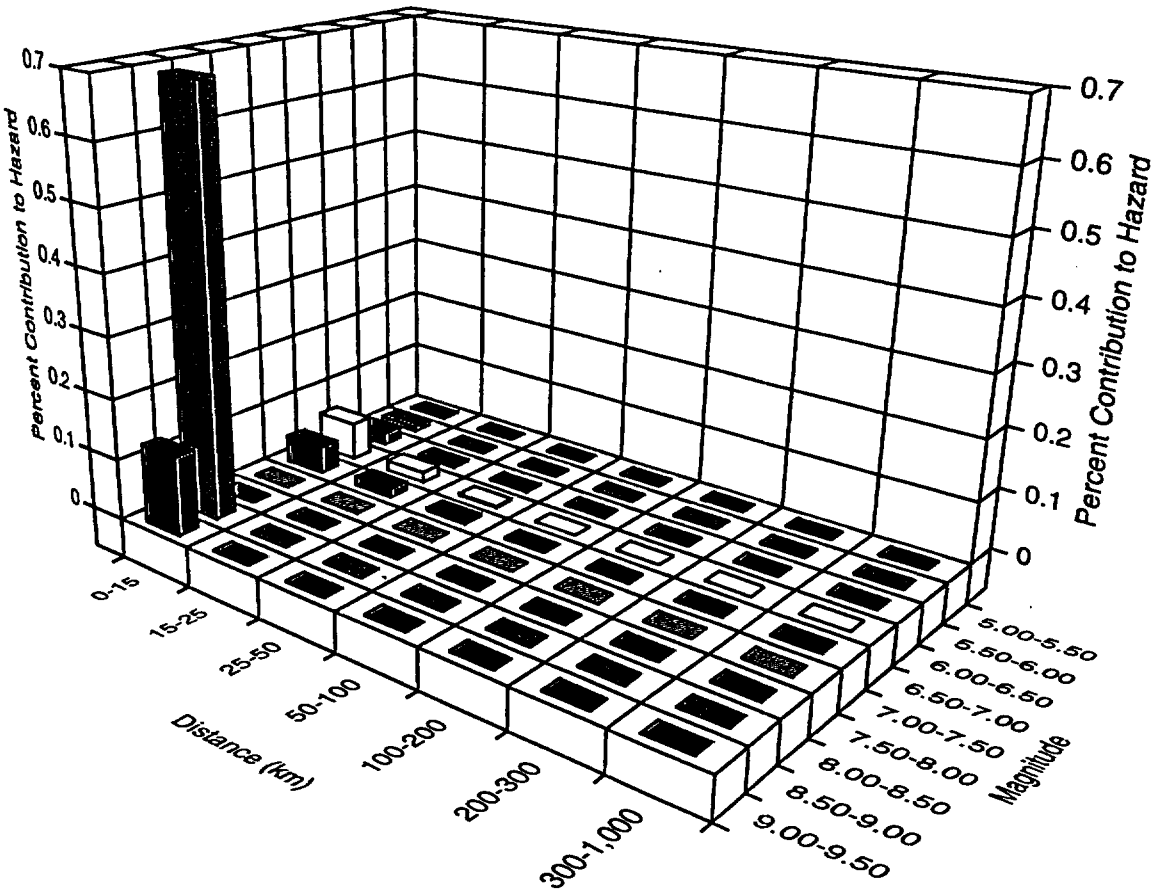

Figure 9.5-4 Deaggregation for the FP component, rock site conditions, T=1.0 sec, for a 2,000 yr return period.

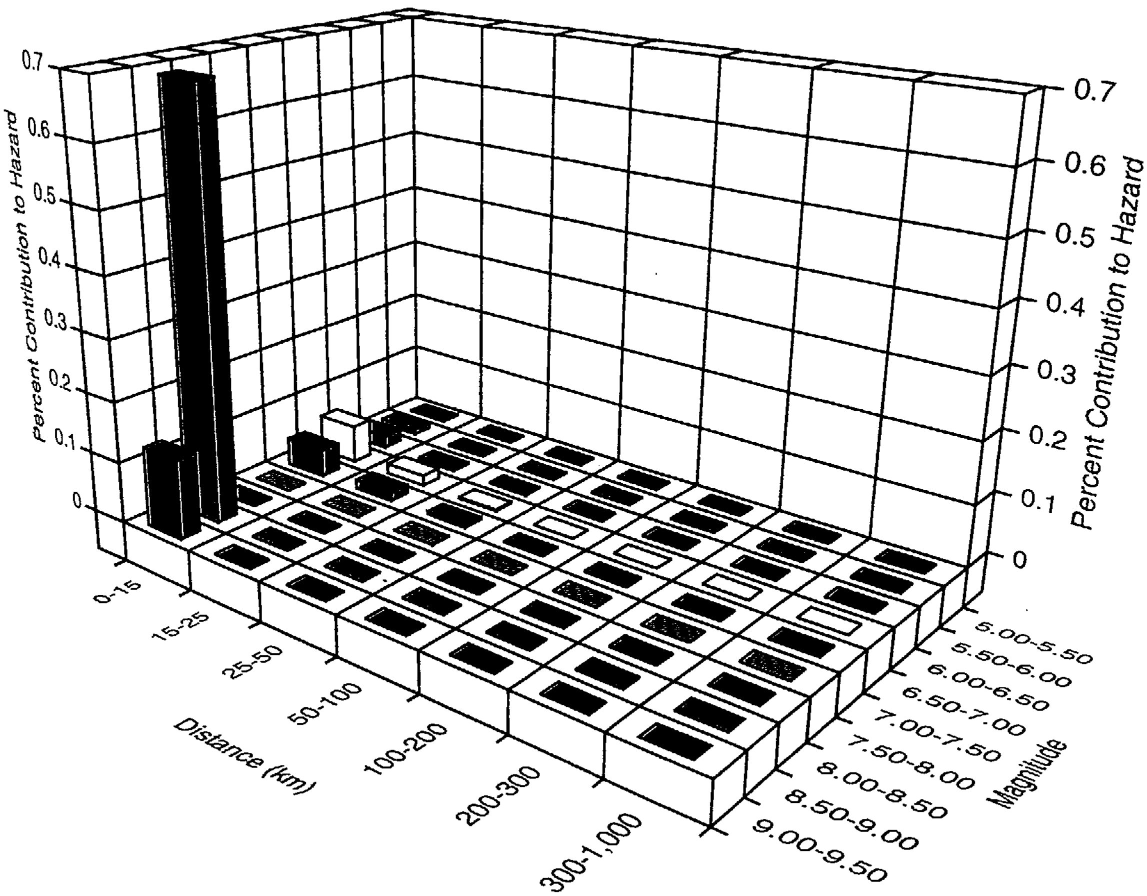

Figure 9.5-4 Deaggregation for the FP component, rock site conditions, T=1.0 sec, for a 2,000 yr return period.

9.6 Soil Hazard for the Fault Normal Component

The hazard curves are shown in Figures 9.6-1 to 9.6-4 for spectral periods of 0.0 (PGA), 0.2 sec, 1.0 sec, and 3.0 sec, respectively. The total hazard curve is interpolated using equation 7-1 to compute the equal hazard spectra for return periods of 1, 25, 50, 100, 500, 1000, 2000, 5000, and 10000 years. The equal hazard spectra are listed in Table 9.6-1 and are plotted in Figure 9.6-5a.

The spectral shape constraint is then applied. First, the spectral shape for each equal hazard spectrum is computed by dividing the spectral acceleration by the peak acceleration. The resulting spectral shape is then compared to the empirical constraint from Table 6-14 for periods less than 0.2 sec. For this case, the spectral values at periods of 0.03 and 0.1 sec fall below the empirical constraint. The modified spectra for these spectra periods are computed by scaling the PGA by the empirical spectral shape. The modified values are listed in Table 9.6-2 and they are plotted in Figure 9.6-5b.

The deaggregation in magnitude and distance space for a 2000 year return period for spectral periods of 0.0 (PGA), 0.2 sec, 1.0 sec, and 3.0 sec is shown in Figures 9.6-6, 9.6-7, 9.6-8, and 9.6-9, respectively. These plots show that at short periods (PGA and 0.2 sec), the hazard is dominated by moderate magnitude events with little contribution from the Cascadia – Little Salmon synchronous rupture. At long periods (1 sec and 3 sec), the situation is reversed with the hazard dominated by the Cascadia – Little Salmon synchronous rupture.

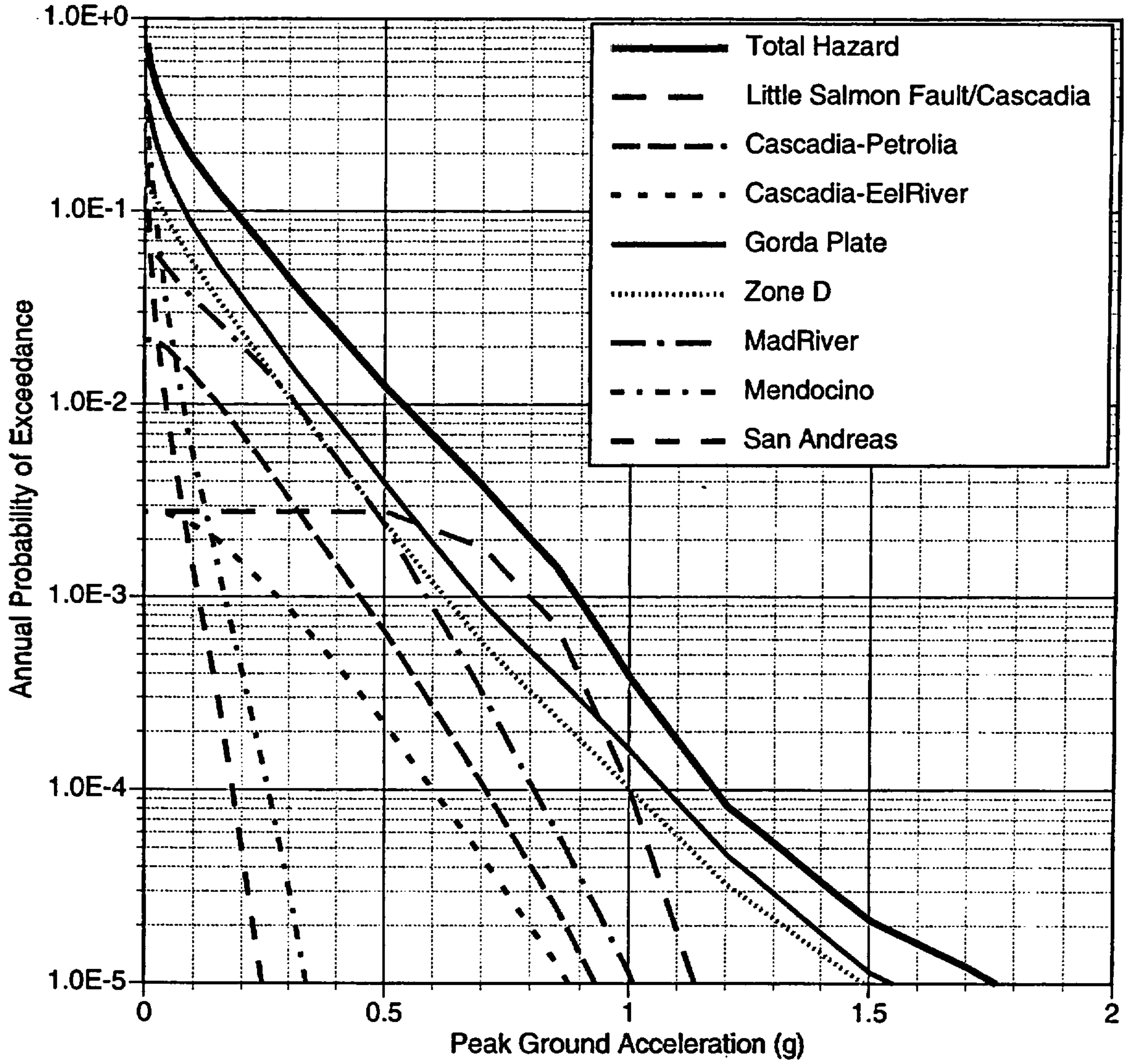

Figure 9.6-1. Mean hazard curve by source, FN component, Soil, PGA.

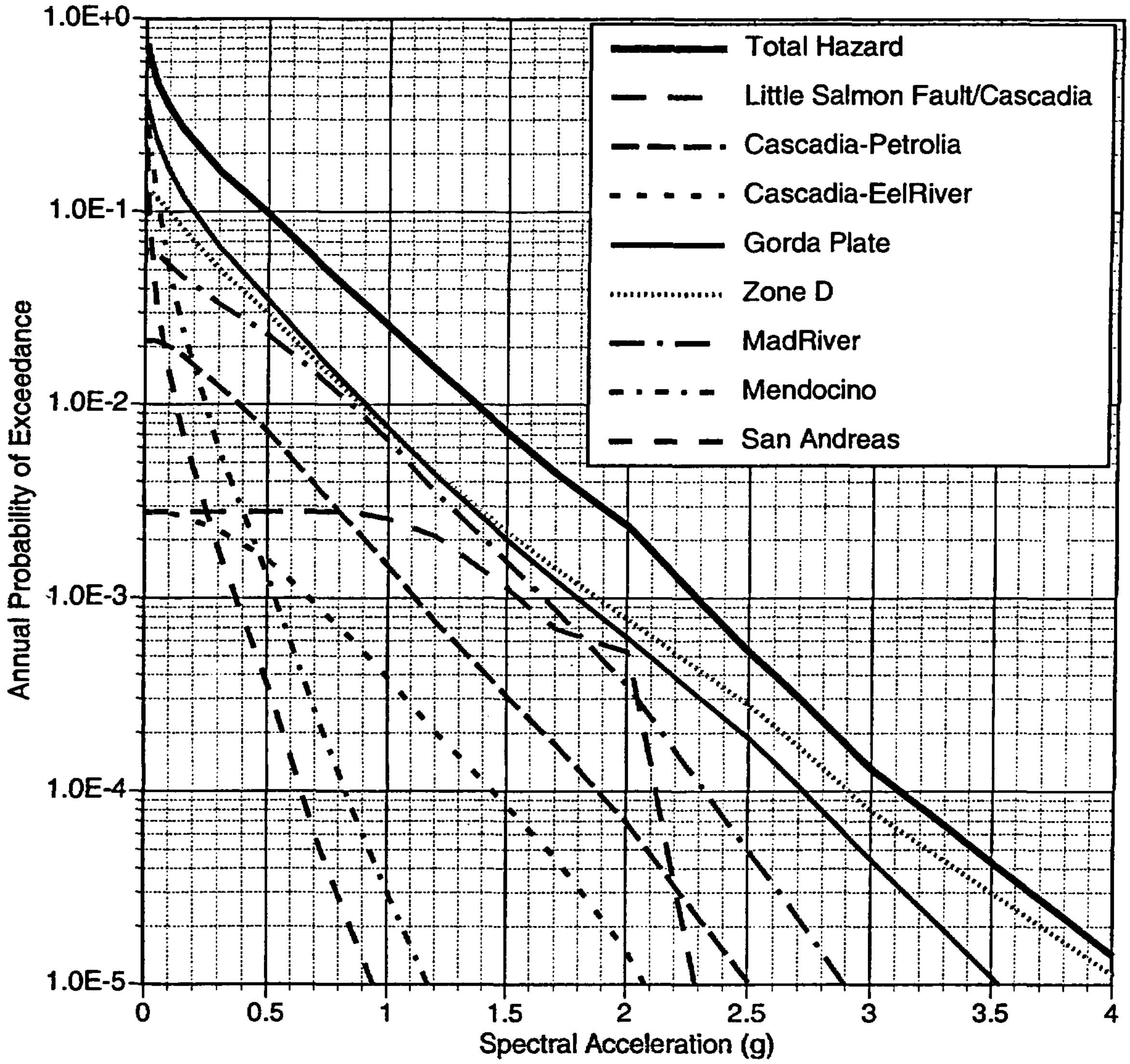

Figure 9.6-2. Mean hazard curve by source, FN component, Soil, T=0.2.

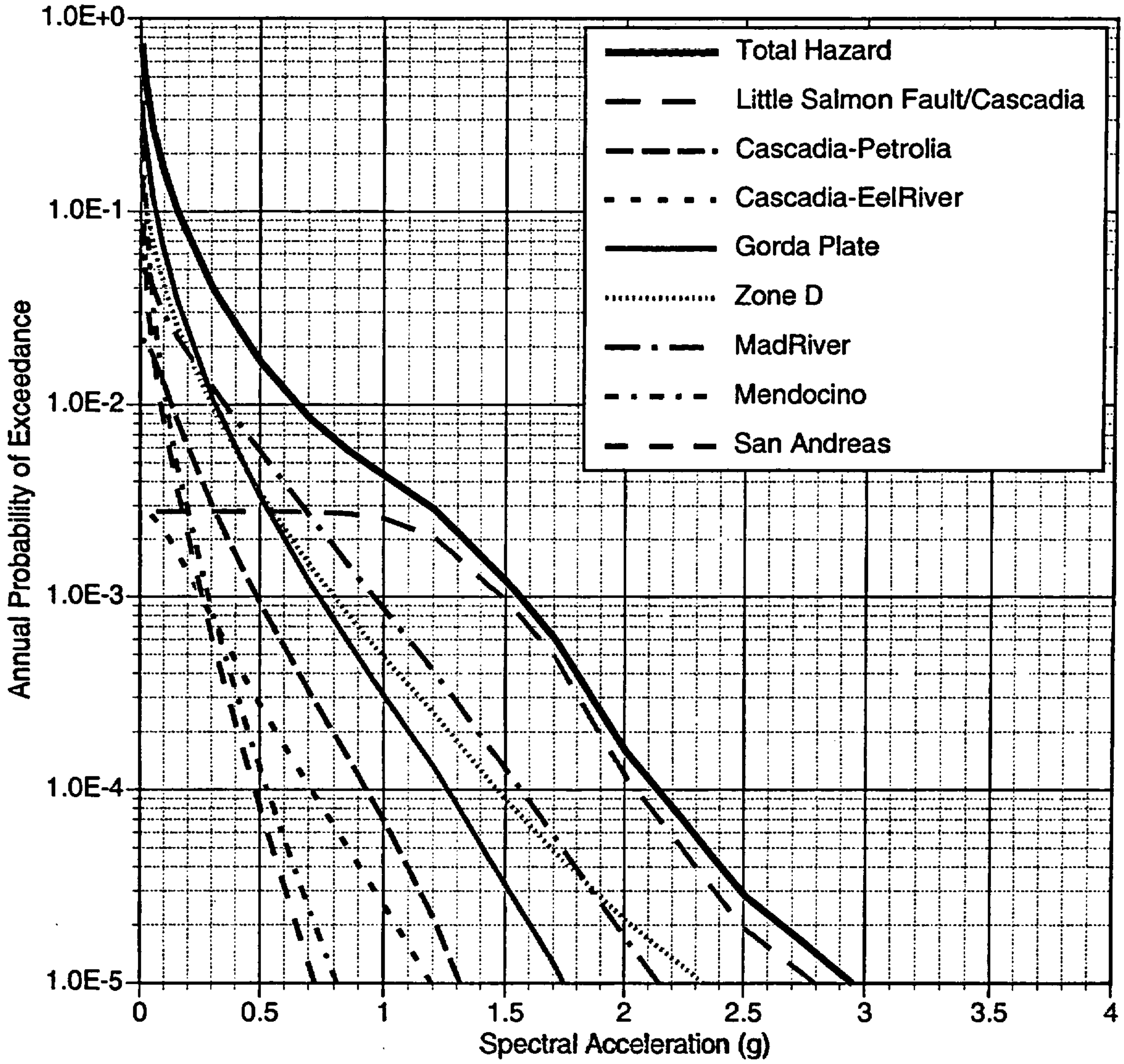

Figure 9.6-3. Mean hazard curve by source, FN component, Soil, T=1.0.

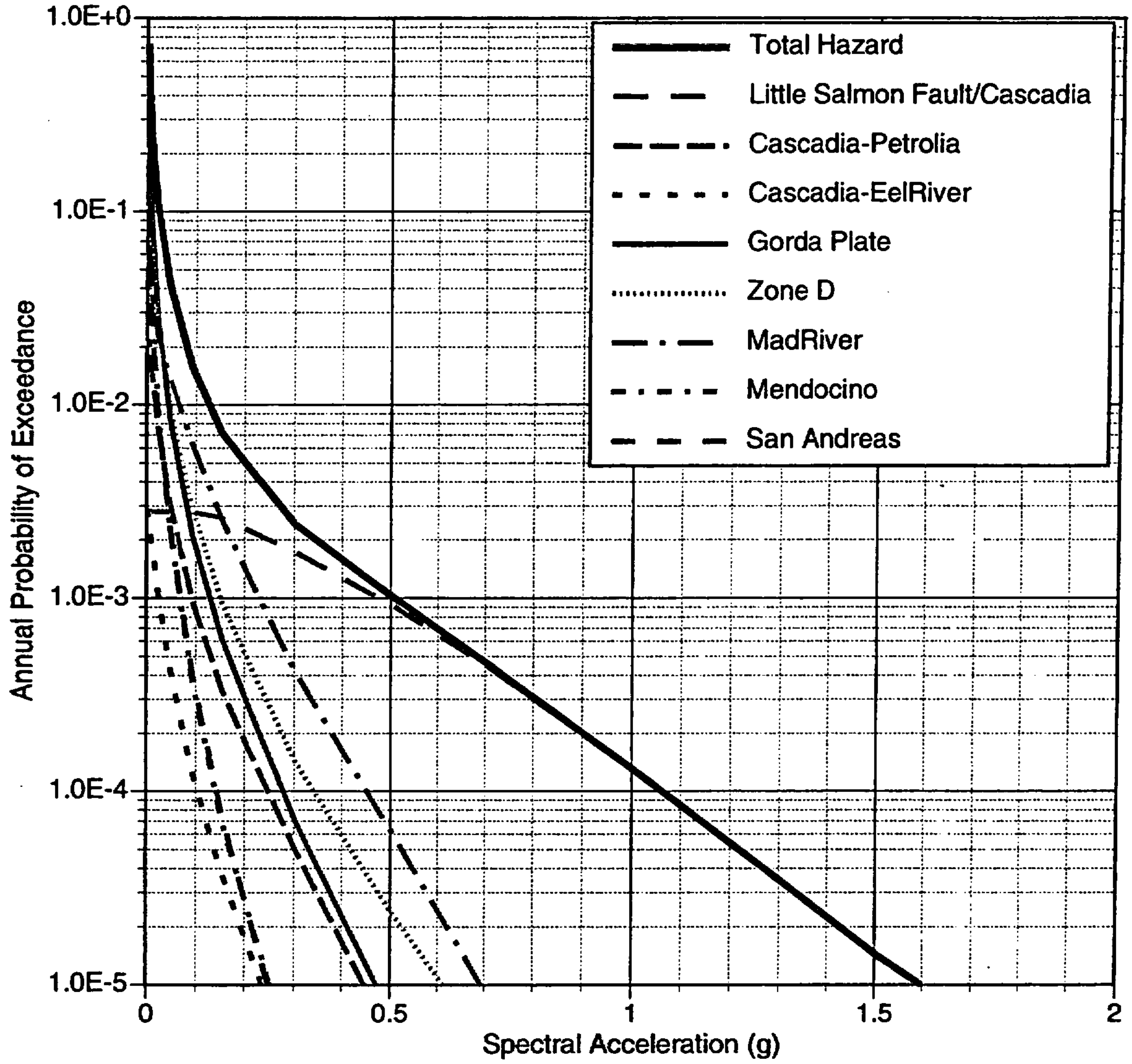

Figure 9.6-4. Mean hazard curve by source, FN component, Soil, T=3 sec.

Table 9.6-1 Equal hazard spectra (g) for the fault normal component for soil site conditions.

Period (sec)	1 Yr	25 yr	50 yr	100 yr	500 yr	1,000 yr	2,000 yr	5,000 yr	10,000 yr
0.01	0.0042	0.3118	0.4109	0.5294	0.7957	0.8890	0.9674	1.0798	1.1726
0.03	0.0042	0.3118	0.4109	0.5294	0.7957	0.8890	0.9674	1.0798	1.1726
0.10	0.0076	0.5219	0.6601	0.7940	1.0803	1.1889	1.3109	1.4922	1.6107
0.15	0.0088	0.6578	0.8621	1.0533	1.5286	1.6959	1.8015	1.9487	2.0767
0.20	0.0110	0.8266	1.0890	1.3608	2.0493	2.2716	2.5157	2.8337	3.1006
0.25	0.0104	0.8450	1.1837	1.5217	2.2760	2.6377	2.9280	3.2399	3.4770
0.30	0.0094	0.7644	1.1031	1.4322	2.2161	2.4778	2.7427	3.0941	3.3236
0.35	0.0087	0.6646	0.9734	1.3427	2.1535	2.4478	2.6454	2.8930	3.1113
0.40	0.0082	0.6128	0.8953	1.2384	2.0439	2.2503	2.4775	2.6986	2.8719
0.50	0.0069	0.5380	0.7870	1.0810	1.8927	2.1027	2.2800	2.5320	2.7128
0.60	0.0051	0.4335	0.6546	0.9338	1.7485	1.9607	2.1531	2.4228	2.6165
0.80	0.0040	0.3210	0.4837	0.6964	1.4445	1.6883	1.8618	2.0882	2.2517
1.00	0.0038	0.2985	0.4469	0.6452	1.3165	1.5507	1.7382	1.9419	2.1210
1.50	0.0025	0.2000	0.3196	0.4764	1.0821	1.3129	1.5282	1.8083	2.0373
2.00	0.0013	0.1205	0.1967	0.3111	0.8237	1.0551	1.2766	1.5738	1.7904
3.00	0.0001	0.0465	0.0763	0.1216	0.3356	0.5055	0.6782	0.8977	1.0571

Table 9.6-4 Equal hazard spectra (g) for the fault normal component for soil site conditions with spectral shape constraints.

Period (sec)	1 Yr	25 yr	50 yr	100 yr	500 yr	1,000 yr	2,000 yr	5,000 yr	10,000 yr
0.01	0.0042	0.3118	0.4109	0.5294	0.7957	0.8890	0.9674	1.0798	1.1726
0.03	0.0043	0.3168	0.4175	0.5379	0.8084	0.9032	0.9829	1.0971	1.1914
0.10	0.0076	0.5219	0.6601	0.7940	1.1012	1.2304	1.3389	1.4944	1.6229
0.15	0.0088	0.6578	0.8621	1.0533	1.5286	1.6959	1.8015	1.9487	2.0767
0.20	0.0110	0.8266	1.0890	1.3608	2.0493	2.2716	2.5157	2.8337	3.1006
0.25	0.0104	0.8450	1.1837	1.5217	2.2760	2.6377	2.9280	3.2399	3.4770
0.30	0.0094	0.7644	1.1031	1.4322	2.2161	2.4778	2.7427	3.0941	3.3236
0.35	0.0087	0.6646	0.9734	1.3427	2.1535	2.4478	2.6454	2.8930	3.1113
0.40	0.0082	0.6128	0.8953	1.2384	2.0439	2.2503	2.4775	2.6986	2.8719
0.50	0.0069	0.5380	0.7870	1.0810	1.8927	2.1027	2.2800	2.5320	2.7128
0.60	0.0051	0.4335	0.6546	0.9338	1.7485	1.9607	2.1531	2.4228	2.6165
0.80	0.0040	0.3210	0.4837	0.6964	1.4445	1.6883	1.8618	2.0882	2.2517
1.00	0.0038	0.2985	0.4469	0.6452	1.3165	1.5507	1.7382	1.9419	2.1210
1.50	0.0025	0.2000	0.3196	0.4764	1.0821	1.3129	1.5282	1.8083	2.0373
2.00	0.0013	0.1205	0.1967	0.3111	0.8237	1.0551	1.2766	1.5738	1.7904
3.00	0.0001	0.0465	0.0763	0.1216	0.3356	0.5055	0.6782	0.8977	1.0571

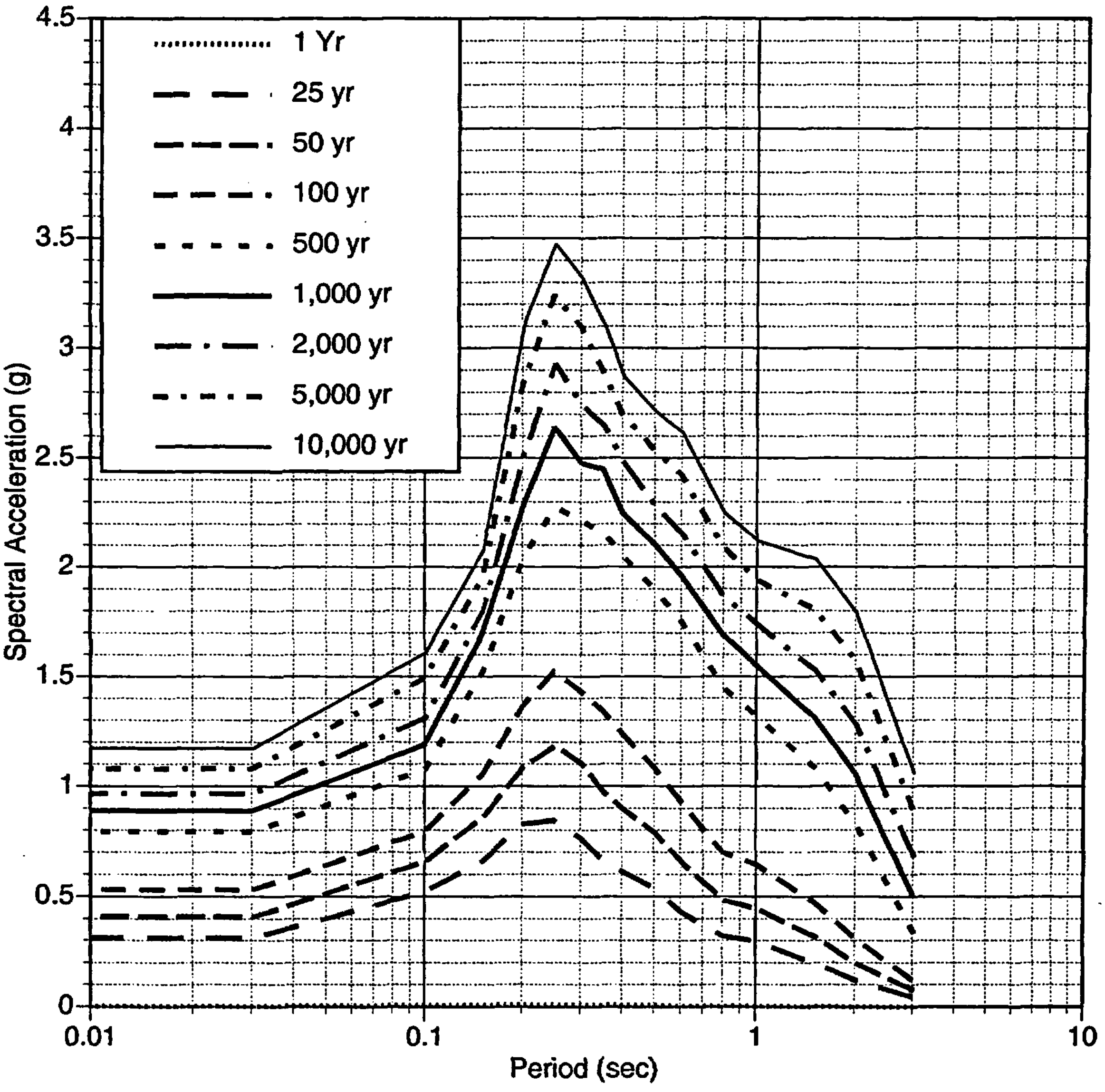

Figure 9.6-5a. Equal hazard spectra for the FN component, soil site conditions before the spectral shape constraint is applied.

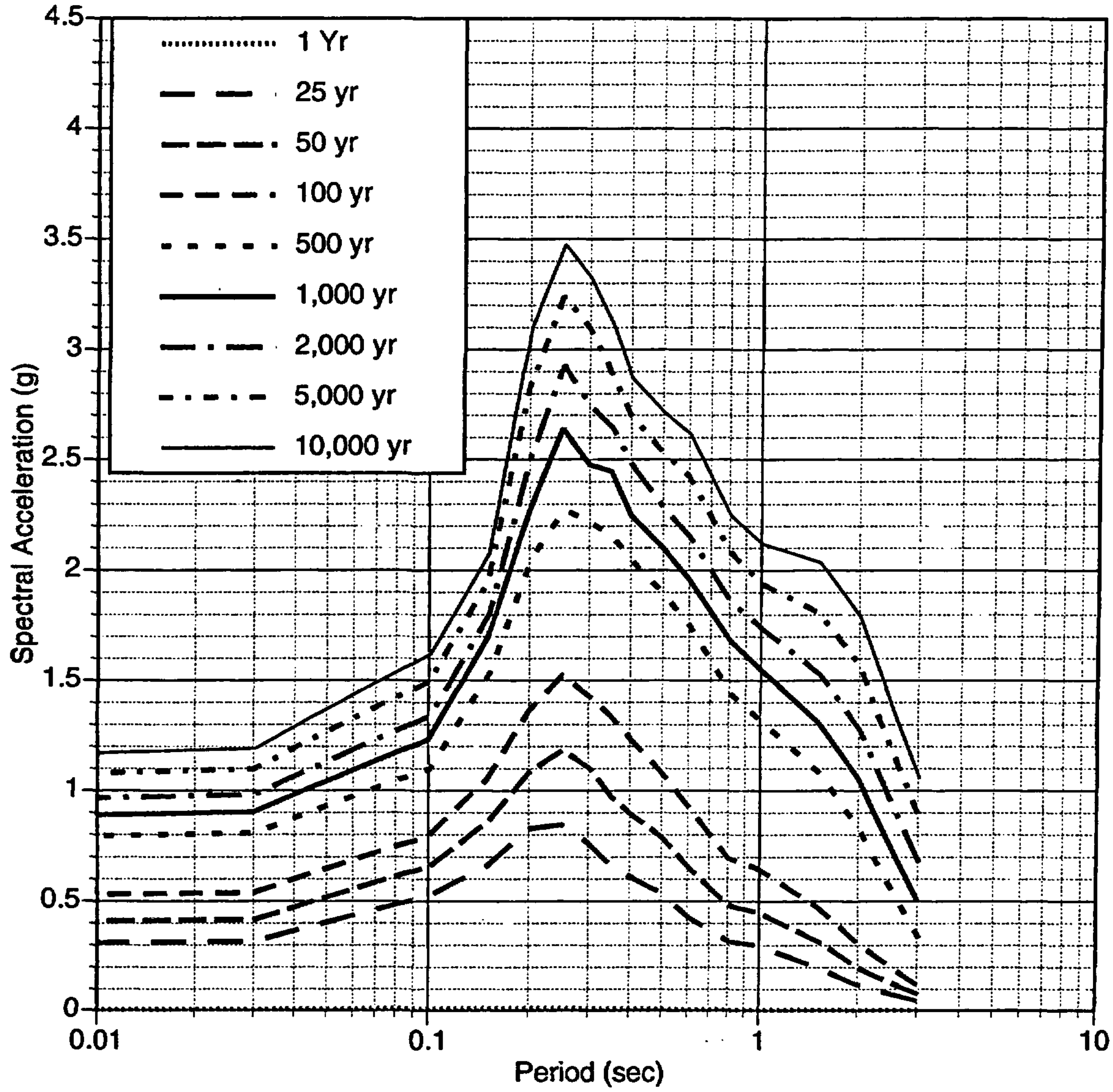

Figure 9.6-5b. Equal hazard spectra for the FN component, soil site conditions after the spectral shape constraint is applied.

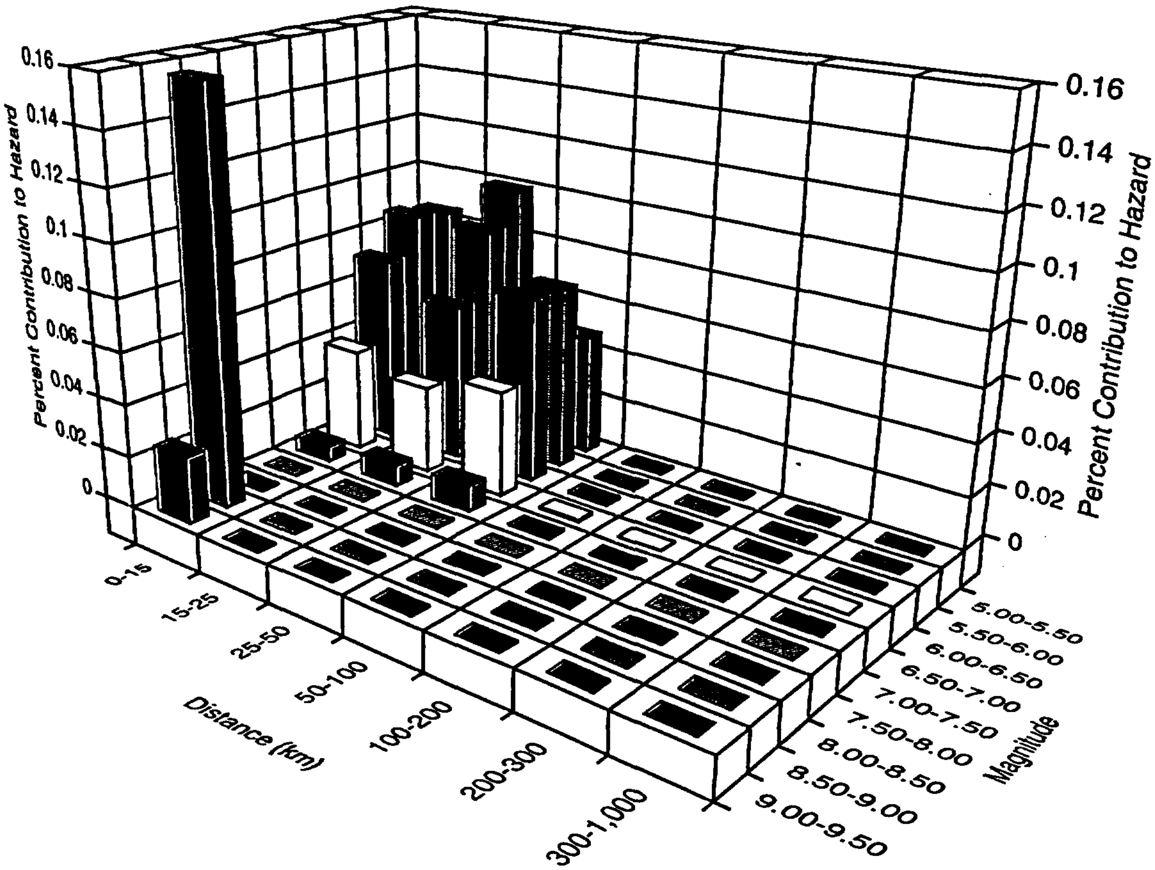

Figure 9.6-6 Deaggregation for the FN component, Soil site conditions, PGA, for a 2,000 yr return period.

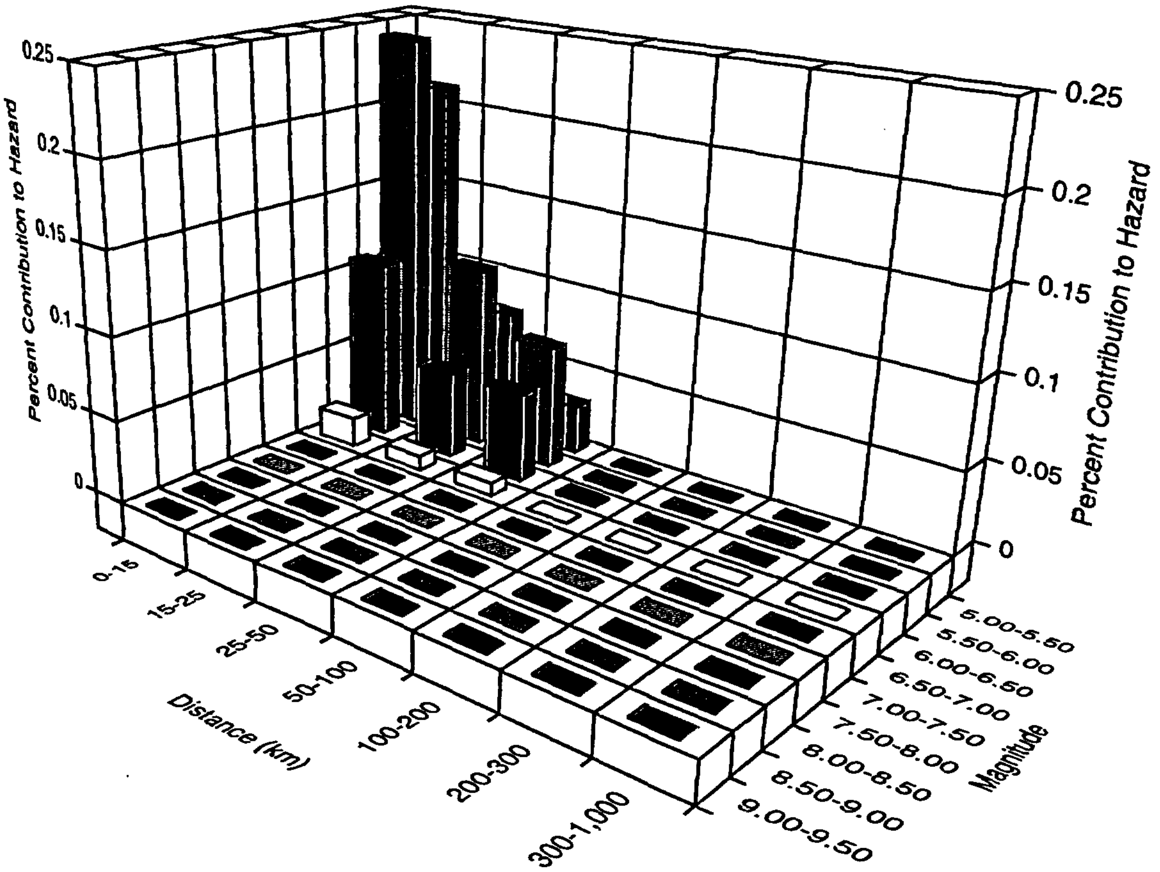

Figure 9.6-7 Deaggregation for the FN component, Soil site conditions, T=0.2 sec, for a 2,000 yr return period.

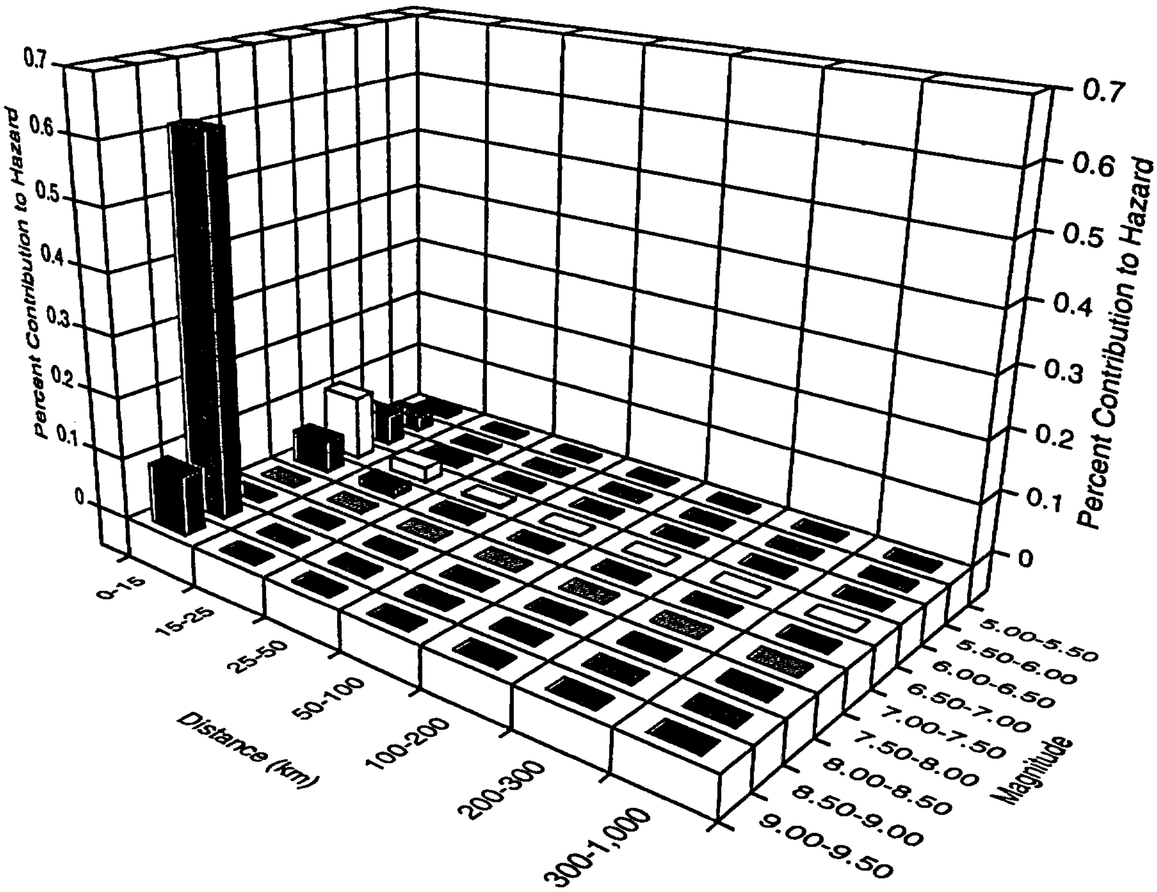

Figure 9.6-8 Deaggregation for the FN component, Soil site conditions, T=1.0 sec, for a 2,000 yr return period.

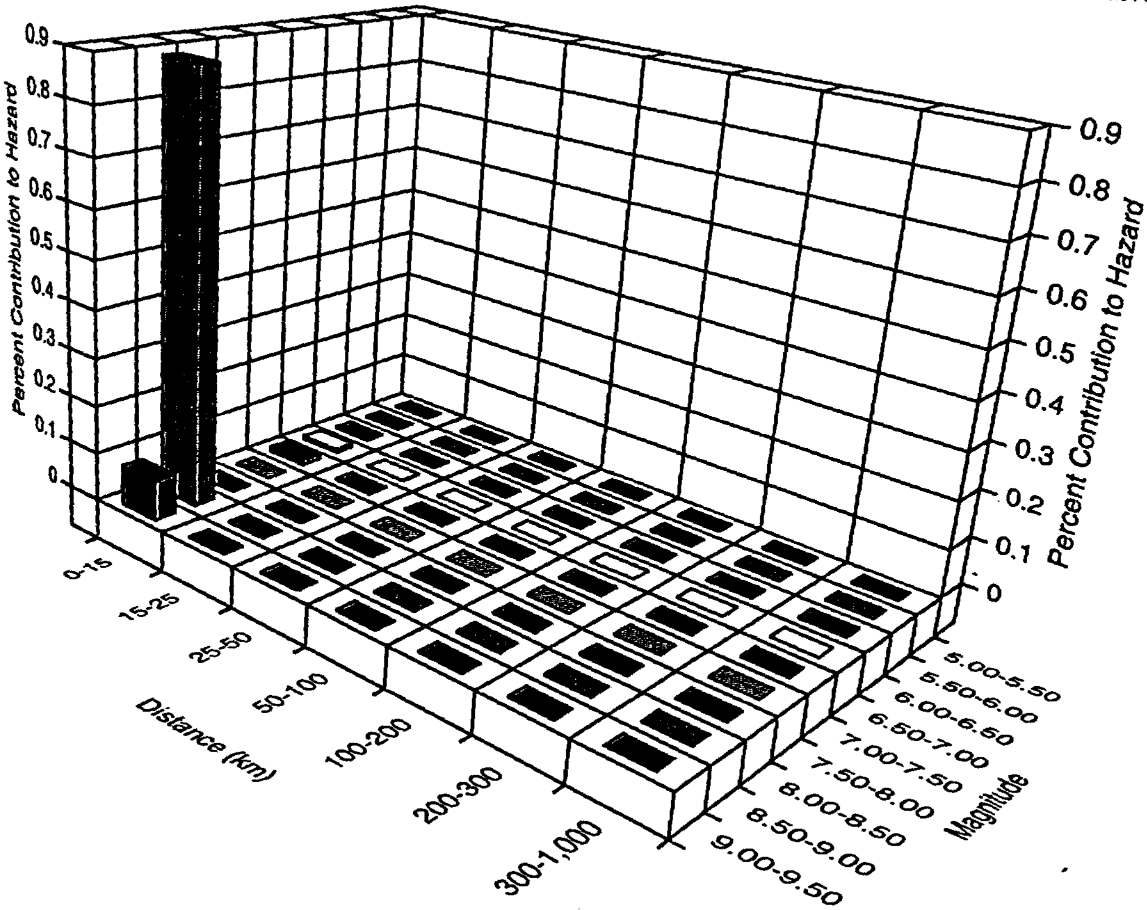

Figure 9.6-9 Deaggregation for the FN component, Soil site conditions, T=3.0 sec, for a 2,000 yr return period.

9.7 Soil Hazard for the Fault Parallel Component

The FP component is identical to the FN component for periods less than 0.6 sec. Therefore, the hazard is only recomputed for spectral period of 0.8 sec, 1.0 sec, 1.5 sec, 2.0 sec, and 3.0 sec.

The hazard curves are shown in Figures 9.7-1 to 9.7-2 for spectral periods1.0 sec, and 3.0 sec, respectively. The total hazard curve is interpolated using equation 7-1 to compute the equal hazard spectra for return periods of 1, 25, 50, 100, 500, 1000, 2000, 5000, and 10000 years. The equal hazard spectra are listed in Table 9.7-1 and are plotted in Figure 9.7-3a.

The spectral shape constraint is taken from the FN component since it is the same. The equal hazard spectra with the spectral shape constraint is shown in Figure 9.7-3b.

The deaggregation in magnitude and distance space for a 2000 year return period for spectral periods of 1.0 sec, and 3.0 sec is shown in Figures 9.7-4 and 9.7-5, respectively. These plots show that at long periods, the hazard dominated by the Cascadia – Little Salmon synchronous rupture.

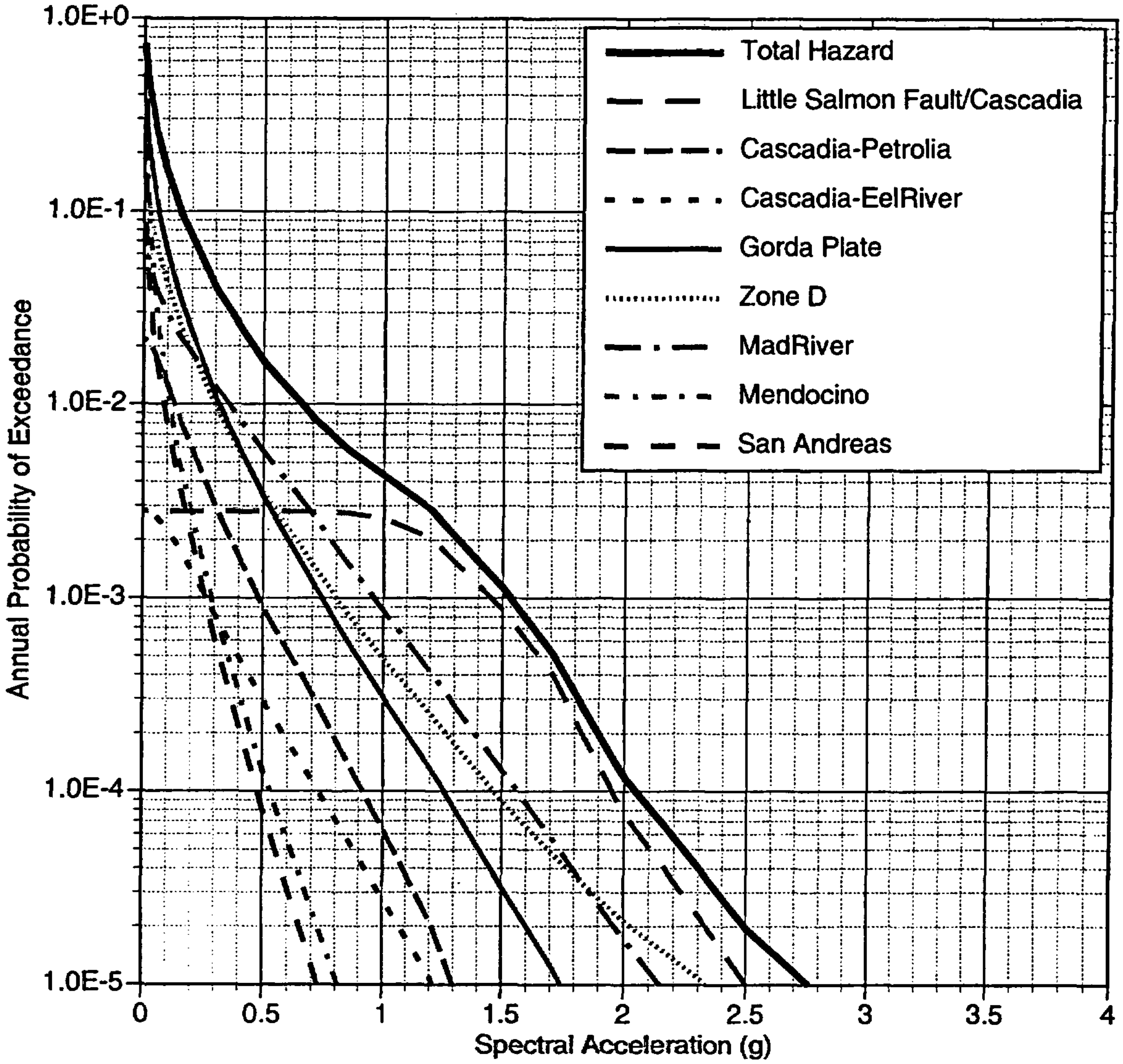

Figure 9.7-1. Mean hazard curve by source, FP component, Soil, T=1.0 sec

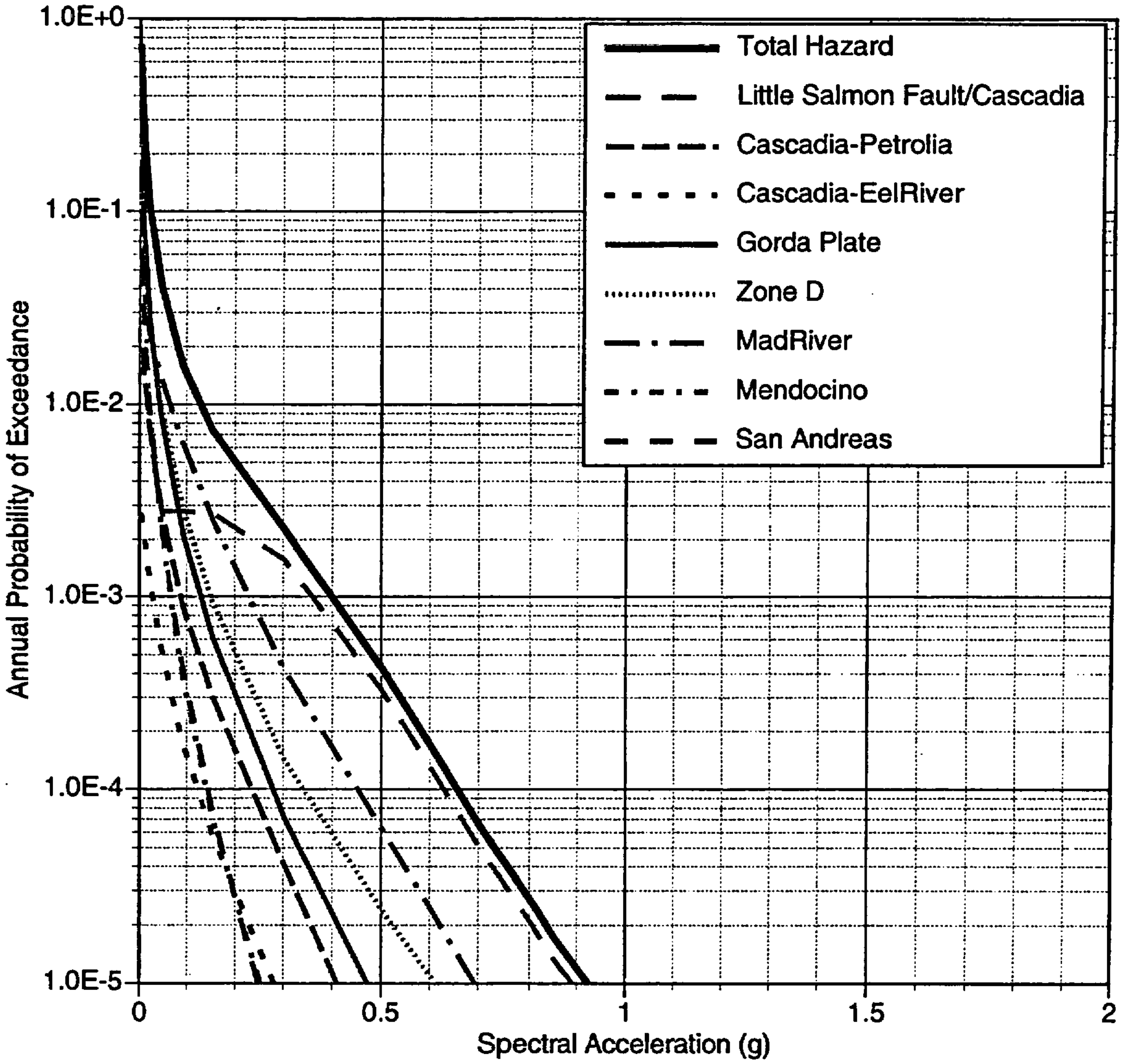

Figure 9.7-2. Mean hazard curve by source, FP component, Soil, T=3.0 sec

Table 9.7-1 Equal hazard spectra (g) for the fault parallel component for soil site conditions.

Period (sec)	1 Yr	25 yr	50 yr	100 yr	500 yr	1,000 yr	2,000 yr	5,000 yr	10,000 yr
0.01	0.0042	0.3118	0.4109	0.5294	0.7957	0.8890	0.9674	1.0798	1.1726
0.03	0.0042	0.3118	0.4109	0.5294	0.7957	0.8890	0.9674	1.0798	1.1726
0.10	0.0076	0.5219	0.6601	0.7940	1.0803	1.1889	1.3109	1.4922	1.6107
0.15	0.0088	0.6578	0.8621	1.0533	1.5286	1.6959	1.8015	1.9487	2.0767
0.20	0.0110	0.8266	1.0890	1.3608	2.0493	2.2716	2.5157	2.8337	3.1006
0.25	0.0104	0.8450	1.1837	1.5217	2.2760	2.6377	2.9280	3.2399	3.4770
0.30	0.0094	0.7644	1.1031	1.4322	2.2161	2.4778	2.7427	3.0941	3.3236
0.35	0.0087	0.6646	0.9734	1.3427	2.1535	2.4478	2.6454	2.8930	3.1113
0.40	0.0082	0.6128	0.8953	1.2384	2.0439	2.2503	2.4775	2.6986	2.8719
0.50	0.0069	0.5380	0.7870	1.0810	1.8927	2.1027	2.2800	2.5320	2.7128
0.60	0.0051	0.4335	0.6546	0.9338	1.7485	1.9607	2.1531	2.4228	2.6165
0.80	0.0040	0.3210	0.4838	0.6959	1.4360	1.6696	1.8373	2.0551	2.2098
1.00	0.0038	0.2985	0.4468	0.6452	1.3053	1.5272	1.7066	1.8845	2.0361
1.50	0.0025	0.2000	0.3196	0.4766	1.0630	1.2631	1.4237	1.6423	1.8033
2.00	0.0013	0.1205	0.1966	0.3114	0.7924	0.9638	1.1069	1.2808	1.4055
3.00	0.0001	0.0464	0.0763	0.1223	0.3109	0.3840	0.4744	0.5714	0.6470

Table 9.7-4 Equal hazard spectra (g) for the fault parallel component for soil site conditions with the spectral shape constraint.

Period (sec)	1 Yr	25 yr	50 yr	100 yr	500 yr	1,000 yr	2,000 yr	5,000 yr	10,000 yr
0.01	0.0042	0.3118	0.4109	0.5294	0.7957	0.8890	0.9674	1.0798	1.1726
0.03	0.0043	0.3168	0.4175	0.5379	0.8084	0.9032	0.9829	1.0971	1.1914
0.10	0.0076	0.5219	0.6601	0.7940	1.1012	1.2304	1.3389	1.4944	1.6229
0.15	0.0088	0.6578	0.8621	1.0533	1.5286	1.6959	1.8015	1.9487	2.0767
0.20	0.0110	0.8266	1.0890	1.3608	2.0493	2.2716	2.5157	2.8337	3.1006
0.25	0.0104	0.8450	1.1837	1.5217	2.2760	2.6377	2.9280	3.2399	3.4770
0.30	0.0094	0.7644	1.1031	1.4322	2.2161	2.4778	2.7427	3.0941	3.3236
0.35	0.0087	0.6646	0.9734	1.3427	2.1535	2.4478	2.6454	2.8930	3.1113
0.40	0.0082	0.6128	0.8953	1.2384	2.0439	2.2503	2.4775	2.6986	2.8719
0.50	0.0069	0.5380	0.7870	1.0810	1.8927	2.1027	2.2800	2.5320	2.7128
0.60	0.0051	0.4335	0.6546	0.9338	1.7485	1.9607	2.1531	2.4228	2.6165
0.80	0.0040	0.3210	0.4838	0.6959	1.4360	1.6696	1.8373	2.0551	2.2098
1.00	0.0038	0.2985	0.4468	0.6452	1.3053	1.5272	1.7066	1.8845	2.0361
1.50	0.0025	0.2000	0.3196	0.4766	1.0630	1.2631	1.4237	1.6423	1.8033
2.00	0.0013	0.1205	0.1966	0.3114	0.7924	0.9638	1.1069	1.2808	1.4055
3.00	0.0001	0.0464	0.0763	0.1223	0.3109	0.3840	0.4744	0.5714	0.6470

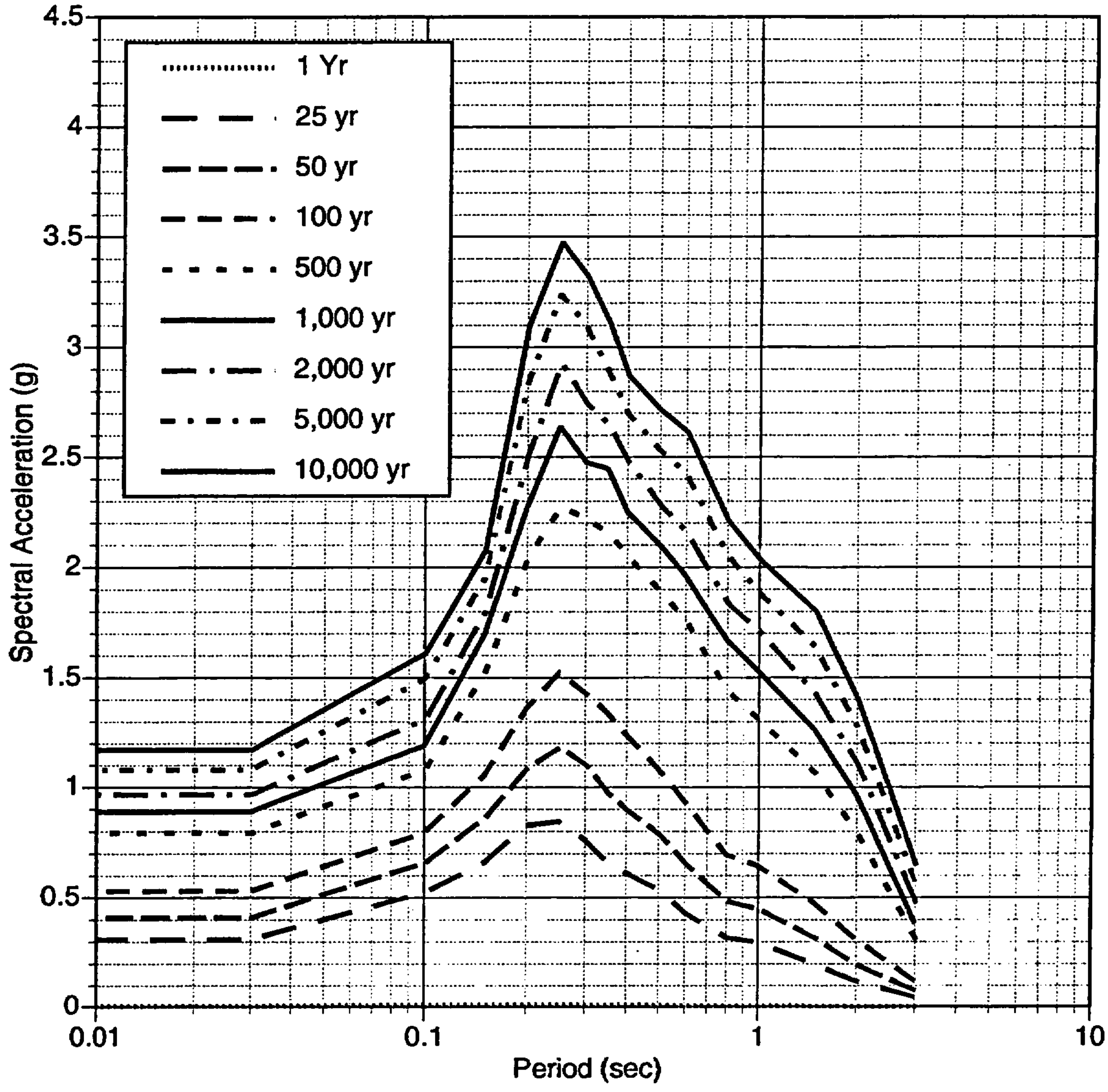

Figure 9.7-3a. Equal hazard spectra for the FP component, soil site conditions before the spectral shape constraint is applied.

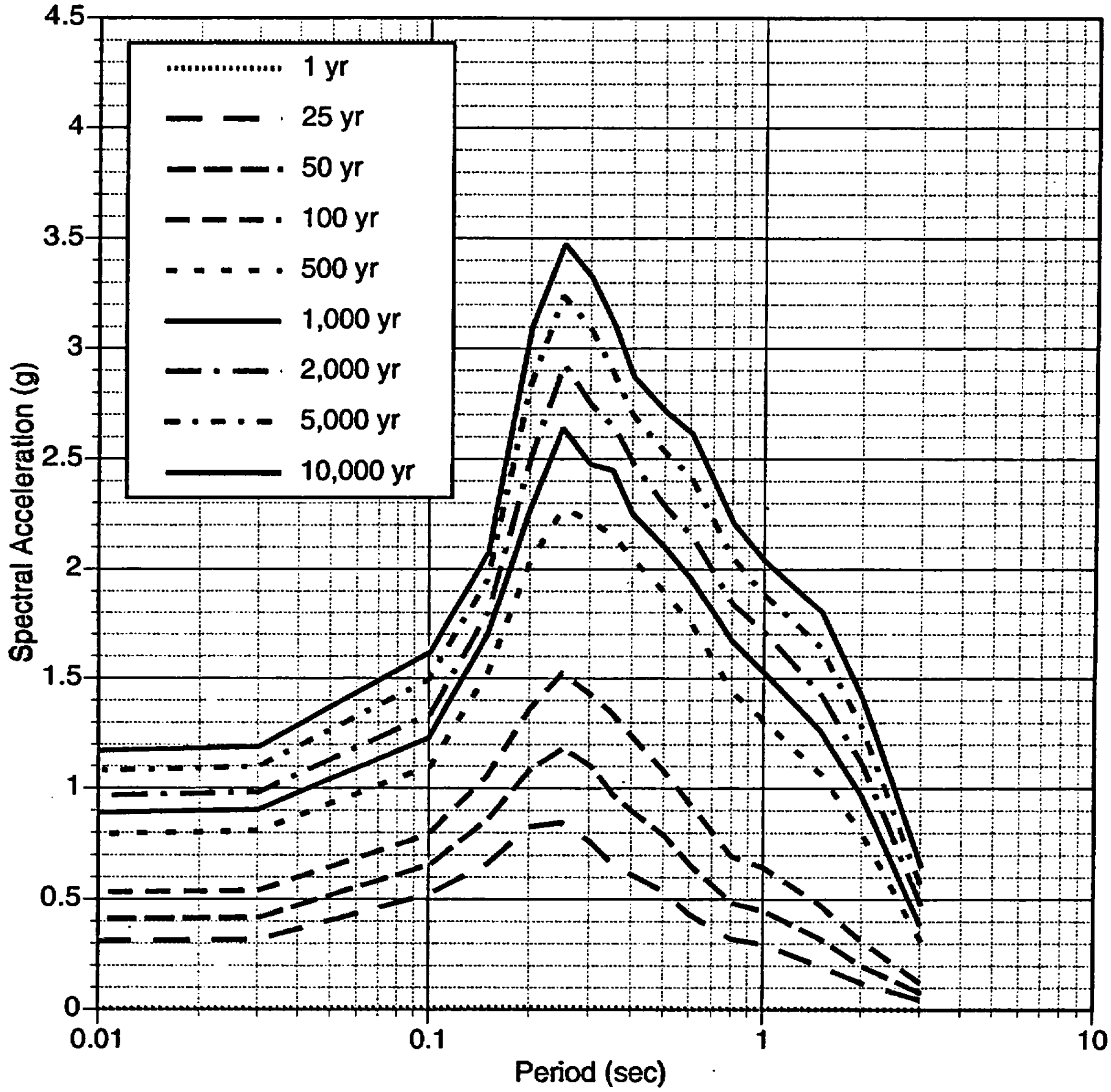

Figure 9.7-3b. Equal hazard spectra for the FP component, soil site conditions after the spectral shape constraint is applied.

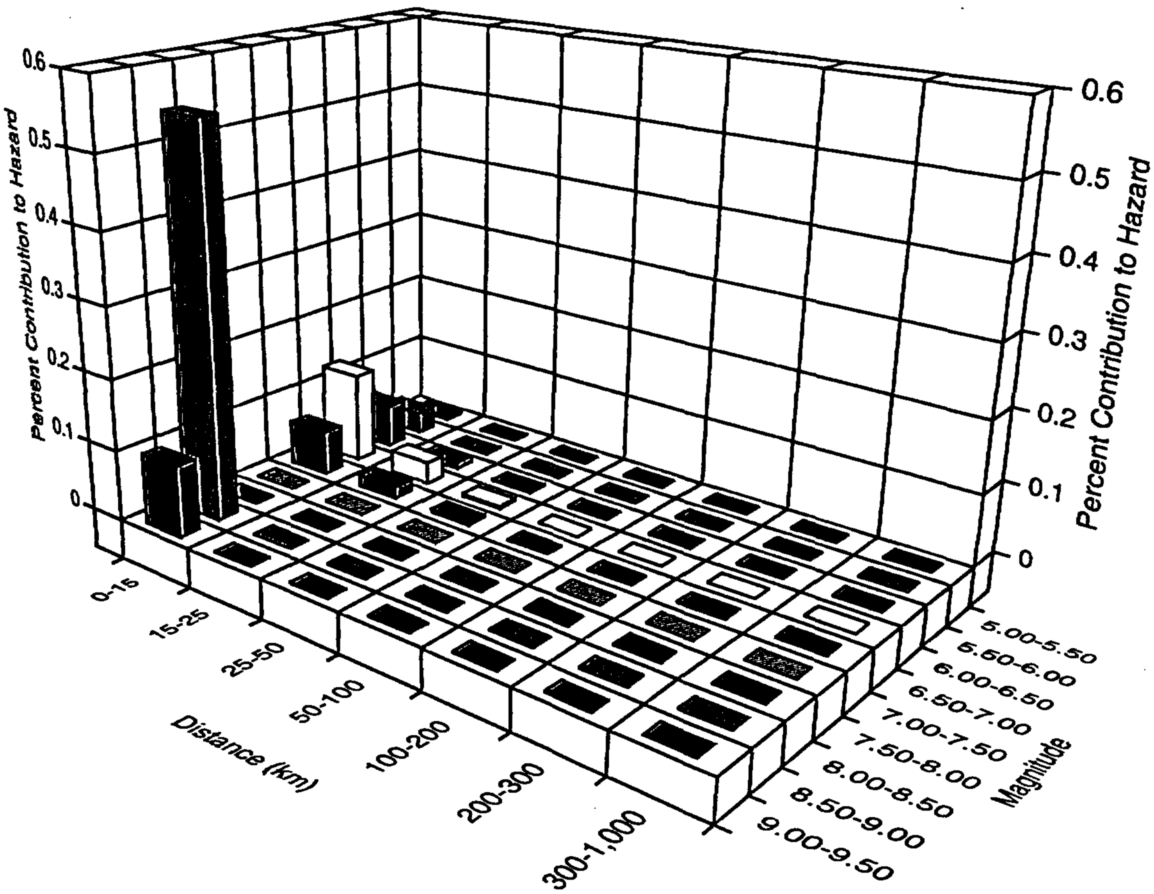

Figure 9.7-4 Deaggregation for the FP component, Soil site conditions, T=1.0 sec, for a 2,000 yr return period.

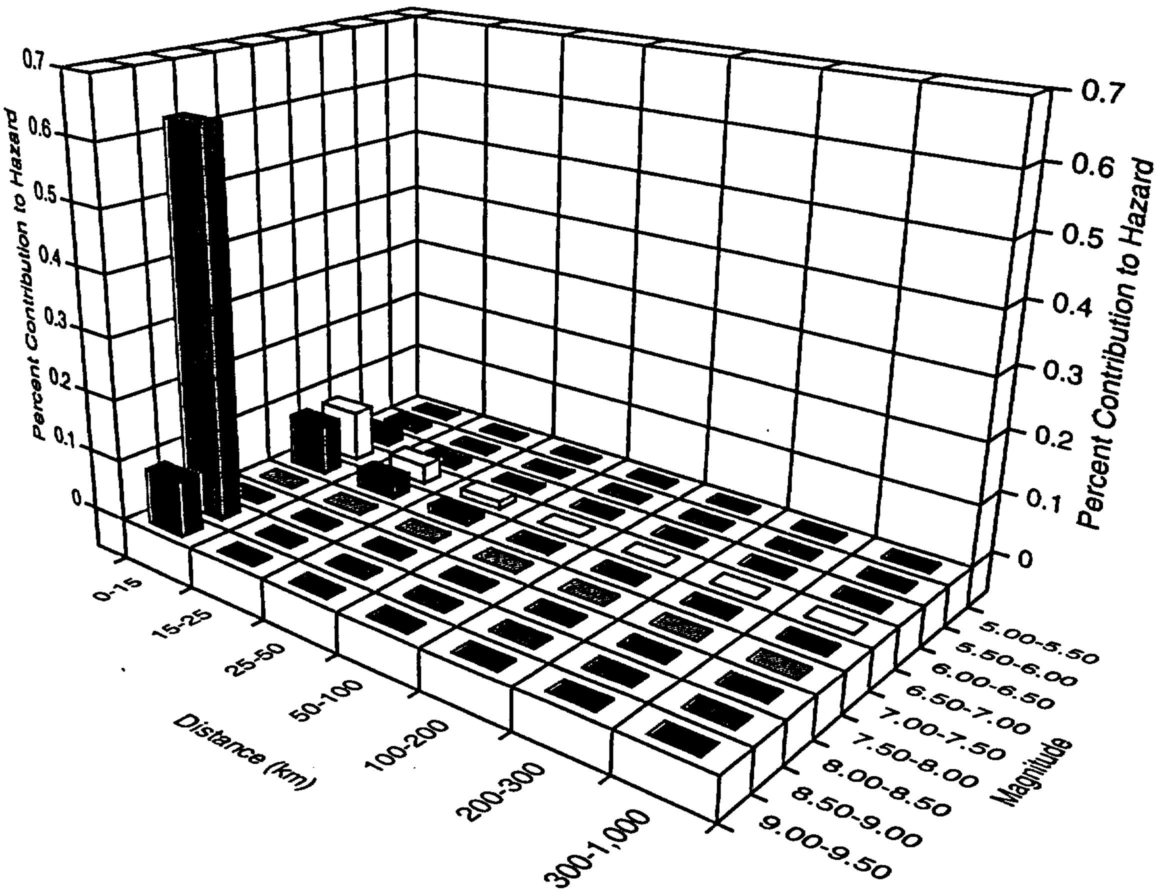

Figure 9.7-5 Deaggregation for the FP component, Soil site conditions, T=3.0 sec, for a 2,000 yr return period.

9.8 Equal Hazard Spectra for the Vertical Component

Following the method described in section 7.2.9, the vertical spectra are computed by scaling the average rock horizontal spectra from sections 9.4 and 9.5 by the ratio of the vertical soil spectrum to the horizontal rock spectral acceleration at T=0.1 sec and T=1 sec computed for the controlling source at 0.1 sec and 1 sec, respectively, and then taking the larger of the two.

The average horizontal spectra are computed in Table 9.8-1 using the geometric mean of the fault normal and fault parallel components for the rock motion.

The controlling magnitude and distance for T=0.1 sec and T=1 sec are given in Table 9-8-2 for each return period.

Using these magnitudes and distances, the horizontal spectral acceleration on rock is computed using the Abrahamson and Silva attenuation relation (for rock sites) given in Section 7.3.5 with the magnitude and distances given in Table 9.8-2. These horizontal spectral accelerations are given in Table 9.8-3.

Next, for each return period, the vertical spectrum on soil is computed computed using the Abrahamson and Silva attenuation relation (for soil sites) given in Section 7.3.5 using the magnitudes and distances given in Table 9.8-2. The values are listed in Tables 9.8-4 to 9.8-11 for return periods from 1 to 10,000 years.

The vertical spectra values (columns 3 and 4) are multiplied by the horzontal spectrum (column 2) and then divided by the corresponding horizontal acceleration given in Table 9.8-3. The resulting vertical spectral valuesare listed in columns 5 and 6 in Table 9.8-4 to 9.8-11.

Finally, the larger of the two spectral values at each period (columns 5 and 6) is given in the last column of Tables 9.8-4 to 9.8-11.

The resulting equal hazard spectra for the vertical component are summarized in Table 9.8-12 and are plotted in Figure 9.8-1.

Table 9.8-1. Equal hazard spectra for the average horizontal component for rock.

Period (sec)	1 Yr	25 yr	50 yr	100 yr	500 yr	1,000 yr	2,000 yr	5,000 yr	10,000 yr
0.01	0,0031	0.2392	0.3567	0.5050	1.0038	1.2046	1.3770	1.6116	1.7746
0.03	0.0031	0.2392	0.3567	0.5050	1.0038	1.2046	1.3770	1.6116	1.7746
0.10	0.0051	0.4739	0.7003	0.9874	1.9180	2.2938	2.6647	3.1087	3.3901
0.15	0.0056	0.5147	0.7643	1.0870	2.1860	2.6738	3.1111	3.6067	4.0334
0.20	0.0057	0.5180	0.7738	1.1064	2.2869	2.8133	3.2488	3.8176	4.3133
0.25	0.0054	0.4738	0.7142	1.0262	2.1669	2.6883	3.1470	3.6958	4.1736
0.30	0.0050	0.4351	0.6610	0.9558	2.0612	2.5685	3.0401	3.5653	4.0221
0.40	0.0042	0.3615	0.5530	0.8053	1.7978	2.2449	2.6815	3.2065	3.5847
0.50	0.0037	0.3126	0.4766	0.6962	1.6081	2.0283	2.3997	2.8776	3.1860
0.60	0.0032	0.2557	0.3943	0.5830	1.3696	1.7500	2.0821	2.5074	2.8100
0.80	0.0022	0.1839	0.2867	0.4247	1.0494	1.2421	1.3854	1.5770	1.7165
1.00	0.0017	0.1439	0.2202	0.3336	0.8422	1.0073	1.1302	1.2872	1.4069
1.50	0.0011	0.0860	0.1350	0.2053	0.5142	0.6283	0.7436	0.8671	0.9611
2.00	0.0005	0.0575	0.0926	0.1400	0.3392	0.4310	0.5259	0.6305	0.7030
3.00	0.0002	0.0291	0.0483	0.0745	0.1787	0.2344	0.2915	0.3772	0.4283

Table 9.8-2a. Mean magnitude from the deaggregation of the horizontal component.

Period (sec)	1 Yr	25 yr	50 yr	100 yr	500 yr	1,000 yr	2,000 yr	5,000 yr	10,000 yr
0.10	5.58	6.31	6.54	6.89	7.74	7.80	7.78	7.61	7.36
1.00	5.61	6.60	6.85	7.23	8.48	8.55	8.54	8.50	8.46

Table 9.8-2b. Mean distance from the deaggregation of the horizontal component.

Period (sec)	1 Yr	25 yr	50 yr	100 yr	500 yr	1,000 yr	2,000 yr	5,000 yr	10,000 yr
0.10	99.7	25.4	21.3	16.9	8.1	7.1	6.7	6.5	6.1
1.00	106.7	29.0	23.3	16.2	2.8	2.3	2.2	2.2	2.2

Table 9.8-3 Median horizontal spectral acceleration on rock using the Abrahamson and Silva (1997) attenuation relation with the event defined based on the deaggregation (from Table 9.8-2)

Return Period (yr)	Mean Mag for T=0.1	Mean Distance (km) for T=0.1	Horizontal Rock Sa (g) at T=0.1 sec	Mean Mag for T=1	Mean Distance (km) for T=1	Horizontal Rock Sa(g) at T=1 sec
1	5.58	99.7	0.020	5.61	106.7	0.019
25	6.31	25.4	0.216	6.60	29.0	0.217
50	6.54	21.3	0.296	6.85	23.3	0.295
100	6.89	16.9	0.409	7.23	16.2	0.465
500	7.74	8.1	0.896	8.48*	2.8	1.416
1,000	7.80	7.1	0.981	8.55*	2.3	1.459
2,000	7.78	6.7	1.010	8.54*	2.2	1.468
5,000	7.61	6.5	0.996	8.50*	2.2	1.468
10,000	7.36	6.1	0.991	8.46*	2.2	1.468

* largest magnitude used is 8.0 because the Abrahamson and Silva attenuation relation is not reliable for M>8.

Table 9.8-4. Development of the vertical spectral for a return period of 1 year.

Vertical Spectrum: 1 year, Soil						
Period (sec)	Horizontal, 1 yr	Median Vertical Sa (g) Using T=0.1 sec M,D	Median Vertical Sa (g) Using T=1 sec M,D	T=0.1 Sec Vertical Soil Spectrum (g)	T=1 Sec Vertical Soil Spectrum (g)	Vertical Soil Spectrum 1 yr
0.01	0.0031	0.0069	0.0066	0.0011	0.0011	0.0011
0.03	0.0031	0.0081	0.0077	0.0013	0.0013	0.0013
0.10	0.0051	0.0116	0.0109	0.0030	0.0029	0.0030
0.15	0.0056	0.0141	0.0134	0.0039	0.0039	0.0039
0.20	0.0057	0.0139	0.0134	0.0040	0.0040	0.0040
0.25	0.0054	0.0137	0.0133	0.0037	0.0038	0.0038
0.30	0.0050	0.0133	0.0129	0.0033	0.0034	0.0034
0.40	0.0042	0.0118	0.0115	0.0025	0.0025	0.0025
0.50	0.0037	0.0104	0.0102	0.0019	0.0020	0.0020
0.60	0.0032	0.0098	0.0097	0.0016	0.0016	0.0016
0.80	0.0022	0.0085	0.0084	0.0009	0.0010	0.0010
1.00	0.0017	0.0067	0.0067	0.0006	0.0006	0.0006
1.50	0.0011	0.0043	0.0043	0.0002	0.0002	0.0002
2.00	0.0005	0.0030	0.0030	0.0001	0.0001	0.0001
3.00	0.0002	0.0013	0.0013	0.0000	0.0000	0.0000

Table 9.8-5. Development of the vertical spectral for a return period of 25 years.

Vertical Spectrum: 25 year, Soil						
Period (sec)	Horizontal, 25 yr	Median Vertical Sa (g) Using T=0.1 sec M,D	Median Vertical Sa (g) Using T=1 sec M,D	T=0.1 Sec Vertical Soil Spectrum (g)	T=1 Sec Vertical Soil Spectrum (g)	Vertical Soil Spectrum 25 yr
0.01	0.2392	0.0848	0.0878	0.0939	0.0968	0.0968
0.03	0.2392	0.1084	0.1114	0.1200	0.1228	0.1228
0.10	0.4739	0.1688	0.1729	0.3703	0.3776	0.3776
0.15	0.5147	0.1683	0.1766	0.4010	0.4189	0.4189
0.20	0.5180	0.1457	0.1553	0.3494	0.3707	0.3707
0.25	0.4738	0.1296	0.1399	0.2843	0.3055	0.3055
0.30	0.4351	0.1149	0.1254	0.2314	0.2514	0.2514
0.40	0.3615	0.0951	0.1048	0.1592	0.1746	0.1746
0.50	0.3126	0.0802	0.0892	0.1161	0.1285	0.1285
0.60	0.2557	0.0736	0.0824	0.0871	0.0971	0.0971
0.80	0.1839	0.0609	0.0692	0.0518	0.0586	0.0586
1.00	0.1439	0.0497	0.0570	0.0331	0.0378	0.0378
1.50	0.0860	0.0341	0.0402	0.0136	0.0159	0.0159
2.00	0.0575	0.0259	0.0312	0.0069	0.0083	0.0083
3.00	0.0291	0.0148	0.0191	0.0020	0.0026	0.0026

Table 9.8-6. Development of the vertical spectral for a return period of 50 years.

Vertical Spectrum: 50 year, Soil						
Period (sec)	Horizontal, 50 yr	Median Vertical Sa (g) Using T=0.1 sec M,D	Median Vertical Sa (g) Using T=1 sec M,D	T=0.1 Sec Vertical Soil Spectrum (g)	T=1 Sec Vertical Soil Spectrum (g)	Vertical Soil Spectrum 50 yr
0.01	0.3567	0.1204	0.1251	0.1451	0.1513	0.1513
0.03	0.3567	0.1557	0.1608	0.1876	0.1944	0.1944
0.10	0.7003	0.2452	0.2529	0.5801	0.6004	0.6004
0.15	0.7643	0.2390	0.2507	0.6171	0.6495	0.6495
0.20	0.7738	0.2041	0.2164	0.5336	0.5676	0.5676
0.25	0.7142	0.1796	0.1919	0.4333	0.4646	0.4646
0.30	0.6610	0.1577	0.1698	0.3522	0.3805	0.3805
0.40	0.5530	0.1296	0.1405	0.2421	0.2634	0.2634
0.50	0.4766	0.1088	0.1188	0.1752	0.1919	0.1919
0.60	0.3943	0.0997	0.1093	0.1328	0.1461	0.1461
0.80	0.2867	0.0822	0.0911	0.0796	0.0885	0.0885
1.00	0.2202	0.0676	0.0755	0.0503	0.0564	0.0564
1.50	0.1350	0.0472	0.0539	0.0215	0.0247	0.0247
2.00	0.0926	0.0364	0.0423	0.0114	0.0133	0.0133
3.00	0.0483	0.0220	0.0272	0.0036	0.0045	0.0045

Table 9.8-7. Development of the vertical spectral for a return period of 100 years.

Vertical Spectrum: 100 year, Soil						
Period (sec)	Horizontal, 100 yr	Median Vertical Sa (g) Using T=0.1 sec M,D	Median Vertical Sa (g) Using T=1 sec M,D	T=0.1 Sec Vertical Soil Spectrum (g)	T=1 Sec Vertical Soil Spectrum (g)	Vertical Soil Spectrum 100 yr
0.01	0.5050	0.1776	0.2128	0.2193	0.2311	0.2311
0.03	0.5050	0.2328	0.2795	0.2874	0.3035	0.3035
0.10	0.9874	0.3720	0.4485	0.8981	0.9524	0.9524
0.15	1.0870	0.3521	0.4231	0.9358	0.9891	0.9891
0.20	1.1064	0.2958	0.3547	0.8002	0.8440	0.8440
0.25	1.0262	0.2567	0.3074	0.6441	0.6784	0.6784
0.30	0.9558	0.2227	0.2664	0.5204	0.5476	0.5476
0.40	0.8053	0.1815	0.2170	0.3574	0.3758	0.3758
0.50	0.6962	0.1515	0.1812	0.2579	0.2713	0.2713
0.60	0.5830	0.1384	0.1656	0.1973	0.2076	0.2076
0.80	0.4247	0.1137	0.1364	0.1181	0.1246	0.1246
1.00	0.3336	0.0941	0.1135	0.0768	0.0814	0.0814
1.50	0.2053	0.0670	0.0820	0.0336	0.0362	0.0362
2.00	0.1400	0.0526	0.0651	0.0180	0.0196	0.0196
3.00	0.0745	0.0340	0.0438	0.0062	0.0070	0.0070

Table 9.8-8. Development of the vertical spectral for a return period of 500 years.

Vertical Spectrum: 500 year, Soil						
Period (sec)	Horizontal, 500 yr	Median Vertical Sa (g) Using T=0.1 sec M,D	Median Vertical Sa (g) Using T=1 sec M,D	T=0.1 Sec Vertical Soil Spectrum (g)	T=1 Sec Vertical Soil Spectrum (g)	Vertical Soil Spectrum 500 yr
0.01	1.0038	0.4552	0.7530	0.5100	0.5338	0.5338
0.03	1.0038	0.6193	1.0529	0.6938	0.7464	0.7464
0.10	1.9180	1.0242	1.7810	2.1924	2.4124	2.4124
0.15	2.1860	0.8885	1.4457	2.1677	2.2319	2.2319
0.20	2.2869	0.7205	1.1819	1.8390	1.9088	1.9088
0.25	2.1669	0.6060	0.9955	1.4656	1.5234	1.5234
0.30	2.0612	0.5102	0.8380	1.1737	1.2198	1.2198
0.40	1.7978	0.4083	0.6869	0.8192	0.8721	0.8721
0.50	1.6081	0.3353	0.5735	0.6018	0.6513	0.6513
0.60	1.3696	0.3030	0.5204	0.4632	0.5033	0.5033
0.80	1.0494	0.2442	0.4225	0.2860	0.3131	0.3131
1.00	0.8422	0.2030	0.3493	0.1908	0.2078	0.2078
1.50	0.5142	0.1470	0.2513	0.0844	0.0913	0.0913
2.00	0.3392	0.1172	0.1993	0.0444	0.0477	0.0477
3.00	0.1787	0.0814	0.1391	0.0162	0.0176	0.0176

Table 9.8-9. Development of the vertical spectral for a return period of 1,000 years.

Vertical Spectrum: 1,000 year, Soil						
Period (sec)	Horizontal, 1,000 yr	Median Vertical Sa (g) Using T=0.1 sec M,D	Median Vertical Sa (g) Using T=1 sec M,D	T=0.1 Sec Vertical Soil Spectrum (g)	T=1 Sec Vertical Soil Spectrum (g)	Vertical Soil Spectrum 1,000 yr
0.01	1.2046	0.5044	0.7751	0.6194	0.6399	0.6399
0.03	1.2046	0.6899	1.0858	0.8471	0.8965	0.8965
0.10	2.2938	1.1460	1.8397	2.6796	2.8923	2.8923
0.15	2.6738	0.9815	1.4863	2.6752	2.7238	2.7238
0.20	2.8133	0.7943	1.2187	2.2779	2.3499	2.3499
0.25	2.6883	0.6664	1.0291	1.8262	1.8962	1.8962
0.30	2.5685	0.5595	0.8683	1.4649	1.5286	1.5286
0.40	2.2449	0.4476	0.7165	1.0243	1.1024	1.1024
0.50	2.0283	0.3672	0.6022	0.7592	0.8372	0.8372
0.60	1.7500	0.3314	0.5484	0.5912	0.6578	0.6578
0.80	1.2421	0.2664	0.4483	0.3373	0.3817	0.3817
1.00	1.0073	0.2213	0.3704	0.2272	0.2557	0.2557
1.50	0.6283	0.1602	0.2662	0.1026	0.1146	0.1146
2.00	0.4310	0.1277	0.2109	0.0561	0.0623	0.0623
3.00	0.2344	0.0888	0.1472	0.0212	0.0236	0.0236

Table 9.8-10. Development of the vertical spectral for a return period of 2,000 years.

Vertical Spectrum: 2,000 year, Soil						
Period (sec)	Horizontal, 2,000 yr	Median Vertical Sa (g) Using T=0.1 sec M,D	Median Vertical Sa (g) Using T=1 sec M,D	T=0.1 Sec Vertical Soil Spectrum (g)	T=1 Sec Vertical Soil Spectrum (g)	Vertical Soil Spectrum 2,000 yr
0.01	1.3770	0.5177	0.7792	0.7058	0.7309	0.7309
0.03	1.3770	0.7096	1.0920	0.9674	1.0243	1.0243
0.10	2.6647	1.1807	1.8507	3.1151	3.3594	3.3594
0.15	3.1111	1.0060	1.4938	3.0988	3.1658	3.1658
0.20	3.2488	0.8138	1.2257	2.6177	2.7126	2.7126
0.25	3.1470	0.6823	1.0354	2.1259	2.2196	2.2196
0.30	3.0401	0.5724	0.8741	1.7229	1.8102	1.8102
0.40	2.6815	0.4580	0.7223	1.2160	1.3194	1.3194
0.50	2.3997	0.3757	0.6079	0.8926	0.9937	0.9937
0.60	2.0821	0.3389	0.5541	0.6986	0.7859	0.7859
0.80	1.3854	0.2722	0.4536	0.3734	0.4281	0.4281
1.00	1.1302	0.2260	0.3748	0.2529	0.2886	0.2886
1.50	0.7436	0.1635	0.2693	0.1204	0.1364	0.1364
2.00	0.5259	0.1302	0.2133	0.0678	0.0764	0.0764
3.00	0.2915	0.0905	0.1489	0.0261	0.0296	0.0296

Table 9.8-11. Development of the vertical spectral for a return period of 5,000 years.

Vertical Spectrum: 5,000 year, Soil						
Period (sec)	Horizontal, 5,000 yr	Median Vertical Sa (g) Using T=0.1 sec M,D	Median Vertical Sa (g) Using T=1 sec M,D	T=0.1 Sec Vertical Soil Spectrum (g)	T=1 Sec Vertical Soil Spectrum (g)	Vertical Soil Spectrum 5,000 yr
0.01	1.6116	0.4962	0.7792	0.8029	0.8554	0.8554
0.03	1.6116	0.6808	1.0920	1.1016	1.1988	1.1988
0.10	3.1087	1.1335	1.8507	3.5379	3.9191	3.9191
0.15	3.6067	0.9628	1.4938	3.4865	3.6701	3.6701
0.20	3.8176	0.7790	1.2257	2.9859	3.1875	3.1875
0.25	3.6958	0.6530	1.0354	2.4230	2.6067	2.6067
0.30	3.5653	0.5477	0.8741	1.9606	2.1229	2.1229
0.40	3.2065	0.4384	0.7223	1.4114	1.5777	1.5777
0.50	2.8776	0.3596	0.6079	1.0389	1.1916	1.1916
0.60	2.5074	0.3243	0.5541	0.8164	0.9464	0.9464
0.80	1.5770	0.2603	0.4536	0.4121	0.4873	0.4873
1.00	1.2872	0.2159	0.3748	0.2790	0.3286	0.3286
1.50	0.8671	0.1558	0.2693	0.1356	0.1591	0.1591
2.00	0.6305	0.1238	0.2133	0.0784	0.0916	0.0916
3.00	0.3772	0.0855	0.1489	0.0324	0.0383	0.0383

Table 9.8-12. Development of the vertical spectral for a return period of 10,000 years.

Vertical Spectrum: 10,000 year, Soil						
Period (sec)	Horizontal, 10,000 yr	Median Vertical Sa (g) Using T=0.1 sec M,D	Median Vertical Sa (g) Using T=1 sec M,D	T=0.1 Sec Vertical Soil Spectrum (g)	T=1 Sec Vertical Soil Spectrum (g)	Vertical Soil Spectrum 10,000 yr
0.01	1.7746	0.4706	0.7792	0.8427	0.9419	0.9419
0.03	1.7746	0.6471	1.0920	1.1588	1.3201	1.3201
0.10	3.3901	1.0784	1.8507	3.6891	4.2739	4.2739
0.15	4.0334	0.9103	1.4938	3.7049	4.1043	4.1043
0.20	4.3133	0.7367	1.2257	3.2065	3.6014	3.6014
0.25	4.1736	0.6173	1.0354	2.5998	2.9437	2.9437
0.30	4.0221	0.5175	0.8741	2.1003	2.3949	2.3949
0.40	3.5847	0.4146	0.7223	1.4997	1.7638	1.7638
0.50	3.1860	0.3401	0.6079	1.0934	1.3193	1.3193
0.60	2.8100	0.3065	0.5541	0.8691	1.0606	1.0606
0.80	1.7165	0.2456	0.4536	0.4254	0.5304	0.5304
1.00	1.4069	0.2032	0.3748	0.2885	0.3592	0.3592
1.50	0.9611	0.1458	0.2693	0.1414	0.1763	0.1763
2.00	0.7030	0.1153	0.2133	0.0818	0.1021	0.1021
3.00	0.4283	0.0784	0.1489	0.0339	0.0434	0.0434

Table 9.8-13. Equal hazard spectra for the vertical component.

Period (sec)	1 Yr	25 yr	50 yr	100 yr	500 yr	1,000 yr	2,000 yr	5,000 yr	10,000 yr
0.01	0.0011	0.0968	0.1513	0.2311	0.5338	0.6399	0.7309	0.8554	0.9419
0.03	0.0013	0.1228	0.1944	0.3035	0.7464	0.8965	1.0243	1.1988	1.3201
0.10	0.0030	0.3776	0.6004	0.9524	2.4124	2.8923	3.3594	3.9191	4.2739
0.15	0.0039	0.4189	0.6495	0.9891	2.2319	2.7238	3.1658	3.6701	4.1043
0.20	0.0040	0.3707	0.5676	0.8440	1.9088	2.3499	2.7126	3.1875	3.6014
0.25	0.0038	0.3055	0.4646	0.6784	1.5234	1.8962	2.2196	2.6067	2.9437
0.30	0.0034	0.2514	0.3805	0.5476	1.2198	1.5286	1.8102	2.1229	2.3949
0.40	0.0025	0.1746	0.2634	0.3758	0.8721	1.1024	1.3194	1.5777	1.7638
0.50	0.0020	0.1285	0.1919	0.2713	0.6513	0.8372	0.9937	1.1916	1.3193
0.60	0.0016	0.0971	0.1461	0.2076	0.5033	0.6578	0.7859	0.9464	1.0606
0.80	0.0010	0.0586	0.0885	0.1246	0.3131	0.3817	0.4281	0.4873	0.5304
1.00	0.0006	0.0378	0.0564	0.0814	0.2078	0.2557	0.2886	0.3286	0.3592
1.50	0.0002	0.0159	0.0247	0.0362	0.0913	0.1146	0.1364	0.1591	0.1763
2.00	0.0001	0.0083	0.0133	0.0196	0.0477	0.0623	0.0764	0.0916	0.1021
3.00	0.0000	0.0026	0.0045	0.0070	0.0176	0.0236	0.0296	0.0383	0.0434

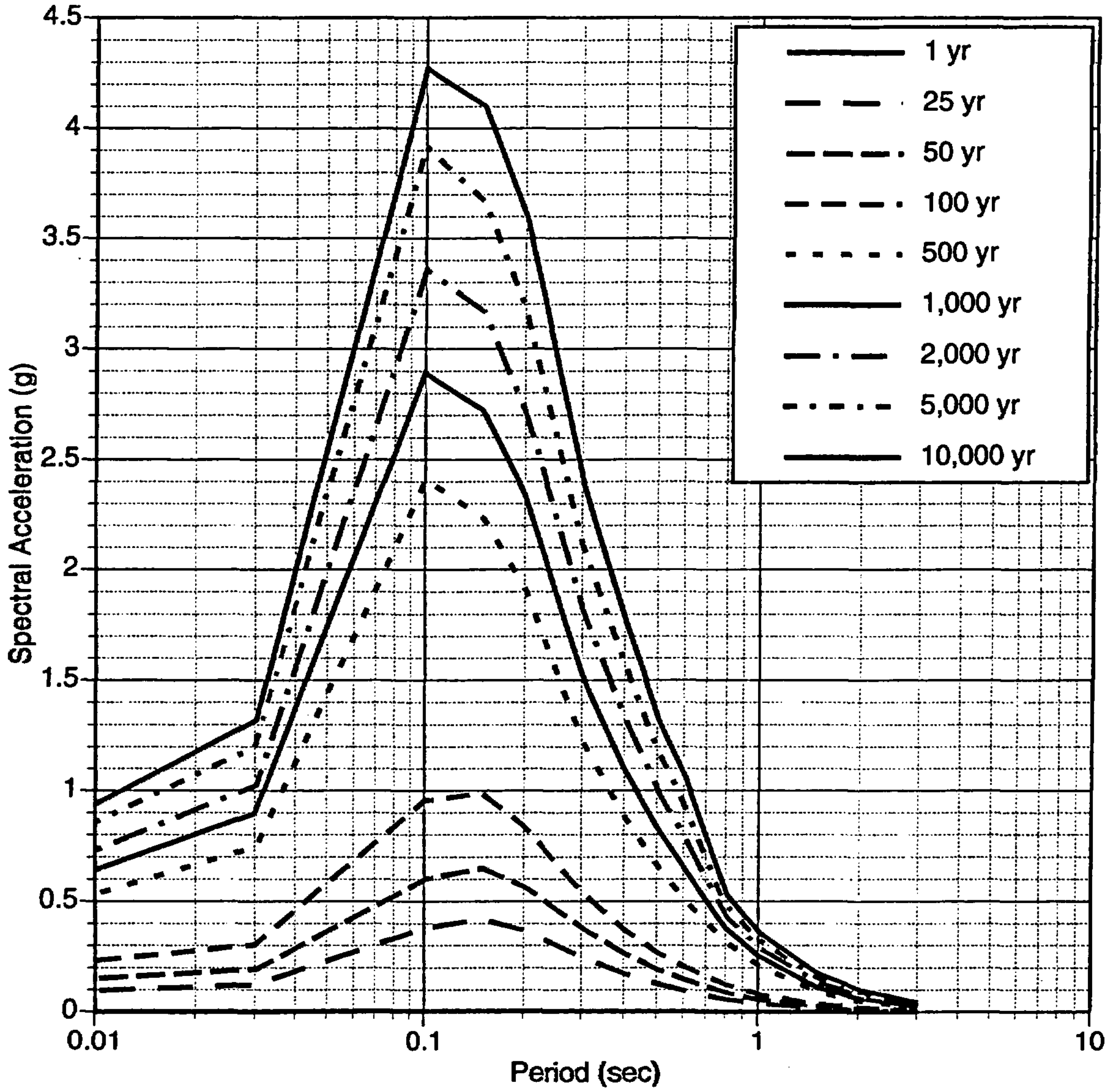

Figure 9.8-1 Equal hazard spectra for the vertical component for soil.

10.0 RESULTS AND CONCLUSIONS

The mean equal hazard spectra for rock for the fault normal and fault parallel components are given in Tables 10.1, and 10.2.

The mean equal hazard spectra for soil for the fault normal, fault parallel, and vertical components are given in Tables 10.3, 10.4, and 10.5, respectively.

The equal hazard spectrum could not be estimated for the 1 month return period because the rate of magnitude 5 or larger earthquakes considered does not result in an earthquake every month. The response spectrum for a 1 month return period is so small that it is negligible for engineering analyses.

Table 10.1 Equal hazard spectra for rock, fault normal component.

Period (sec)	1 Yr	25 yr	50 yr	100 yr	500 yr	1,000 yr	2,000 yr	5,000 yr	10,000 yr
0.01	0.0031	0.2392	0.3567	0.5050	1.0038	1.2046	1.3770	1.6116	1.7746
0.03	0.0031	0.2392	0.3567	0.5050	1.0038	1.2046	1.3770	1.6116	1.7746
0.10	0.0051	0.4739	0.7003	0.9874	1.9180	2.2938	2.6647	3.1087	3.3901
0.15	0.0056	0.5147	0.7643	1.0870	2.1860	2.6738	3.1111	3.6067	4.0334
0.20	0.0057	0.5180	0.7738	1.1064	2.2869	2.8133	3.2488	3.8176	4.3133
0.25	0.0054	0.4738	0.7142	1.0262	2.1669	2.6883	3.1470	3.6958	4.1736
0.30	0.0050	0.4351	0.6610	0.9558	2.0612	2.5685	3.0401	3.5653	4.0221
0.40	0.0042	0.3615	0.5530	0.8053	1.7978	2.2449	2.6815	3.2065	3.5847
0.50	0.0037	0.3126	0.4766	0.6962	1.6081	2.0283	2.3997	2.8776	3.1860
0.60	0.0032	0.2557	0.3943	0.5830	1.3696	1.7500	2.0821	2.5074	2.8100
0.80	0.0022	0.1839	0.2868	0.4249	1.0528	1.2490	1.3986	1.5944	1.7408
1.00	0.0017	0.1440	0.2202	0.3335	0.8473	1.0184	1.1526	1.3160	1.4438
1.50	0.0011	0.0860	0.1350	0.2050	0.5188	0.6531	0.7788	0.9297	1.0406
2.00	0.0005	0.0575	0.0926	0.1399	0.3471	0.4620	0.5668	0.7089	0.8008
3.00	0.0002	0.0291	0.0483	0.0743	0.1889	0.2717	0.3514	0.4686	0.5457

Table 10.2 Equal hazard spectra for rock, fault parallel component.

Period (sec)	1 Yr	25 yr	50 yr	100 yr	500 yr	1,000 yr	2,000 yr	5,000 yr	10,000 yr
0.01	0.0031	0.2392	0.3567	0.5050	1.0038	1.2046	1.3770	1.6116	1.7746
0.03	0.0031	0.2392	0.3567	0.5050	1.0038	1.2046	1.3770	1.6116	1.7746
0.10	0.0051	0.4739	0.7003	0.9874	1.9180	2.2938	2.6647	3.1087	3.3901
0.15	0.0056	0.5147	0.7643	1.0870	2.1860	2.6738	3.1111	3.6067	4.0334
0.20	0.0057	0.5180	0.7738	1.1064	2.2869	2.8133	3.2488	3.8176	4.3133
0.25	0.0054	0.4738	0.7142	1.0262	2.1669	2.6883	3.1470	3.6958	4.1736
0.30	0.0050	0.4351	0.6610	0.9558	2.0612	2.5685	3.0401	3.5653	4.0221
0.40	0.0042	0.3615	0.5530	0.8053	1.7978	2.2449	2.6815	3.2065	3.5847
0.50	0.0037	0.3126	0.4766	0.6962	1.6081	2.0283	2.3997	2.8776	3.1860
0.60	0.0032	0.2557	0.3943	0.5830	1.3696	1.7500	2.0821	2.5074	2.8100
0.80	0.0022	0.1839	0.2866	0.4246	1.0461	1.2352	1.3724	1.5597	1.6925
1.00	0.0017	0.1439	0.2203	0.3338	0.8371	0.9964	1.1082	1.2591	1.3709
1.50	0.0011	0.0861	0.1351	0.2056	0.5096	0.6045	0.7099	0.8087	0.8877
2.00	0.0005	0.0575	0.0926	0.1401	0.3314	0.4021	0.4880	0.5607	0.6171
3.00	0.0002	0.0291	0.0483	0.0747	0.1690	0.2022	0.2418	0.3036	0.3361

Table 10.3 Equal hazard spectra for soil, fault normal component.

Period (sec)	1 Yr	25 yr	50 yr	100 yr	500 yr	1,000 yr	2,000 yr	5,000 yr	10,000 yr
0.01	0.0042	0.3118	0.4109	0.5294	0.7957	0.8890	0.9674	1.0798	1.1726
0.03	0.0042	0.3118	0.4109	0.5294	0.7957	0.8890	0.9674	1.0798	1.1726
0.10	0.0076	0.5219	0.6601	0.7940	1.0803	1.1889	1.3109	1.4922	1.6107
0.15	0.0088	0.6578	0.8621	1.0533	1.5286	1.6959	1.8015	1.9487	2.0767
0.20	0.0110	0.8266	1.0890	1.3608	2.0493	2.2716	2.5157	2.8337	3.1006
0.25	0.0104	0.8450	1.1837	1.5217	2.2760	2.6377	2.9280	3.2399	3.4770
0.30	0.0094	0.7644	1.1031	1.4322	2.2161	2.4778	2.7427	3.0941	3.3236
0.35	0.0087	0.6646	0.9734	1.3427	2.1535	2.4478	2.6454	2.8930	3.1113
0.40	0.0082	0.6128	0.8953	1.2384	2.0439	2.2503	2.4775	2.6986	2.8719
0.50	0.0069	0.5380	0.7870	1.0810	1.8927	2.1027	2.2800	2.5320	2.7128
0.60	0.0051	0.4335	0.6546	0.9338	1.7485	1.9607	2.1531	2.4228	2.6165
0.80	0.0040	0.3210	0.4837	0.6964	1.4445	1.6883	1.8618	2.0882	2.2517
1.00	0.0038	0.2985	0.4469	0.6452	1.3165	1.5507	1.7382	1.9419	2.1210
1.50	0.0025	0.2000	0.3196	0.4764	1.0821	1.3129	1.5282	1.8083	2.0373
2.00	0.0013	0.1205	0.1967	0.3111	0.8237	1.0551	1.2766	1.5738	1.7904
3.00	0.0001	0.0465	0.0763	0.1216	0.3356	0.5055	0.6782	0.8977	1.0571

Table 10.4 Equal hazard spectra for soil, fault parallel component.

Period (sec)	1 Yr	25 yr	50 yr	100 yr	500 yr	1,000 yr	2,000 yr	5,000 yr	10,000 yr
0.01	0.0042	0.3118	0.4109	0.5294	0.7957	0.8890	0.9674	1.0798	1.1726
0.03	0.0043	0.3168	0.4175	0.5379	0.8084	0.9032	0.9829	1.0971	1.1914
0.10	0.0076	0.5219	0.6601	0.7940	1.1012	1.2304	1.3389	1.4944	1.6229
0.15	0.0088	0.6578	0.8621	1.0533	1.5286	1.6959	1.8015	1.9487	2.0767
0.20	0.0110	0.8266	1.0890	1.3608	2.0493	2.2716	2.5157	2.8337	3.1006
0.25	0.0104	0.8450	1.1837	1.5217	2.2760	2.6377	2.9280	3.2399	3.4770
0.30	0.0094	0.7644	1.1031	1.4322	2.2161	2.4778	2.7427	3.0941	3.3236
0.35	0.0087	0.6646	0.9734	1.3427	2.1535	2.4478	2.6454	2.8930	3.1113
0.40	0.0082	0.6128	0.8953	1.2384	2.0439	2.2503	2.4775	2.6986	2.8719
0.50	0.0069	0.5380	0.7870	1.0810	1.8927	2.1027	2.2800	2.5320	2.7128
0.60	0.0051	0.4335	0.6546	0.9338	1.7485	1.9607	2.1531	2.4228	2.6165
0.80	0.0040	0.3210	0.4838	0.6959	1.4360	1.6696	1.8373	2.0551	2.2098
1.00	0.0038	0.2985	0.4468	0.6452	1.3053	1.5272	1.7066	1.8845	2.0361
1.50	0.0025	0.2000	0.3196	0.4766	1.0630	1.2631	1.4237	1.6423	1.8033
2.00	0.0013	0.1205	0.1966	0.3114	0.7924	0.9638	1.1069	1.2808	1.4055
3.00	0.0001	0.0464	0.0763	0.1223	0.3109	0.3840	0.4744	0.5714	0.6470

Table 10.5 Equal hazard spectra for soil, vertical component.

Period (sec)	1 Yr	25 yr	50 yr	100 yr	500 yr	1,000 yr	2,000 yr	5,000 yr	10,000 yr
0.01	0.0011	0.0968	0.1513	0.2311	0.5338	0.6399	0.7309	0.8554	0.9419
0.03	0.0013	0.1228	0.1944	0.3035	0.7464	0.8965	1.0243	1.1988	1.3201
0.10	0.0030	0.3776	0.6004	0.9524	2.4124	2.8923	3.3594	3.9191	4.2739
0.15	0.0039	0.4189	0.6495	0.9891	2.2319	2.7238	3.1658	3.6701	4.1043
0.20	0.0040	0.3707	0.5676	0.8440	1.9088	2.3499	2.7126	3.1875	3.6014
0.25	0.0038	0.3055	0.4646	0.6784	1.5234	1.8962	2.2196	2.6067	2.9437
0.30	0.0034	0.2514	0.3805	0.5476	1.2198	1.5286	1.8102	2.1229	2.3949
0.40	0.0025	0.1746	0.2634	0.3758	0.8721	1.1024	1.3194	1.5777	1.7638
0.50	0.0020	0.1285	0.1919	0.2713	0.6513	0.8372	0.9937	1.1916	1.3193
0.60	0.0016	0.0971	0.1461	0.2076	0.5033	0.6578	0.7859	0.9464	1.0606
0.80	0.0010	0.0586	0.0885	0.1246	0.3131	0.3817	0.4281	0.4873	0.5304
1.00	0.0006	0.0378	0.0564	0.0814	0.2078	0.2557	0.2886	0.3286	0.3592
1.50	0.0002	0.0159	0.0247	0.0362	0.0913	0.1146	0.1364	0.1591	0.1763
2.00	0.0001	0.0083	0.0133	0.0196	0.0477	0.0623	0.0764	0.0916	0.1021
3.00	0.0000	0.0026	0.0045	0.0070	0.0176	0.0236	0.0296	0.0383	0.0434

11.0 LIMITATIONS

The equal hazard spectra developed in this calculation are based on the state of the knowledge at the time the calculation was performed. With time, new models of the source characterization and ground motion attenuation will be developed that may significantly change these results.

The equal hazard spectra were computed for spectral periods of 0 to 3 seconds. The spectra were not computed for periods greater than 3 seconds because the longest period for which the attenuation relation (for subduction events) is defined is 3 seconds. If needed, the spectra can be extended to longer periods by extrapolating the equal hazard spectral values (see Calculation GEO.HBIP.02.04).

12.0 IMPACT EVALUATION

The results from this study impact the design ground motions for the HBIP ISFSI. The new regulations require that a PSHA be conducted and that the 2000 year return period ground motions be used. This impacts the previous structural and geotechnical evaluations that were based on the deterministic approach used in GEO.HBIP.02.04. As long as the 2000 year equal hazard spectra from this current calculation are smaller than the deterministic spectra from GEO.HBIP.02.04, then other calculation based on the deterministic ground motion will still meet the criteria of DG3021.

13.0 REFERENCES

Abe, K. (1981). Magnitudes of large shallow earthquakes from 1904-1980, *Physics of the Earth and Planetary Interiors*, Vol. **27**, p. 72-92.

Abe, K. (1984). Complements to "Magnitudes of large shallow earthquakes from 1904-1980," *Physics of the Earth and Planetary Interiors*, Vol. **34**, p. 17-23.

Abrahamson, N. A. and W. Silva (1997). Empirical Response Spectral Attenuation Relations for Shallow Crustal Earthquakes, *Seis. Res. Letters*, Vol. **68**, No. 1, p. 94-127.

Campbell, K. (1997). Empirical near-source attenuation relationships for horzontal and vertical components of peak ground acceleration, peak ground velcoity, and pseudo-absolute acceleration response sepctra, Seism. Res. Let, 154-179.

Cao, T., W A. Bryant, B. Rowshandel, D. Branum, and C. J. Wills (2003). The Revised 2002 California Probabilistic Seismic Hazard Maps, June 2003, California Geological Survey Internet Web Report, http://www.consrv.ca.gov/CGS/rghm/psha/index.htm

Clarke, S. H., Jr. and G. A. Carver (1992). Late Holocene Tectonics and Paleoseismicity, Southern Cascadia Subduction Zone, *Science*, Vol. **255**, p. 188-192.

Clarke, S. H., Jr. (1992). Geology of the Eel River Basin and Adjacent Region: Implications for Late Cenozoic Tectonics of the Southern Cascadia Subduction Zone and Mendocino Triple Junction, *American Association of Petroleum Geologist Bulletin*, Vol. **76**, p. 199-224.

Geomatrix (1992). Seismic Ground Motion Study for Richmond – San Rafael Bridge, Contra Costa County, California, Report prepared for Caltrans, Caltrans Contract No. 59N772, March 1992.

Geomatrix (1993). Seismic Margin Earthquake for the Trojan site, Final unpublished report prepared for Portland General Electric Trojan Nuclear Power Plant, Ranier, Oregon.

Geomatrix (1994). Seismic Hazard Ground Motion Study for Humboldt Bay Bridges on Route 255, Report for Caltrans, Division of Structures, Sacramento, California, March 1994.

Geomatrix (1995). Seismic Design Mapping State of Oregon, Report for Oregon Department of Transportation, Salem, Oregon, January, 1995.

Gutenberg, B., and C. F. Richter (1956). Earthquake Magnitude, Intensity, Energy, and Acceleration, *Bull Seism. Soc. Am.*, Vol. **46**, p. 105-145.

Idriss, I. M. (1995). An overview of earthquake ground motions pertinent to seismic zonation, Proc. Fifth International Conference on Seismic Zonation, Vol. III, 2111-2126.

Idriss. I. M. (1991). Selection of earthquake ground motions at rock sites, report prepared for the Structures Division, Building and Fire Research Laboratory, National Institute of Standard and Technology, Department of Civil Engineering, University of California, Davis.

Jennings, C. W. (1994). Fault Activity Map of California and Adjacent Areas with Locations and Ages of Recent Volcanic Eruptions, California Division of Mines and Geology, California Geologic Data Map Series, Map No. 06.

McGuire, R. K., W. J. Silva, and C. J. Constantino (2001). Technical basis for revision of Regulatory Guidance on Design Ground Motions: Hazard- and Rick-Consistent Ground Motion Spectra Guidelines, NUREG/CR-6728.

Pacific Gas and Electric (2002a). Humboldt Bay ISFSI Project, Technical Report, TR-xHBIP-2002-01.

Pacific Gas and Electric (2002b). Geosciences Calculation Log GEO.HBIP.02.03 – Development of maximum credible earthquake magnitudes and distances for HBIP, Dated October 4, 2002.

Pacific Gas and Electric (2002c). Geosciences Calculation Log GEO.HBIP.02.04 – Development of response spectra for the HBIP ISFSI, Dated November 4, 2002.

Pacific Gas and Electric (2003a). Action Request A0583100 – Develop PHSA for the Humboldt Bay ISFSI, Dated May 20, 2003.

Pacific Gas and Electric (2003b). Geosciences Calculation Log GEO.HBIP.03.03 – Verification of PHSA software HAZ36, Revision 0, September 12, 2003.

Pacific Gas and Electric (2003c). Geosciences Calculations Log GEO.HBIP.03.02 – Amplification Factors for Probabilistic Seismic Hazard Analysis at HBPP ISFSI Site, Dated August 27, 2003.

Peterson, M., W. Bryant, C. Cramer, T. Cao, M. Reichle, A. Frankel, J. Lienkaemper, P. McCrory, and D. Schwartz (1996). Probabilistic seismic hazard assessment for the State of California, California Department of Conservation, Div. Mines and Geology, OFR 96-08, USGS OFR 96-706.

Sadigh, K., C-Y Chang, J. A. Egan, F. Makdisi, and R. R. Youngs (1997). Attenuation relationships for shallow crustal earthquakes based on California strong motion data, *Seis. Res. Letters*, Vol. **68**, p. 180-189.

Senior Seismic Hazard Analysis Committee (SSHAC) (2997). Recommendations for Probabilistic Seismic Hazard Analysis: Guidence on Uncertainty and Use of Experts, NUREG/CR-6372.

Somerville, P. G., N. F. Smith, R. W. Graves, and N. A. Abrahamson (1997). Modification of Empirical Strong Ground Motion Attenuation Relations to Include the Amplitude and Duration Effects of Rupture Directivity, *Seis. Res. Letters*, Vol. **68**, p. 199-222.

Tanioka, Y., K. Satake, and L. Ruff (1995). Seismotectonics of the April 25, 1992 Petrolia earthquake and the Mendocino Triple Junction Region, *Tectonics*, **14**, 1095-1103.

U.S. NRC (2002). Site Evaluations and determiniation of design earhtquake ground motions for seismic design of independent spent fuel storage installations and monitored retrievable staorage installations, Draft Regulatory Guide DG-3021, July 2002.

U.S. NRC (1997). Identification and characterization of seismic sources and determination of safe shutdown earthquake ground motion, Regulatory Guide 1.165, March 1997.

Utsu, T. (1970). Aftershock and earthquake statistics (II) – Further investigation of aftershocks and other earthquakes sequences based on a new classificsation of earthquake sequences, Journal of the Faculty of Science, Hokkaido University, Ser. VII (Geophsics), Vol III, No. 4, pp 197-266.

Wells, D. and K. Coppersmith (1994). Updated empirical relationships among magnitude, rupture length, rupture area, and surface displacement, *Bull Seism. Soc. Am.*, Vol. **84**, p. 974-1002.

Youngs, R. R., S. J. Chiou, W. J. Silva and J. R. Humphrey (1997). Strong ground motion attenuation relationships for subduction zone earthquakes, *Seis. Res. Letters*, Vol. **68**, No. 1, p. 58-73.

Youngs, R. R. and K. Coppersmith (1985). Implications for fault slip rates and earthquake recurrence models to probabilistic seismic hazard estimates, *Bull. Seism. Soc. Am.*, Vol. **75**, p. 939-964.

14.0 ENCLOSURES

Source characterization section from Geomatrix (1994)

Source characterization section from Geomatrix (1995)

CD ROM (dated 9/29/03)

Appendix 1	Fault File
Appendix 2	Input and output files for rock FN
Appendix 3	Input and output files for rock FP
Appendix 4	Input and output files for soil FN
Appendix 5	Input and output files for soil FP
Appendix 6	Contents of CD ROM

Pages 132 through 760 are attachments of computer input and output data, and are not printed. They exist in electronic format on a CD in records retention system.